

ผลของโปรตีนคาวิโอลิน-1 ต่อภาวะเครียดออกซิเดชัน
และการตายของเซลล์มะเร็งปอดที่ถูกเหนี่ยวนำด้วยไฮโดรเจนเปอร์ออกไซด์

นายวงศกร สุชาวรินทร์

วิทยานิพนธ์นี้เป็นส่วนหนึ่งของการศึกษาตามหลักสูตรปริญญาเภสัชศาสตรมหาบัณฑิต
สาขาวิชาเภสัชวิทยา ภาควิชาเภสัชวิทยาและสรีรวิทยา
คณะเภสัชศาสตร์ จุฬาลงกรณ์มหาวิทยาลัย
ปีการศึกษา 2554
ลิขสิทธิ์ของจุฬาลงกรณ์มหาวิทยาลัย

บทคัดย่อและแฟ้มข้อมูลฉบับเต็มของวิทยานิพนธ์ตั้งแต่ปีการศึกษา 2554 ที่ให้บริการในคลังปัญญาจุฬาฯ (CUIR)
เป็นแฟ้มข้อมูลของนิสิตเจ้าของวิทยานิพนธ์ที่ส่งผ่านทางบัณฑิตวิทยาลัย
The abstract and full text of theses from the academic year 2011 in Chulalongkorn University Intellectual Repository(CUIR)
are the thesis authors' files submitted through the Graduate School.


EFFECT OF CAVEOLIN-1 ON HYDROGEN PEROXIDE-MEDIATED
OXIDATIVE STRESS AND CELL DEATH
IN LUNG CARCINOMA CELLS

Mr. Wongsakorn Suchaoin


A Thesis Submitted in Partial Fulfillment of the Requirements
for the Degree of Master of Science in Pharmacy Program in Pharmacology
Department of Pharmacology and Physiology
Faculty of Pharmaceutical Sciences
Chulalongkorn University
Academic Year 2011
Copyright of Chulalongkorn University


Thesis Title EFFECT OF CAVEOLIN-1 ON HYDROGEN PEROXIDE-
MEDIATED OXIDATIVE STRESS AND CELL DEATH
IN LUNG CARCINOMA CELLS
By Mr. Wongsakorn Suchaoin
Field of Study Pharmacology
Thesis Advisor Assistant Professor Pithi Chanvorachote, Ph.D.

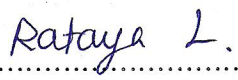
Accepted by the Faculty of Pharmaceutical Sciences, Chulalongkorn University
in Partial Fulfillment of the Requirements for the Master's Degree


..... Dean of the Faculty of Pharmaceutical
Sciences
(Associate Professor Pintip Pongpech, Ph.D.)

THESIS COMMITTEE


..... Chairman
(Associate Professor Pol. Lt. Col. Somsong Lawanprasert, Ph.D.)


..... Thesis Advisor
(Assistant Professor Pithi Chanvorachote, Ph.D.)


..... Examiner
(Assistant Professor Rataya Luechapudiporn, Ph.D.)


..... External Examiner
(Assistant Professor Patamawan Phuagphong, Ph.D.)

วงศกร สุเขาวินทร์: ผลของโปรตีนคาวีโอลิน-1 ต่อภาวะเครียดออกซิเดชันและการตาย
ของเซลล์มะเร็งปอดที่ถูกเหนี่ยวนำด้วยไฮโดรเจนเปอร์ออกไซด์. (EFFECT OF
CAVEOLIN-1 ON HYDROGEN PEROXIDE-MEDIATED OXIDATIVE STRESS
AND CELL DEATH IN LUNG CARCINOMA CELLS)

อ. ที่ปรึกษาวิทยานิพนธ์หลัก: ผศ. ภค. ดร. ปิติ จันทร์วรโชติ, 99 หน้า.

ภาวะเครียดออกซิเดชันที่เกิดขึ้นภายในเซลล์มีบทบาทสำคัญต่อพฤติกรรม และการดำเนินไปของโรคมะเร็ง มักพบการเพิ่มขึ้นของระดับอนุมูลออกซิเจนที่ว่องไวหลายชนิด โดยเฉพาะไฮโดรเจนเปอร์ออกไซด์ในบริเวณแวดล้อมของก้อนเซลล์มะเร็งปอด นอกจากนี้ยังพบว่าในเซลล์มะเร็งที่มีความรุนแรงหรือเซลล์มะเร็งที่อยู่ในระยะลุกลามจะมีระดับโปรตีนคาวีโอลิน-1 เพิ่มขึ้นด้วย ในการศึกษาที่มีวัตถุประสงค์เพื่อศึกษาผลของโปรตีนคาวีโอลิน-1 ต่อสภาวะเครียดออกซิเดชันและการตายของเซลล์มะเร็งปอดเมื่อถูกเหนี่ยวนำด้วยไฮโดรเจนเปอร์ออกไซด์ ผลการศึกษาพบว่าโปรตีนคาวีโอลิน-1 มีผลลดสภาวะเครียดออกซิเดชันซึ่งถูกเหนี่ยวนำด้วยไฮโดรเจนเปอร์ออกไซด์ โดยไฮโดรเจนเปอร์ออกไซด์มีผลเพิ่มระดับอนุมูลออกซิเจนภายในเซลล์และเป็นผลให้เกิดการตายแบบอะพอพโทซิสในเซลล์มะเร็งปอดชนิดเอช 460 และเมื่อทำการตรวจวัดระดับของอนุมูลออกซิเจนที่ว่องไวแต่ละชนิดร่วมกับการใช้สารต้านอนุมูลอิสระที่จำเพาะต่ออนุมูลออกซิเจนแต่ละชนิด ผลการศึกษาพบว่าอนุมูลอิสระไฮดรอกซิลแรดดิคัลเป็นตัวการสำคัญที่ทำให้เกิดการตายของเซลล์มะเร็งปอด และเมื่อทำการทรานส์เฟกชันให้เซลล์มะเร็งปอดมีการแสดงออกของระดับโปรตีนคาวีโอลิน-1 ที่แตกต่างกัน ผลการศึกษาพบว่า เซลล์มะเร็งปอดที่มีระดับของโปรตีนคาวีโอลิน-1 เพิ่มขึ้นจะเกิดภาวะเครียดออกซิเดชันและการตายของเซลล์เมื่อถูกเหนี่ยวนำด้วยไฮโดรเจนเปอร์ออกไซด์น้อยกว่าเซลล์มะเร็งปอดที่มีระดับคาวีโอลิน-1 ปกติอย่างมีนัยสำคัญ ในขณะที่เซลล์ที่มีระดับของโปรตีนคาวีโอลิน-1 ลดลงจะเกิดภาวะเครียดออกซิเดชันและการตายของเซลล์มากกว่าเซลล์ที่มีระดับคาวีโอลิน-1 ปกติอย่างมีนัยสำคัญ งานวิจัยนี้แสดงให้เห็นว่า ไฮโดรเจนเปอร์ออกไซด์ส่งผลให้เซลล์มะเร็งปอดเกิดภาวะเครียดออกซิเดชันและการตายแบบอะพอพโทซิสผ่านการสร้างไฮดรอกซิลแรดดิคัลภายในเซลล์ และโปรตีนคาวีโอลิน-1 มีบทบาทในการลดภาวะเครียดออกซิเดชันและการตายของเซลล์มะเร็งปอดเมื่อเหนี่ยวนำด้วยไฮโดรเจนเปอร์ออกไซด์ ซึ่งข้อมูลจากงานวิจัยดังกล่าวจะเป็นข้อมูลเบื้องต้นของโปรตีนคาวีโอลิน-1 ซึ่งเป็นเป้าหมายใหม่ที่สำคัญในการพัฒนาแนวทางในการรักษาโรคมะเร็ง และทำให้เข้าใจสภาวะของเซลล์มะเร็งที่คือต่อยาซึ่งมีกลไกการออกฤทธิ์ผ่านการสร้างอนุมูลออกซิเจนได้มากยิ่งขึ้น

ภาควิชา เกษัตริศาสตร์และสัตวศาสตร์

ลายมือชื่อนิติกร วงศกร สุเขาวินทร์

สาขาวิชา เกษัตริศาสตร์

ลายมือชื่อ อ.ที่ปรึกษาวิทยานิพนธ์หลัก ปิติ จันทร์วรโชติ

ปีการศึกษา 2554

5376559833: MAJOR Pharmacology

KEYWORDS : caveolin-1 / hydrogen peroxide / lung cancer / oxidative stress / reactive oxygen species

WONGSAKORN SUCHAOIN: EFFECT OF CAVEOLIN-1 ON HYDROGEN PEROXIDE-MEDIATED OXIDATIVE STRESS AND CELL DEATH IN LUNG CARCINOMA CELLS.

ADVISOR: ASST PROF. PITHI CHANVORACHOTE, Ph.D., 99 pp.

Oxidative stress plays an important role in cancer cell behavior and tumor progression. In lung cancer, various kinds of reactive oxygen species (ROS) especially hydrogen peroxide (H2O2) has been up-regulated in tumor microenvironment. Moreover, caveolin-1 (Cav-1) has been shown to overexpress in both primary and metastatic cancers and may be critical in the regulation of oxidative status of cancer cells. This study has reported for the first time that Cav-1 suppressed cellular oxidative stress induced by H2O2. The treatment of H2O2 in human lung carcinoma H460 cells significantly increased ROS inside the cells and resulted in cell apoptosis. Furthermore, using of specific ROS detecting assay and pretreatment with specific antioxidants revealed that superoxide anion was not associated with H2O2-induced oxidative stress whereas the hydroxyl radical was the key ROS which was responsible for oxidative damage in H460 cells. To study the effect of Cav-1 on H2O2-induced oxidative stress and cell death, H460 cells were transfected with Cav-1 overexpressing (H460/Cav-1) or knockdown plasmids (H460/shCav-1). The resulted showed that ROS level and cell death of H460/Cav-1 cells were decreased after H2O2 treatment in comparison to those of H460 control cells while H460/shCav-1 cells exhibited enhanced ROS signal and increased number of apoptotic cells. In conclusion, this study suggested that hydroxyl radical was the main ROS causing oxidative stress and cell death and Cav-1 protein attenuated cellular oxidative damage induced by H2O2 in lung carcinoma cells. These findings may provide the novel information of Cav-1 in cancer research and the better understanding on cancer resistance to ROS-generating chemotherapy.

Department : Pharmacology and Physiology
Field of Study : Pharmacology
Academic Year : 2011

Student's Signature Wongsakorn Suchaoin
Advisor's Signature Pithi Chanvorachote

ACKNOWLEDGEMENTS

First of all, I would like to express my appreciation to my advisor, Assistant Professor Pithi Chanvorachote for his best guidance and supporting. Without his assistance, this research would never be complete.

My sincere thanks to Associate Professor Somsong Lawanprasert for her kindness and giving me an opportunity to study in the Department of Pharmacology and Physiology, Chulalongkorn University with grants so that I can deeply focus on this research.

I would like to express my thanks to Dr. Varisa Pongrakhananon, Mr. Hasseri Halim, Mr. Chatchai choatham, Mr. Preedakorn Chunchacha, Miss Kanittha Pongjit, Miss Chuanpit Ninsontia, Miss Thitiporn Songserm, Miss Apiriya Dhumrongvaraporn, Miss Nuttida Yongsanguanchai and other members in my laboratory for technical teaching, supporting and sharing their comments and experiences which help me find the way to solve any problem while I was doing this project.

My special thanks to my close friends; Miss Warunya Arunotayanun, Miss Sarunya Sornpao, Miss Jiraporn Owatsakul, Miss Piyaporn Chummongkon and Miss Niramom Kaewratanapathama for their helpfulness, encouraging and understanding. Their suggestions and advices are always admirable and give me strength to carry on this work until success.

I would like to thank my family for their supporting and believing in me. In the memorial of their love, I also dedicate all the goodness of this research to my father and grandmother.

This work was supported by Chulalongkorn University Graduate Scholarship to Commemorate the 72nd Anniversary of His Majesty King Bhumibol Adulyadej.

CONTENTS

	Page
ABSTRACT (THAI).....	iv
ABSTRACT (ENGLISH).....	v
ACKNOWLEDGEMENTS.....	vi
CONTENTS.....	vii
LIST OF TABLES.....	viii
LIST OF FIGURES.....	x
LIST OF ABBREVIATIONS.....	xii
CHAPTER	
I INTRODUCTION.....	1
II LITERATURE REVIEW.....	4
1. Lung cancer.....	4
2. Caveolin-1.....	5
3. Role of caveolin-1 in cancer.....	8
4. Reactive Oxygen Species.....	10
5. Cellular target of ROS	13
6. Role of hydrogen peroxide as a signaling molecule.....	15
7. Role of hydrogen peroxide in cancer and chemotherapeutic agent.....	16
8. Studies of ROS and caveolin-1 in lung cancer cells.....	18
III MATERIALS AND METHODS.....	20
IV RESULTS.....	29
V DISCUSSION AND CONCLUSION.....	69
REFERENCES.....	72
APPENDIX.....	81
VITA.....	99

LIST OF TABLES

	Page
Table 1. ROS intensity of H460 cells after treatment with various concentration of hydrogen peroxide and determined by using DCFH ₂ -DA probe.	82
Table 2. The percentage of H460 cell viability was determined by MTT assay after treatment with various concentration of hydrogen peroxide for 24 h.....	84
Table 3. The percentage of H460 cell viability was determined by MTT assay after treatment with 200 μM hydrogen peroxide at various time point.....	84
Table 4. The percentage of H460 cell viability was determined by MTT assay after pretreatment with various kinds of antioxidant prior to 200 μM hydrogen peroxide at 24 h.....	85
Table 5. The percentage of H460 cell viability was determined by MTT assay after treatment with various kinds of antioxidant at 24 h	86
Table 6. ROS intensity of H460 cells after pretreatment with various kinds of antioxidant prior to 200 μM of hydrogen peroxide and determined by using DCFH ₂ -DA probe.....	87
Table 7. Specific ROS intensity of H460 cells after 200 μM of hydrogen peroxide treatment and determined by using DCFH ₂ -DA, HPF and DHE probe.....	89
Table 8. HPF intensity of H460 cells after 200 μM of hydrogen peroxide treatment with or without pretreatment with deferoxamine and determined by using HPF probe.....	90
Table 9. DCF intensity of H460/control, H460/shCav-1 and H460/Cav-1 cells after 200 μM of hydrogen peroxide treatment and determined by using DCFH ₂ -DA.....	91
Table 10. HPF intensity of H460/control, H460/shCav-1 and H460/Cav-1 cells after 200 μM of hydrogen peroxide treatment and determined by using HPF probe.....	92

	Page
Table 11. The percentage of H460/shCav-1 cell viability was determined by MTT assay after treatment with various concentration of hydrogen peroxide for 24 h.....	93
Table 12. The percentage of H460/Cav-1 cell viability was determined by MTT assay after treatment with various concentration of hydrogen peroxide for 24 h.	93
Table 13. The percentage of H460/control, H460/shCav-1 and H460/Cav-1 cell viability was determined by MTT assay after treatment with 200 μ M of hydrogen peroxide for various time point.....	94
Table 14. The percentage of H460/control, H460/shCav-1 and H460/Cav-1 cell viability was determined by MTT assay after treatment with 200 μ M of hydrogen peroxide with the presence or absence of hydroxyl radical modulators for 24 h.....	94
Table 15. DCF intensity of H460/control, H460/shCav-1 and H460/Cav-1 cells after pretreatment with deferoxamine prior to 200 μ M hydrogen peroxide and determined by using DCFH ₂ -DA	95
Table 16. DCF intensity of H460/control, H460/shCav-1 and H460/Cav-1 cells after pretreatment with ferrous sulfate prior to 200 μ M hydrogen peroxide and determined by using DCFH ₂ -DA.....	96
Table 17. HPF intensity of H460/control, H460/shCav-1 and H460/Cav-1 cells after pretreatment with deferoxamine prior to 200 μ M hydrogen peroxide and determined by using HPF probe.....	97
Table 18. HPF intensity of H460/control, H460/shCav-1 and H460/Cav-1 cells after pretreatment with ferrous sulfate prior to 200 μ M hydrogen peroxide and determined by using HPF probe....	98

LIST OF FIGURES

	Page
Figure 2.1 The structure of caveola and caveolin.....	6
Figure 2.2 Role of caveolin-1 in cancer cell progression	9
Figure 2.3 The pathway of ROS production and clearance	12
Figure 2.4 Role of hydrogen peroxide in apoptotic pathway.....	15
Figure 3.1 Experimental design of this study	24
Figure 3.2 Conceptual framework of this study	25
Figure 4.1 Effect of hydrogen peroxide on oxidative stress in H460 cells	31
Figure 4.2 Effect of various concentrations of hydrogen peroxide on cell death in H460 cells.....	33
Figure 4.3 A time-dependent study of hydrogen peroxide-induced cell death in H460 cells	35
Figure 4.4 Effect of antioxidants on H460 cell death induced by hydrogen peroxide	37
Figure 4.5 Effect of antioxidants on cell viability of H460 cells	38
Figure 4.6 Effect of antioxidants on oxidative stress induced by hydrogen peroxide	40
Figure 4.7 Superoxide anion was not the cause of oxidative stress induced by hydrogen peroxide	43
Figure 4.8 Hydroxyl radical played a predominant role in oxidative stress induced by hydrogen peroxide.....	45
Figure 4.9 Caveolin-1 expression by Western blotting	46
Figure 4.10 Caveolin-1 attenuated hydrogen peroxide-induced ROS in H460 cells	48
Figure 4.11 Caveolin-1 reduced hydroxyl radical level induced by hydrogen peroxide in H460 cells	49
Figure 4.12 Hydrogen peroxide reduced viability of H460/shCav-1 cells and caused cell apoptosis in a dose-dependent manner.....	51
Figure 4.13 Hydrogen peroxide reduced viability of H460/shCav-1 cells and caused cell apoptosis in a time-dependent manner.....	53

	Page
Figure 4.14 Hydrogen peroxide reduced viability of H460/Cav-1 cells and caused cell apoptosis in a dose-dependent manner.....	55
Figure 4.15 Hydrogen peroxide reduced viability of H460/Cav-1 cells and caused cell apoptosis in a time-dependent manner	57
Figure 4.16 Caveolin-1 attenuated oxidative damage to H460 cells.....	59
Figure 4.17 Effect of hydroxyl radical on cell death induced by hydrogen peroxide in H460/Cav-1, H460/control and H460/shCav-1 cell	60
Figure 4.18 Effect of hydroxyl radical inhibitor on cellular oxidative stress.....	63
Figure 4.19 Effect of hydroxyl radical generator on cellular oxidative stress.....	65
Figure 4.20 Effect of hydroxyl radical modulators on cellular hydroxyl radical level.....	67

LIST OF ABBREVIATIONS

%	= percentage
°C	= degree Celsius
μM	= micromolar
ANOVA	= analysis of variance
ATP	= adenosine-5'-triphosphate
Cav-1	= caveolin-1
CAT	= catalase
CO ₂	= carbon dioxide
DCFH ₂ -DA	= 2,7-dichlorofluorescein diacetate
DFO	= deferoxamine
DHE	= dihydroethidium
DMSO	= dimethyl sulfoxide
DNA	= deoxyribonucleic acid
et al.	= et alibi, and others
Fe ²⁺	= ferrous ion
Fe ³⁺	= ferric ion
FeSO ₄	= ferrous sulphate
g	= gram
GPx	= glutathione peroxidase
GSH	= glutathione
h	= hour, hours
H ₂ O ₂	= hydrogen peroxide
HPF	= 3'-(p-hydroxyphenyl) fluorescein
LC ₅₀	= 50% lethal concentration
min	= minute (s)
ml	= milliliter
mM	= millimolar
MnTBAP	= Mn(III)tetrakis (4-benzoic acid) porphyrin chloride
MTT	= 3-(4,5-dimethylthiazol-2-yl)-2,5-diphenyltetrazolium bromide
NAC	= N-acetylcysteine

NADPH	= nicotinamide adenine dinucleotide phosphate
$O_2^{\bullet -}$	= superoxide anion radical
$\bullet OH$	= hydroxyl radical
PBS	= phosphate buffer saline
PI	= propidium iodide
ROS	= reactive oxygen species
RPMI	= Roswell Park Memorial Institute's medium
S.D.	= standard deviation
SOD	= superoxide dismutase
U	= unit

CHAPTER I

INTRODUCTION

Intracellular oxidative stress has been shown to associate with cell and tissue damages in several pathological conditions (Hunt *et al.*, 1998; Madamanchi, Vendrov, and Runge, 2005; Klaunig, Kamendulis, and Hocevar, 2010). In cancers, reactive oxygen species (ROS) and their related oxidative properties have been shown to contribute carcinogenesis and progression of cancer (Arbiser *et al.*, 2002; Polytaichou, Hatziapostolou, and Papadimitriou, 2005; Klaunig *et al.*, 2010). Also, evidence has indicated their role on cancer cell survival and behavior (del Bello *et al.*, 1999; Giannoni *et al.*, 2009).

ROS found in cancer environments come from surrounding immune cells' activity and inflammation reaction (Klaunig *et al.*, 2010). In particular, several studies have documented that ROS level in the lung of lung cancer patients were highly up-regulated (Chung-man Ho *et al.*, 2001; Misthos *et al.*, 2005). It is worthy to note herein that such increase ROS may render cancer cell death since several chemotherapeutic agents including cisplatin induced cancer cell apoptosis through ROS-dependent mechanism (Wang *et al.*, 2008).

Among various kinds of ROS, hydrogen peroxide (H_2O_2) seems to garner most attentions, due to its ability to diffuse and spread for relatively long distance from originated sources compared to the other ROS likes superoxide anion and hydroxyl radical (Ohno and Gallin, 1985; Rhee *et al.*, 2005; Bienert, Schjoerring, and Jahn, 2006). Together with the fact that an increase of H_2O_2 in cancer environment has been continuously reported (Chung-man Ho *et al.*, 2001; Miguel, 2007), the notice regarding role of such ROS on cancer cell behaviors is very interesting. Although the role of H_2O_2 on cancer cell viability is in controversial either to promote cell survival or to induce cell death, many researchers believe that H_2O_2 at basal level and low concentrations could favor cell proliferation and viability (Burdon, 1995; Polytaichou *et al.*, 2005), whereas at high doses, H_2O_2 could induce cell damages through the induction of intracellular oxidative stress (Mao *et al.*, 2006; Miguel,

2007). According to this concept, cancer cells immersing in H₂O₂-rich microenvironments may possess machinery which allows them to survive.

In searching for mentioned mechanism of cancer cells in resisting ROS-mediated cell death, the cellular protein named caveolin-1 (Cav-1) was picked. Not only does such protein was intensively shown to implicate in cancer progression, but also Cav-1 was shown to mediate anoikis resistance and another aggressiveness behaviors of cancer cells (Chanvorachote *et al.*, 2009; Luanpitpong *et al.*, 2010; Rungtabnapa *et al.*, 2011). Moreover, the expression of Cav-1 has been shown to relate to poor prognosis in lung (Ho *et al.*, 2002; Moon *et al.*, 2005) and prostate cancers (Tahir *et al.*, 2001; Karam *et al.*, 2007). Cav-1 has been shown to function as scaffolding protein (Sargiacomo *et al.*, 1995) and to regulate certain proteins such as Src-like kinases, endothelial nitric oxide, and H-Ras (Li *et al.*, 1995; Garcia-Cardena *et al.*, 1996; Li, Couet, and Lisanti, 1996; Shaul *et al.*, 1996; Song *et al.*, 1996). Because there is an evidence indicating that high Cav-1 expression was frequently found in lung cancer cells (Ho *et al.*, 2002; Sunaga *et al.*, 2004), it is very interesting to evaluate whether or not Cav-1 protein could play a role in modulating cellular oxidative condition and implicate in the oxidative stress-induced cell damage.

This study aims to investigate the role of Cav-1 protein in H₂O₂-induced cell death in human lung carcinoma H460 cells which benefits the better understanding in lung cancer cell biology. These findings not only provide the knowledge of cancer cells' behavior in H₂O₂-rich microenvironment, but also give explanation about the cancer cells' reaction and related effect to ROS-generating drugs in cancer therapy.

Research questions

1. What are the effects of hydrogen peroxide on oxidative status and viability of H460 lung carcinoma cell?
2. Which species of ROS are responsible for intracellular oxidative stress and cell death induced by hydrogen peroxide treatment?
3. Whether caveolin-1 plays a role in modulating cellular oxidative stress and cell death in response to hydrogen peroxide?

Hypothesis

Due to previous studies of caveolin-1 and ROS in cancer, caveolin-1 may play a role in attenuating cellular oxidative stress induced by hydrogen peroxide and protect lung carcinoma cells from hydrogen peroxide-mediated death.

Objectives

1. To study the effect of hydrogen peroxide-induced oxidative stress in H460 lung carcinoma cell.
2. To identify species of ROS are responsible for intracellular oxidative stress and cell death induced by hydrogen peroxide.
3. To investigate the role of caveolin-1 in cellular oxidative status in response to hydrogen peroxide.

CHAPTER II

LITERATURE REVIEWS

Lung cancer

Lung cancer is the major cause of cancer deaths in the United States and worldwide (Jemal *et al*, 2010) and can be classified into two subtype namely non-small cell lung cancer (NSCLC) and small cell lung cancer (SCLC). The most common risk factor of lung cancer is smoking, however, lung cancers are also found in non-smoking patients as adenocarcinoma cell type. Smoking not only results in tissue injury, but also causes transcriptional changes in the inflammatory and apoptotic pathway. Moreover, DNA repairing ability of lung cancer patients was reduced, leading to mutation. Then, the premalignant stages occur due to inappropriate activation of proliferation and apoptotic pathway. Consequently, lung cancer develops from the early stage to the advanced stage by invasion, angiogenesis and metastasis of cancer cell. Furthermore, mutation of several cellular signaling molecules such as KRAS, p53, EGFR and HER2 are shown, in which could be used as predictive marker for prognosis of patient and sensitivity to medical therapy (Herbst, Heymach, and Lippman, 2008).

NSCLC, commonly found in lung cancer patient, can be divided into three subtypes which are squamous-cell carcinoma, adenocarcinoma, and large-cell lung cancer. According to the TNM classification for staging disease, NSCLC can be divided into 4 stages depending on progression of the cancer. Unfortunately, it is frequently diagnosed at the advanced stage with a poor prognosis (Herbst *et al.*, 2008). Treatment of NSCLC could be surgery, radiation or chemotherapy alone or in combination. Due to the fact that NSCLC is usually not very sensitive to single chemotherapy at the early stage, platinum combined with another chemotherapeutic agent becomes the standard clinical regimen used in lung cancer treatment such as cisplatin (or carboplatin) plus gemcitabine (or paclitaxel) (Rosell *et al.*, 2001). However, due to its high side effects (e.g. bone marrow suppression and

nephrotoxicity) and unsatisfied responses, targeted therapy becomes an optional choice. Targeted therapy is specific to epidermal growth factor receptor (EGFR) which is overexpressed in NSCLC patients (Fujino *et al.*, 1996; Janku, Stewart, and Kurzrock, 2010). EGFR participates in two main pathways, MAPK and PI3K/Akt pathway, which is crucial for cancer cell proliferation, invasion, angiogenesis and metastasis (Hynes and Lane, 2005). Gefitinib and erlotinib, tyrosine kinase inhibitors (TKIs), are approved to be used in NSCLC because they inhibit autophosphorylation of the receptor resulting in blockage of the downstream signaling molecules. In addition, bevacizumab, monoclonal antibodies which block angiogenesis by inhibition of vascular endothelial growth factor (VEGF) also used as standard first-line treatment in combination with platinum-based chemotherapy. New targeted therapy could improve clinical outcome of patients, however, this strategy do not completely cure cancer but only help prolong the patient's life. Importantly, another limitation of targeted therapy is their cost of treatment (Janku *et al.*, 2010).

Caveolin-1

Caveolae are flask-shaped invaginations of the plasma membrane that play an important role in vesicular trafficking and signal transduction (Carver and Schnitzer, 2003). Figure 2.1 shows the main structural proteins of caveolae which are cholesterol, glycol-sphingolipid and caveolin (Parton and Simons, 2007).

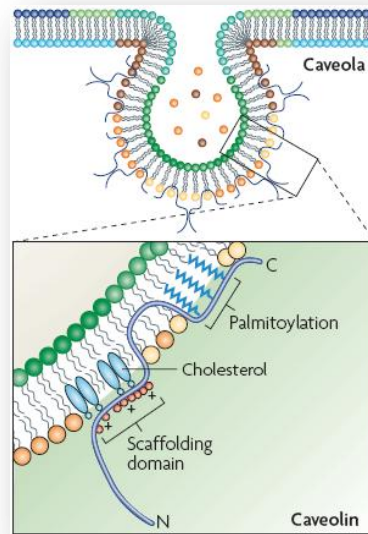


Figure 2.1 The structure of caveola and caveolin (Parton and Simons, 2007).

Three members of the caveolin family namely caveolin-1, -2, and -3 have been identified. Caveolin protein can form homo- and hetero- oligomers which bind directly to cholesterol, allowing them to insert into lipid membrane. Caveolin-1 (Cav-1), a 21 – 24 kDa protein, is found in many cell types including adipocytes, endothelial cells, and fibroblasts. It has two isoforms which are Cav-1 α and Cav-1 β . Caveolin-2, like Cav-1, is found in most non-muscle cells whereas caveolin-3 is highly expressed in muscle cells (Okamoto *et al.*, 1998). Among them, Cav-1 is the most commonly studied because it possess a domain called caveolin scaffolding domain (CSD) which interact with a variety of signaling molecules, for example, Src-like kinases (Li *et al.*, 1996), endothelial nitric oxide synthase (Garcia-Cardena *et al.*, 1996; Shaul *et al.*, 1996), H-Ras (Li *et al.*, 1996; Song *et al.*, 1996) and G-protein (Li *et al.*, 1995; Li *et al.*, 1996). These signal transduction proteins are summarized as following

- Src family tyrosine kinases

Src family kinase is a family of non-receptor tyrosine kinases which its members are c-Src, Fyn and Lyn. The Src-interacting domain of caveolin is localized to caveolin residues 61–101. The evidence show that Cav-1 suppresses the activity of

c-Src and Fyn through interaction via CSD. Cav-1 also manipulates interaction between Src kinases and integrins, a family of cell surface receptors that attach cells to the extracellular matrix and mediate signals from it. This leads to activation of ERK and cell cycle stimulation. Moreover, phosphorylation of Cav-1 by Src contribute to muscle degeneration because it localizes to focal adhesions which mediates cell adhesion and cytoskeleton rearrangement (Li *et al.*, 1996).

- endothelial nitric oxide synthase (eNOS)

eNOS is an enzyme that generates nitric oxide (NO) in blood vessels and involved in controlling vascular tone by inhibiting smooth muscle contraction and platelet aggregation. Interaction between eNOS and Cav-1 inhibits the enzymes' activity. When eNOS dissociates from Cav-1, it can access to the co-activators namely calmodulin and 90-kD heat-shock protein (HSP90) which in turn produce nitric oxide (Garcia-Cardena *et al.*, 1996; Shaul *et al.*, 1996; Carver and Schnitzer, 2003).

- G-protein

GPCRs, heterotrimeric G proteins, and G-protein-regulated effectors are localized within caveolae. For heterotrimeric G-proteins, Cav-1 interacts with the α -subunit of G-proteins via CSD. This interaction maintains G_{α} proteins in an inactive GDP-bound form, resulting in suppression of GTPase activity by inhibition of GDP/GTP exchange (Li *et al.*, 1995; Li *et al.*, 1996).

- H-Ras

H-Ras, small GTP-binding protein of the Ras superfamily, regulates cell division in response to growth factor stimulation and has been shown to be proto-oncogene. H-Ras is also found in caveolae and interacts with residues 61-101 of Cav-1. Thus, H-Ras still maintains in an inactive state (Li *et al.*, 1996; Song *et al.*, 1996).

- Phosphatidylinositol-3-kinase/protein kinase B (PI3K/PKB or Akt)

PI3K/Akt pathway regulates various cellular processes, such as cell growth, cell proliferation, cell survival and cytoskeletal rearrangement (Vivanco and Sawyers, 2002). This pathway could be activated by receptor tyrosine kinases (RTK), for example, epidermal growth factor receptor (EGFR) and insulin-like growth factor receptor (IGF-R) which are localized to caveolae (Vivanco and Sawyers, 2002). In prostate cancer, Cav-1 maintains Akt in the phosphorylated states via interaction with CSD and protein phosphatase 1 and 2A (Li *et al.*, 2003). On the other hand, caveolin overexpression activates Akt and increases cell death in HepG2 cells in response to TNF- α (Ono *et al.*, 2004). In addition, overexpression of Cav-1 in MCF-7 breast cancer cells results in higher levels of phosphorylated Akt and higher stimulation of cell proliferation and migration in response to EGF compared to normal breast cancer cells (Patel, Murray, and Insel, 2008; Agelaki *et al.*, 2009).

- Mitogen-Activated Protein Kinases (MAPK)

MAPK pathway regulates various cellular activities, such as mitosis, differentiation, proliferation and gene expression (Thomas and Haganir, 2004). Overexpression of Cav-1 has been shown to inhibit MEK/ERK signaling pathway (Patel *et al.*, 2008).

Role of Caveolin-1 in cancer

The role of Cav-1 in cancer had been investigated (Sunaga *et al.*, 2004). Some evidences concluded that Cav-1 acts as a tumor suppressor while others suggested that Cav-1 is an oncogene (Lloyd and Hardin, 2011). From the previous studies, Cav-1 levels are down-regulated in some primary human cancers and cancer cell lines such as transformed fibroblasts (Koleske, Baltimore, and Lisanti, 1995). In MCF-7 breast cancer cells, Cav-1 inhibits cell invasion, anchorage-independent growth and anoikis (Fiucci *et al.*, 2002). However, the idea that Cav-1 is a tumor suppressor remains controversial because several cancer cells express high level of Cav-1. Cav-1 level up-regulates in metastatic prostate cancer cells and relate to the poor prognosis in prostate cancer patients (Tahir *et al.*, 2001; Karam *et al.*, 2007). In human lung cancer,

the positive correlation between Cav-1 level and tumor progression has been reported as well (Ho *et al.*, 2002; Moon *et al.*, 2005). Primary lung adenocarcinoma tumors express low level of Cav-1 but in metastatic lung tumors, the higher level of Cav-1 had been shown (Ho *et al.*, 2002). Moreover, high expression of Cav-1 has been reported in non-small cell lung cancer cell lines whereas small cell lung cancer cell lines are loss of Cav-1 (Sunaga *et al.*, 2004). Cav-1 also plays a role in drug resistance. Some multidrug resistant cancer cells also express high level of Cav-1 such as SKLBL1 (vinblastine-resistant ovarian carcinoma) cells and A549-T24 (taxol-resistant lung carcinoma) cells (Yang *et al.*, 1998).

The model of Cav-1 in cancer was developed in order to explain that the level of Cav-1 is dynamic during tumor progression (Figure 2.2). Cav-1 is highly expressed in differentiated cells and controls cellular signal transduction. According to inhibition of cell proliferation, Cav-1 functions as a tumor suppressor. In the early stage, normal cells can undergo oncogenic transformation through various mechanisms. The down-regulation of Cav-1 results in increased cell proliferation and anchorage-independent cell growth. In the later stages, Cav-1 might be increased which enhances anoikis resistance and invasive properties of cancer cells, allowing them to metastasize and survive in the new environment (Carver and Schnitzer, 2003; Lloyd and Hardin, 2011).

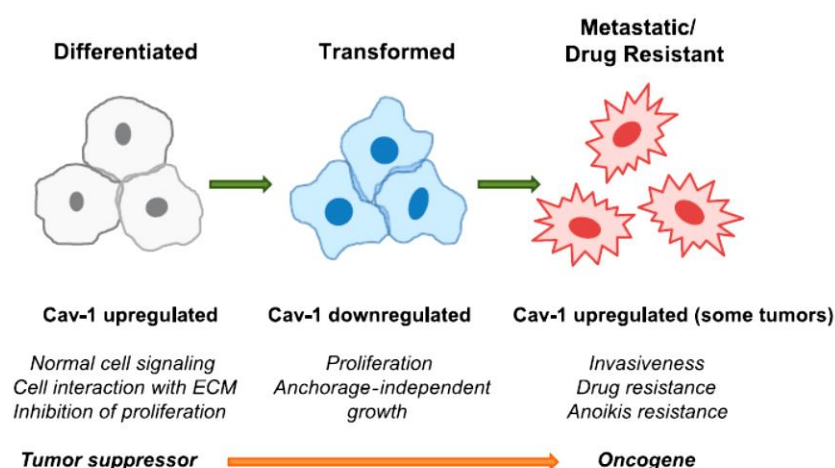


Figure 2.2 Role of caveolin-1 in cancer cell progression (Lloyd and Hardin, 2011).

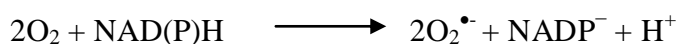
Reactive Oxygen Species (ROS)

Reactive Oxygen Species (ROS) are chemically reactive molecules containing oxygen molecule which normally produced by cellular metabolic process. Despite ROS are essential for cellular biological functions, excessive production of ROS or depletion of cellular antioxidant molecules and/or enzymes leading to oxidative stress and subsequently cellular damage. Cellular oxidative stress has been widely studied and was found to be involved in several diseases such as cancer, neurodegenerative disorder, arteriosclerosis and others (Valko *et al.*, 2004).

ROS are highly reactive because they contain unpaired electron which can be described as O₂-derived free radicals such as superoxide anion (O₂^{•-}), hydroxyl radical (OH[•]), alkoxy (RO[•]) radicals and peroxy radical (RO₂[•]) or O₂-derived non-radical species such as hydrogen peroxide (H₂O₂). In addition, reactive nitrogen species (RNS), other form of reactive molecules, such as nitric oxide (NO[•]) and peroxyxynitrite (ONOO[•]) are also presented inside the cells (Circu and Aw, 2010). Each of the ROS are described as following

- Superoxide anion (O₂^{•-})

During electron transport chain in mitochondria, approximately 3% of the oxygen molecules are converted into superoxide anion. Phase I cytochrome P-450 which detoxify foreign compounds or drugs by using oxygen to oxidize them also produces superoxide anion by electron leakage from oxidation or hydroxylation reactions. Moreover, NADPH oxidase found in phagocytes also generates superoxide anion to destroy the foreign particles (e.g. bacteria and virus) by the process called respiratory burst (Valko *et al.*, 2004).



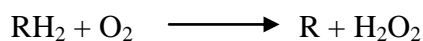
Furthermore, superoxide anion is also produced by other enzymes namely xanthine oxidase, lipoxygenase and cyclooxygenase (Valko *et al.*, 2004). Superoxide anion may interact with cellular molecules, however, it can be converted to much less reactive hydrogen peroxide (H₂O₂) by superoxide dismutase (SOD) enzyme. In

mammalian tissue, there are two forms of SOD which are copper, zinc (CuZnSOD), and manganese (MnSOD). CuSOD and ZnSOD localize in the cytosol and extracellular space while MnSOD is found in the mitochondria (Chung-man Ho *et al.*, 2001).

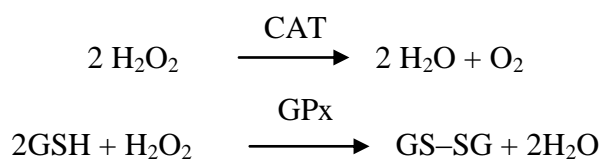


- Hydrogen peroxide (H_2O_2)

H_2O_2 can be produced by SOD (as mentioned above) or peroxisome in oxidative reaction (Valko *et al.*, 2004).



H_2O_2 diffuses and spreads for relatively long distance from the originated sources and can be removed by the antioxidant enzymes which are catalase (CAT) and glutathione peroxidase (GPx) (Chung-man Ho *et al.*, 2001).



The pathway of ROS production and clearance are summarized as shown in the figure below (Droge, 2002).

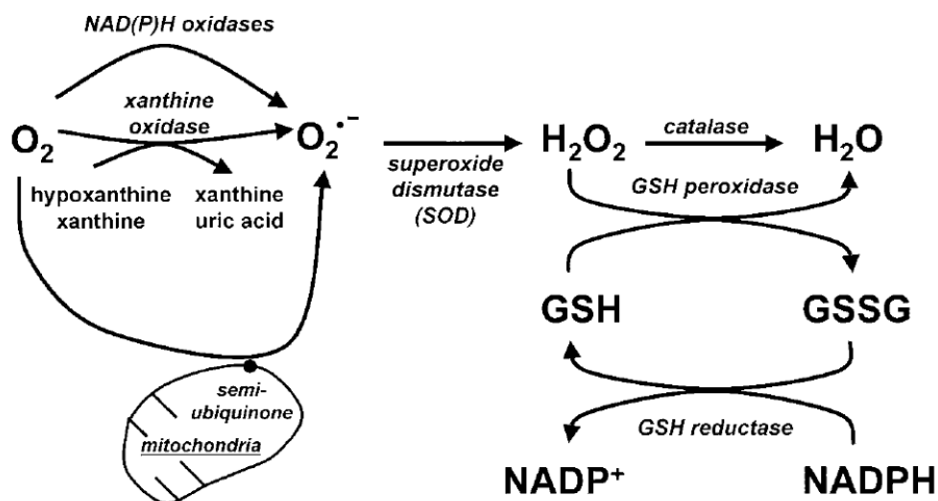
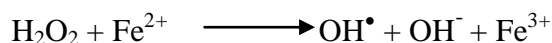


Figure 2.3 The pathway of ROS production and clearance (Droge, 2002).

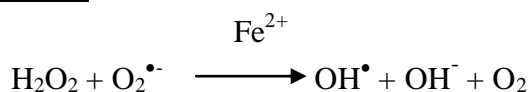
- Hydroxyl radical (OH^\bullet)

Hydroxyl radical is formed by H_2O_2 through two main reactions which are Fenton reaction and Haber-Weiss reaction. These reactions are catalyzed by ferrous ion (Fe^{2+}) or another metal ion (Valko *et al.*, 2004).

Fenton reaction

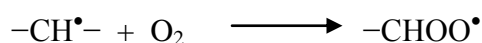
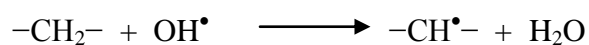


Haber-Weiss reaction

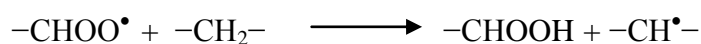


Hydroxyl radical is the most highly reactive and can react with the target near the site of its formation, however, it has very short half-life (< 1 ns) (Valko *et al.*, 2004). Hydroxyl radical causes DNA damages or strand breaks resulting from reaction with DNA bases or deoxyribosyl backbone of DNA. Besides, when hydroxyl radical attack membrane lipid, it causes lipid peroxidation and damages cell membrane (Valko *et al.*, 2004).

- Peroxyl radicals (RO₂•)



The above reactions show the step of initiation and propagation of peroxyl radicals. When a hydrogen atom is abstracted from methylene group by hydroxyl radicals, the initial step begins. Then, peroxyl radical is produced under aerobic condition. Moreover, peroxyl radicals can abstract hydrogen atom from another molecules and subsequently begins the process of propagation (Gueraud *et al.*, 2010).



Peroxyl radicals can be found in various kinds of molecule such as cholesterol derivatives and fatty acid. Peroxyl radicals are associated with lipid peroxidation, DNA damage and protein modification (Valko *et al.*, 2004).

Cellular target of ROS

ROS can attack protein and cause protein fragmentation by oxidation of amino acid residue, protein-protein cross-links and oxidation of protein backbone. Besides, protein is indirectly damaged by lipid peroxidation leading to abnormal structure and function of the protein such as enzymes, receptors and signaling molecules. (Berlett and Stadtman, 1997; Valko *et al.*, 2004).

Phospholipid of cell membrane is an excellent target of ROS because of the polyunsaturated fatty acid which contains multiple double bonds. In the initial step, lipid peroxidation starts with generation of lipid radical when lipid is oxidized by ROS. Lipid radical reacts with the oxygen molecule and become lipoperoxyl radical (LOO•). Next, the step of propagation is followed by the reaction between lipid and lipoperoxyl radical which in turns yield lipid hydroperoxide (LOOH). Finally, the reaction stops by the combination of radical species to non-radical species (Valko *et al.*, 2004; Gueraud *et al.*, 2010). Lipid peroxidation causes change in cell membrane permeability and fluidity leading to cellular damage. Previous studies had shown that

lipid peroxidation is associated with some pathophysiological states and diseases such as atherosclerosis, inflammation and cancer (Madamanchi *et al.*, 2005; Klaunig *et al.*, 2010; Negre-Salvayre *et al.*, 2010).

ROS cause DNA damage in various forms such as DNA-protein crosslink, DNA strand break, DNA bases modification, chromosome abnormalities and others. As a result of misrepairing of DNA damage, mutation occurs resulting in carcinogenesis (Klaunig *et al.*, 2010). Oxidative damage by ROS has been shown to stimulate signal transduction pathway such as Ras pathway which modulate gene expression for cell growth, cell proliferation and tumor promotion (Valko *et al.*, 2004). Hydroxyl radical, highly reactive ROS, can react with all DNA molecules. Previous study has showed that hydroxyl radical can activate oncogenes such as K-Ras and C-Raf-1 and has been reported to inhibit cell's ability to repair damaged DNA (Jackson, 1994). Moreover, hydroxyl radical causes OH-adduct radical when add to the double bond of DNA. In addition, peroxy radical is also formed by this reaction (Valko *et al.*, 2004).

Oxidative stress modulates apoptotic or necrotic cell death (Chandra, Samali, and Orrenius, 2000; Miguel, 2007; Lin *et al.*, 2010). Apoptosis is characterized by chromatin condensation, DNA fragmentation and formation of apoptotic bodies while necrosis is characterized by cell membrane rupture in response to severe stress leading to releasing of cells' content into the extracellular space. Necrosis results in inflammation of neighboring cells and tissues while apoptosis does not.

There are two main proposed mechanisms for apoptosis, the intrinsic and extrinsic pathway. The extrinsic pathway is involved in "death receptor", Fas or TNF-R. Caspases play an important role in this pathway by serial activation of these enzymes when death ligand binds to its receptor (Nicholson and Thornberry, 1997; DeLong, 1998; Droge, 2002). Instead of association with cell surface receptor, the intrinsic pathway or the mitochondrial pathway relies on pro-apoptotic proteins such as Bax, Bad and Bak. Pro-apoptotic protein causes the release of cytochrome c from the mitochondria, followed by serial activation of caspases, leading to apoptosis (Nicholson and Thornberry, 1997). However, ROS-induced apoptosis can switch into

necrosis by the depletion of cellular ATP resulting from ROS-induced mitochondrial dysfunction (Leist *et al.*, 1999; Chandra *et al.*, 2000). Another mechanism is oxidation of the thiol group in the caspases active site which in turns inactivate the enzyme (Nobel *et al.*, 1997; Chandra *et al.*, 2000).

H_2O_2 induces apoptosis by up-regulation of the Fas-FasL system. Then, the downstream caspases are activated as shown in Figure 2.4. Moreover, H_2O_2 also disrupts the mitochondrial membrane potential and triggers the release of cytochrome c from mitochondria into the cytosol. Then, cytochrome c activates caspase enzyme by forming apoptosome with Apaf-1 (apoptotic protease activating factor 1). In addition, H_2O_2 directly activates transcription factor in the nucleus such as p53, AP-1 and NF- κ B and modulates gene transcription of survival- or death-regulated proteins (Chandra *et al.*, 2000).

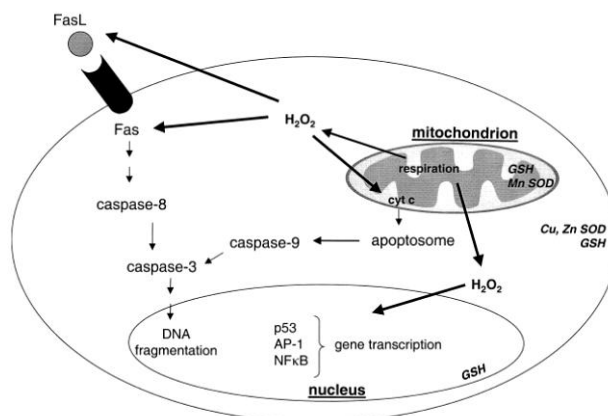


Figure 2.4 Role of hydrogen peroxide in apoptotic pathway (Chandra *et al.*, 2000).

Role of hydrogen peroxide as a signaling molecule

In normal physiological state, H_2O_2 functions as a signaling molecule in both intracellular and intercellular signal (Bienert *et al.*, 2006). H_2O_2 has longer half-life (1 ms in lymphocytes) and is more stable than other ROS. (The half-life of superoxide anion is 1 μ s while hydroxyl radical is less than 1 ns) (Reth, 2002). Moreover, it can diffuse through cell membrane (Bienert *et al.*, 2006). Due to its properties, previous studies showed that H_2O_2 plays a role as an intercellular signaling molecule. Human epidermal keratinocytes produce H_2O_2 to modulate melanogenesis

of nearby melanocytes (Pelle *et al.*, 2005). Furthermore, myofibroblasts induce lung epithelial cell death by releasing H₂O₂ (Waghray *et al.*, 2005). For intracellular signaling, H₂O₂ can change intracellular level of Ca²⁺ in several cell types and activates MAPK in response to osmotic stress or other stimuli (Bienert *et al.*, 2006). In addition, H₂O₂ also play a crucial role in apoptotic cell death (Chandra *et al.*, 2000) as mentioned above.

Role of hydrogen peroxide in cancer and chemotherapeutic agents

The excessive production of ROS results in oxidative stress and cause carcinogenesis (Klaunig *et al.*, 2010). Previous studies indicated that H₂O₂ plays an important role in cancer because there are up-regulation of the enzyme SOD which generates H₂O₂ in cancer cells (Chung-man Ho *et al.*, 2001). Furthermore, H₂O₂-induced cell proliferation, invasion, metastasis, angiogenesis and apoptosis resistance have been reported (Polytarchou *et al.*, 2005; Miguel, 2007; Rungtabnapa *et al.*, 2011). On the contrary, up-regulation of catalase, the enzyme that detoxifies H₂O₂, inhibits cell proliferation and triggers cell apoptosis in some cell types (Brown *et al.*, 1999; Zanetti, Katusic, and O'Brien, 2002). H₂O₂ also activates HIF-1 (hypoxia-inducible factor 1) which is responsible for cancer cell invasion, metastasis, angiogenesis and apoptosis resistance. Overexpression of HIF-1 has been found in various cancer cells and is related to the increased mortality of cancer patients (Miguel, 2007). Moreover, carcinogenesis induced by H₂O₂ can be reverse by catalase and glutathione peroxidase. These obviously suggested the role of H₂O₂ in promoting tumor. In contrast, several studies showed the role of H₂O₂ in killing cancer cells (Burdon, 1995; Mao *et al.*, 2006; Miguel, 2007). These different effects of H₂O₂ depend on cellular concentration. H₂O₂ at low concentration functions as a signaling molecule while at high concentration, H₂O₂ causes oxidative stress and cell damage (Miguel, 2007).

According to the mechanisms of some chemotherapeutic agents such as cisplatin (Wang *et al.*, 2008) and doxorubin (Gewirtz, 1999) which kill cancer cell through ROS production, ROS are widely studied in cancer research as another strategy of cancer treatment. Cisplatin which commonly used in various kinds of

tumor, induces cancer cell damage by two main mechanisms. First mechanism is the formation of DNA-adduct. Cisplatin binds to DNA resulting in intra- and interstrand cross-links in DNA (Alan, 1987). Then, DNA replication and transcription are blocked causing cell-cycle arrest and cell death (Wang and Lippard, 2005). Another mechanism is ROS generated by cisplatin and contribute to cellular oxidative damage (Brozovic *et al.*, 2010). In lung carcinoma cell, cisplatin generated H_2O_2 which induced cell apoptosis (Wang *et al.*, 2008). Indeed, cisplatin decreases mitochondrial membrane potential and disrupts mitochondrial function through interruption of electron transfer in respiratory chain leading to excessive ROS production (Kruidering *et al.*, 1997; Brozovic *et al.*, 2010).

Doxorubicin, the anthracycline antibiotics, has various mechanism of action such as formation of DNA adduct, inhibition of macromolecule synthesis and interference with helicase and Topoisomerase II enzyme (Gewirtz, 1999). Doxorubicin also generates ROS because its structure. When quinone ring attacked by the unpaired electron, it will converted into semiquinone. This structure acts like the free radical and then interact with DNA or membrane phospholipid, leading to DNA damage and lipid peroxidation, respectively. Moreover, semiquinone can interact with oxygen molecule to yield ROS such as superoxide anion, H_2O_2 and hydroxyl radical (Bates and Winterbourn, 1982; Gewirtz, 1999).

According to oxidative stress induced by chemotherapeutic drugs mentioned above, the idea of using H_2O_2 as a mediator for killing cancer cells had been discussed (Miguel, 2007). H_2O_2 -generating drug have been developed as an alternative choice for cancer therapy (Fang, Seki, and Maeda, 2009). Interestingly, the concentration used for killing cancer cells is lower than normal cells (Chen *et al.*, 2005). However, the selectivity of H_2O_2 for killing cancer cell has not been explained clearly. H_2O_2 -generating enzyme such as xanthine oxidase and D-amino acid oxidase, have been developed as “oxidation therapy” so far. Macromolecules (e.g. polymer) or nanoparticles are used to transport H_2O_2 -generating enzymes to the target. Nevertheless, usage of H_2O_2 for killing tumor in cancer patient is still controversial because of consideration between risk and benefit. According to dose-dependent killing effect, low dose of H_2O_2 will trigger the aggressiveness of cancer cell if the

amount of H_2O_2 given cannot reach the targeted tumor high enough (Fang *et al.*, 2009). Furthermore, concerning about surrounding normal cells near tumor site, direct administration of H_2O_2 to the targeted tumor may be inappropriate and unsafe (Miguel, 2007).

Studies of ROS and Caveolin-1 in lung cancer cells

The role of ROS in migration and invasion of lung carcinoma cells had been investigated. Different species of ROS affect level of Cav-1 differently. Luanpitpong and colleagues showed that Cav-1 is down-regulated by superoxide anion and H_2O_2 resulting in the inhibition of cell migration and invasion. On the other hand, hydroxyl radical up-regulate Cav-1 level and increases cancer cell migration and invasion. Furthermore, the ubiquitin-proteasome pathway participates in Cav-1 degradation in response to superoxide anion and H_2O_2 (Luanpitpong *et al.*, 2010).

Rungtabnapa *et al.* reported that Cav-1 acts as a negative regulator of anoikis in lung carcinoma cell. Down-regulation of Cav-1 occurs after cell detachment, while ROS (H_2O_2 and hydroxyl radical) up-regulate. H_2O_2 plays a major role in preventing anoikis. Treatment of catalase promotes Cav-1 down-regulation and anoikis after cell detachment. Catalase also stimulates ubiquitination and proteasome degradation of Cav-1 during anokis. This study suggests that H_2O_2 regulates Cav-1 level during anoikis (Rungtabnapa *et al.*, 2011).

The role of Cav-1 in drug response has been studied by Pongjit and Chanvorachote. They reported that overexpression of Cav-1 enhanced cisplatin-induced lung carcinoma cell death while knockdown Cav-1 cells decrease cisplatin susceptibility. Moreover, the level of superoxide anion in response to cisplatin in Cav-1 overexpressed cell is higher when compared to normal cell. As a result of superoxide anion, Cav-1 sensitizes cisplatin-induced cell death (Pongjit and Chanvorachote, 2011).

Khan *et al.* reported the relationship between EGFR and Cav-1 in response to H_2O_2 -induced oxidative stress. H_2O_2 had been shown to activate EGFR leading to endocytosis via clathrin-coat pits and receptor degradation by lysosome. Signaling

molecules which participate in cell proliferation such as Akt and ERK1/2 (extracellular signal-regulated kinase 1/2) are also prolonged activated (Ravid *et al.*, 2004). This study showed that EGFR was co-localized with Cav-1 at the membrane of A549 lung carcinoma cells. When EGFR is activated by H₂O₂, Src kinase is activated. Consequently, Tyr-14 of Cav-1 is hyperphosphorylated in a Src dependent manner resulting in trafficking of EGFR and prolonged signaling (Khan *et al.*, 2006).

CHAPTER III

MATERIALS AND METHODS

Materials

1. Chemicals and Reagents

N-acetylcysteine (NAC), reduced glutathione (GSH), sodium pyruvate, hydrogen peroxide (H₂O₂), catalase (CAT), Mn(III)tetrakis(4-Benzoic acid)porphyrin chloride (MnTBAP), propidium iodide (PI), Hoechst 33342, 2',7'-dichlorofluorescein diacetate (DCFH₂-DA), 3-(4,5-dimethylthiazol-2-yl)-2,5-diphenyltetrazolium bromide (MTT), ferrous sulfate and deferoxamine (DFO) were obtained from Sigma Chemical, Inc. (St. Louis, MO); dihydroethidium (DHE) and 3'-(p-hydroxyphenyl) fluorescein (HPF) were purchased from Molecular Probes, Inc (Eugene, OR); Antibody for caveolin-1 and peroxidase-conjugated secondary antibody were obtained from Abcam (Cambridge, MA); The transfecting agent Lipofectamine 2000 was obtained from Invitrogen (Carlsbad, CA).

2. Equipments

Laminar flow cabinet, carbon dioxide incubator, autopipette: 2-10 µl, 10-100 µl, 20-200 µl and 200-1,000 µl, pipette tips for 2-10 µl, 10-100 µl, 20-200 µl, and 200-1,000 µl, cell culture plate: 96-well and 6-well (Nunc), conical tube: 15 ml and 50 ml (Neptune) , bottle: 100 ml, 250 ml, 500 ml, and 1,000 ml (Duran) disposable pipette: 1 ml and 5 ml, pH meter, fluorescence microplate reader (SpectraMax M5, Molecular Devices Corp., Sunnyvale, CA, USA), fluorescence microscope (Eclipse Ti-U, Nikon, Tokyo, Japan).

Methods

1. Sample preparation

Various concentration of hydrogen peroxide was prepared by diluting in phosphate buffer saline (PBS).

2. Cell culture

Human lung cancer H460 cells were obtained from the American Type Culture Collection (Manassas, VA). Cells were cultivated in RPMI 1640 supplemented with 10% fetal bovine serum, 2 mM L-glutamine, and 100 units/mL penicillin/streptomycin in a 5% CO₂ environment at 37°C. The Cav-1 overexpressed (H460/Cav-1) and Cav-1 knockdown (H460/shCav-1) cells were established by transfection of the H460 cells with Cav-1 plasmid obtained from the American Type Culture Collection (Manassas, VA) and Cav-1 knockdown plasmid shRNACav-1 obtained from Santa Cruz Biotechnology (Santa Cruz, CA), respectively.

3. ROS detection

Intracellular ROS were determined by using a fluorescent probe 2',7'-dichlorofluorescein diacetate (DCFH₂-DA), superoxide anion was determined by dihydroethidium (DHE), and hydroxyl radical was determined by 3'-(p-hydroxyphenyl) fluorescein (HPF). Cells were incubated with 10 μM of DCFH₂-DA, HPF, or DHE for 30 min at 4°C. Then, they were washed and immediately analyzed for fluorescence intensity by fluorescence microplate reader using a 480-nm excitation beam and a 530-nm band-pass filter for detecting DCF fluorescence, using a 490-nm excitation beam and a 515-nm band-pass filter for HPF, or using a 488-nm excitation beam and a 610-nm band-pass filter for DHE. The fluorescence intensity was also visualized under fluorescence microscope.

4. Cytotoxicity assay

To determine H₂O₂-mediated cytotoxicity, cell viability was determined by MTT assay which measured ability of the cells to reduce 3-(4,5-Dimethylthiazol-2-yl)-2,5-diphenyltetrazolium bromide (yellow) to purple formazan crystal by using mitochondrial reductase enzyme. After specific treatment, cells in 96-well plates were incubated with 100 μl of 500 μg/ml MTT solution for 4 h at 37 °C. Then, MTT solution was removed and 100 μl of 99.9% DMSO was added to dissolve the formazan crystal. The intensity of formazan product was measured at 570 nm using a

microplate reader. All analyses were performed in at least three independent experiment. Percentage of cell viability was calculated as follow

$$\text{Cell viability (\%)} = \frac{A_{570} \text{ of treatment}}{A_{570} \text{ of control}} \times 100$$

5. Apoptosis and necrosis assay

Apoptotic and necrotic cell death were determined by Hoechst 33342 and propidium iodide (PI) co-staining assay. After specific treatments, cells were incubated with 10 μ M of the Hoechst and 5 μ g/mL PI dye for 30 min at 37°C. The apoptotic cells were shown by having condensed chromatin and/or fragmented nuclei while necrotic cells were stained with PI dye. Cells were visualized using a fluorescence microscope.

6. Plasmid and transfection

The Cav-1 overexpressed (H460/Cav-1) and Cav-1 knockdown (H460/shCav-1) cells were established by transfection of the H460 cells with Cav-1 plasmids and Cav-1 knockdown plasmid shRNACav-1, respectively. Briefly, H460 cells were cultured on 24-well plate in until they reached 60% confluence. Cells were transfected with 15 μ l of Lipofectamine 2000 reagent and 2 μ g of Cav-1, shRNA-Cav-1 or mock control plasmids. After 16 h, the medium was replaced with culture medium containing 10% fetal bovine serum. Approximately 3 days after the beginning of transfection, the single cell suspensions were plated onto 75-ml culture flasks and cultured for 60 days with 400 μ g/ml of Geneticin. The expression of Cav-1 protein in the transfectants was quantified by Western blot analysis.

7. Western blot

Cell lysates were obtained by incubating the cells in ice-cold lysis buffer containing 20 mM Tris-HCl (pH 7.5), 0.5% Triton X-100, 150 mM sodium chloride, 10% glycerol, 1 mM sodium orthovanadate, 50 mM sodium fluoride, 100 mM phenylmethylsulfonyl fluoride, and a protease inhibitor cocktail (Roche Molecular

Biochemicals, Indianapolis, IN, USA) for 60 min on ice. Protein content was determined using the Bradford method (Bio-Rad Laboratories, Hercules, CA, USA) and an equal amount of proteins of each sample (30 μ g) were heated at 95°C for 5 min with Laemmli loading buffer. Then, the lysates were loaded on 10% SDS-polyacrylamide gel electrophoresis. After separation, proteins were transferred onto 0.45 μ m nitrocellulose membranes (Bio-Rad). The transferred membranes were blocked for 1 h in 5% non-fat dry milk in TBST (25 mM Tris-HCl (pH 7.5), 125 mM NaCl, 0.05% Tween 20). Membranes were washed twice with TBST for 7 min and incubated with the anti-Cav-1 antibodies at 4°C for 10 h. Then, Membranes were washed twice with TBST for 7 min and incubated with horseradish peroxidase-coupled isotype-specific secondary antibodies for 2 h at room temperature. The immune complexes were detected by enhanced chemiluminescence substrate (Supersignal West Pico; Pierce) and normalized to the level of β -actin protein.

8. Statistical Analysis

The mean of data from at least three independent experiments were normalized to the non-treated control. Statistical differences between means were determined using an analysis of variance (ANOVA) and post hoc test (Tukey's test) at a significance level of $p < 0.05$, and presented as the mean \pm SD.

9. Experimental designs

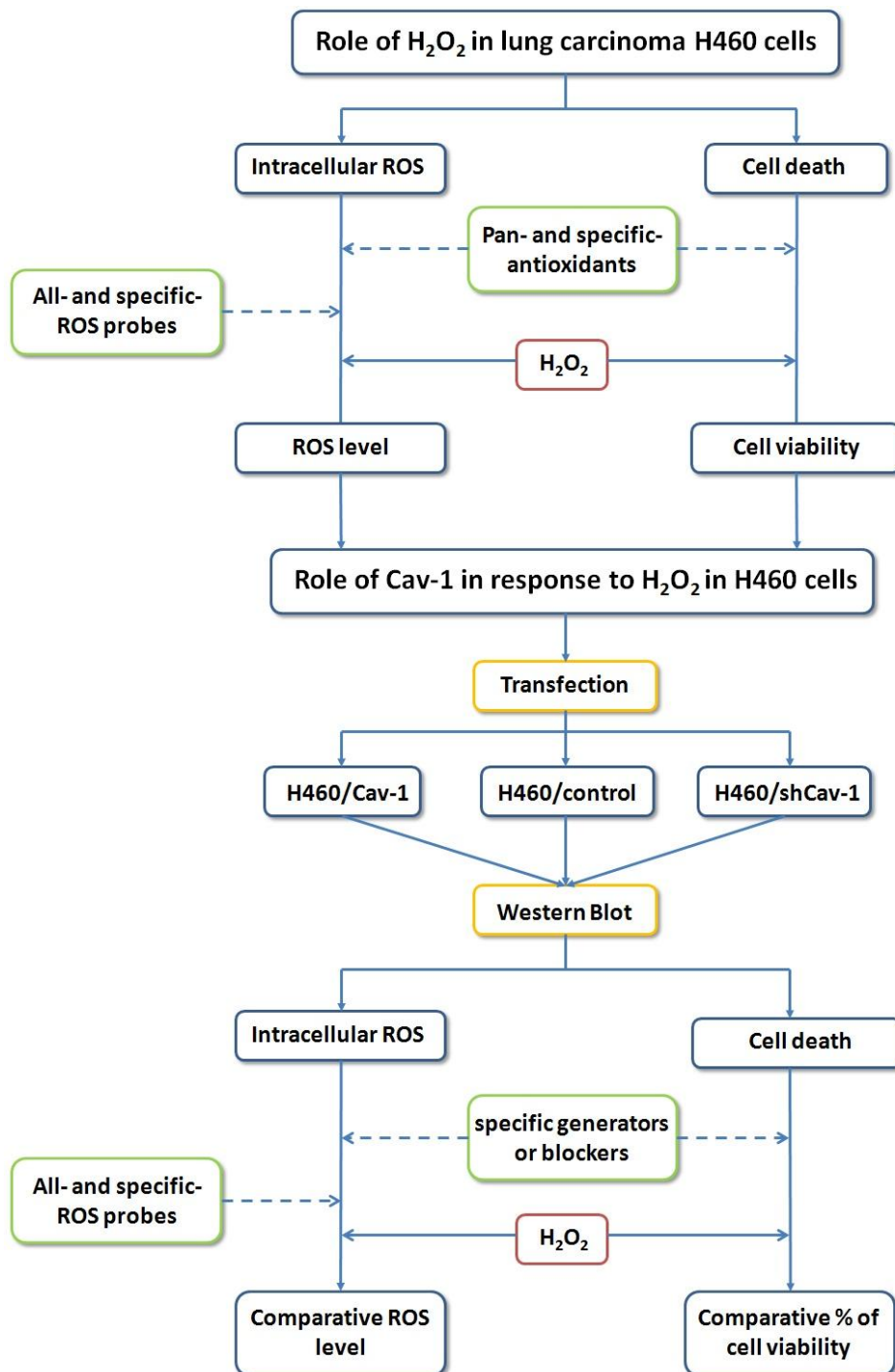


Figure 3.1 Experimental design of this study

9.1. Conceptual framework

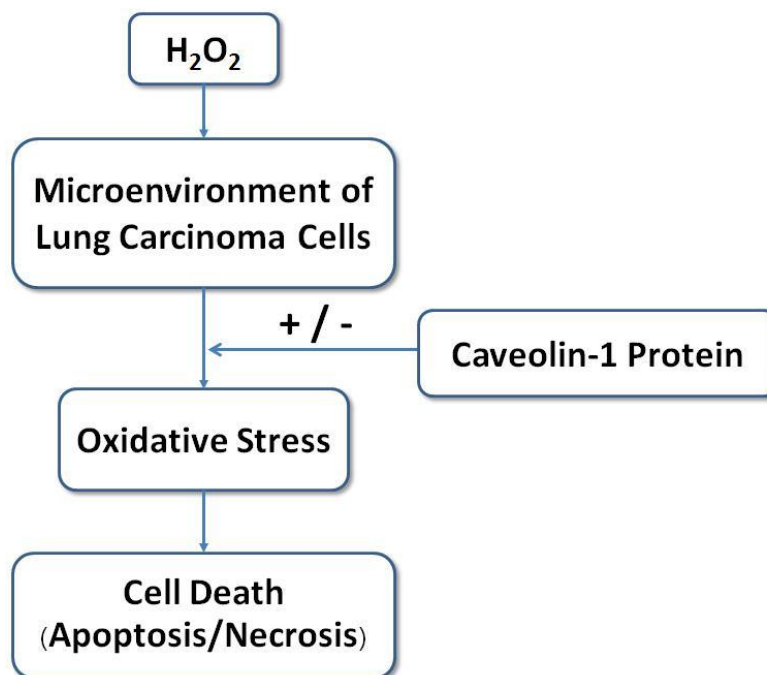


Figure 3.2 Conceptual framework of this study

9.2. Effect of hydrogen peroxide in lung carcinoma cells

9.2.1. Hydrogen peroxide induced oxidative stress in human lung carcinoma H460 cells

To investigate the effects of hydrogen peroxide in lung carcinoma cells, H460 cells were seeded at 8×10^3 cells per well in a 96-well plate overnight. Next day, medium were removed and cells were incubated with medium containing $10 \mu\text{M}$ of DCFH₂-DA at 4°C for 30 min. Next, medium were removed and replaced by medium containing various dose of hydrogen peroxide (0, 10, 50, 100 and $200 \mu\text{M}$). Intracellular ROS level was determined immediately by fluorescence microplate reader using a 480-nm excitation beam and a 530-nm band-pass filter for detecting DCF fluorescence from 0 to 6 h after treatment. Cellular DCF signals were also determined by fluorescence microscope.

9.2.2. Hydrogen peroxide induced cell death in lung carcinoma H460 cell

Cell death induced by hydrogen peroxide was characterized in H460 cells. The lethal concentration fifty (LC₅₀) was determined in order to obtain the optimum concentrations of hydrogen peroxide used for further experiments. Cells were seeded at 8×10^3 cells per well in a 96-well plate overnight. Next day, cells were treated with various concentrations of hydrogen peroxide (0, 10, 50, 100, 200 μ M) and incubated for 24 h. Then, cell viability was investigated by MTT assay. Apoptotic and necrotic cell death was also detected by Hoechst 33342 and propidium iodide (PI) co-staining assay.

For time-dependent study, cells were incubated with hydrogen peroxide (LC₅₀) for various time points (0, 3, 6, 12, 24 h). After that, cell viability was observed by MTT assay. Hoechst 33342 and propidium iodide (PI) co-staining assay was also used to detect apoptotic and necrotic cell death.

9.2.3. Effect of antioxidants on H460 cell death induced by hydrogen peroxide

Cells were seeded at 8×10^3 cells per well in a 96-well plate overnight. Next day, cells were pretreated with pan-antioxidants such as *N*-acetylcysteine (NAC) and reduced glutathione (GSH) or specific antioxidants which were H₂O₂-scavenger (catalase and sodium pyruvate), hydroxyl radical inhibitor (deferoxamine) and superoxide anion scavenger (MnTBAP) for 1 h and followed by hydrogen peroxide (LC₅₀). After incubation for optimum time, cell viability was investigated by MTT assay. Hoechst 33342 and propidium iodide (PI) co-staining assay was also used to detect apoptotic and necrotic cell death.

9.2.4. Effect of antioxidants on cellular oxidative stress induced by hydrogen peroxide in H460 cells

Cells were seeded at 8×10^3 cells per well in a 96-well plate overnight. Next day, cells were pretreated with pan- or specific antioxidants for 1 h. Then,

medium were removed and replaced by medium containing 10 μM of DCFH₂-DA for 30 min at 4°C. After that, cells were washed to remove excess probe and medium containing hydrogen peroxide (LC₅₀) were added. Intracellular ROS level was determined immediately by fluorescence microplate reader from 0 to 3 h. Fluorescence microscope was also used to detect cellular DCF signals.

9.2.5. Hydroxyl radical was responsible for hydrogen peroxide-mediated oxidative stress in H460 cells

To confirm which species were responsible for intracellular oxidative stress, cells were seeded at 8×10^3 cells per well in a 96-well plate overnight. Next day, medium were removed and cells were incubated with medium containing 10 μM of DCFH₂-DA, HPF (hydroxyl radical probe), or DHE (superoxide anion probe) at 4 °C for 30 min. Next, medium was removed and replaced by medium containing hydrogen peroxide (LC₅₀). Intracellular ROS, hydroxyl radical or superoxide anion levels were determined immediately by fluorescence microplate reader from 0 to 3 h. Cellular fluorescence signals were also determined by fluorescence microscope.

To find out whether hydroxyl radical was the main ROS leading to the oxidative stress induced by hydrogen peroxide, H460 cells were pretreated or non-pretreated with deferoxamine, hydroxyl radical blocker, for 1 hr. Then, HPF (hydroxyl radical probe) was added and incubated at 4 °C for 30 min. Next, medium was removed and replaced by medium containing hydrogen peroxide (LC₅₀). Intracellular hydroxyl radical was determined by fluorescence microplate reader from 0 to 3 h.

9.3. Effect of caveolin-1 in response to hydrogen peroxide in lung carcinoma H460 cells

9.3.1. Evaluation for caveolin-1 (Cav-1) expression levels

To study the effects of caveolin-1 (Cav-1) on cellular oxidative stress and cell death induced by hydrogen peroxide, Cav-1 overexpressed H460 (H460/Cav-1) cells, mock control transfected H460 (H460/control) cells and Cav-1 down-

regulated H460 (H460/shCav-1) cells were generated by stably transfecting H460 cells with Cav-1 overexpressing plasmid, mock control plasmid or Cav-1 shRNA plasmid, respectively. After selection, each cell type (H460/Cav-1, H460/control and H460/shCav-1 cells) was seeded at density of 1×10^5 cells per well onto a 6-well plate. Next day, cells were subjected to western blot analysis and evaluated for Cav-1 expression levels. The level of β -actin protein of each cell was also evaluated as control. The band intensity was quantified by using analyst/PC densitometry software (Bio-Rad).

9.3.2. Hydrogen peroxide induced oxidative stress in H460/Cav-1 and H460/shCav-1 cells

H460/Cav-1, H460/control and H460/shCav-1 cells were seeded at 8×10^3 cells per well in a 96-well plate overnight. Next day, medium were removed and cells were incubated with medium containing $10 \mu\text{M}$ of DCFH₂-DA or HPF at 4°C for 30 min. After that, the excess probe were removed and replaced by medium containing hydrogen peroxide (LC_{50} of H460 cells). Intracellular ROS and hydroxyl radical levels were determined immediately by fluorescence microplate reader from 0 to 3 h and cellular fluorescence signals were also determined by fluorescence microscope.

9.3.3. Hydrogen peroxide induced H460/Cav-1 and H460/shCav-1 cell death

H460/Cav-1, H460/control and H460/shCav-1 cells were seeded at 8×10^3 cells per well in a 96-well plate overnight. Next day, cells were treated with various concentrations of hydrogen peroxide (0, 10, 50, 100 and $200 \mu\text{M}$) and incubated for 24 h. Then, cell viability was investigated by MTT assay. Hoechst 33342 and propidium iodide (PI) co-staining assay was also used to detect apoptotic and necrotic cell death.

In order to compare time-dependent effect of hydrogen peroxide to normal H460 cells, H460/Cav-1, H460/control and H460/shCav-1 cells were treated with hydrogen peroxide (LC_{50} of H460 cells) for various time point (0, 3, 6, 12, 24 h).

Then, cell viability was investigated by MTT assay. Hoechst 33342 and propidium iodide (PI) co-staining assay was also investigated.

9.3.4. Effect of hydroxyl radical modulators on viability of H₂O₂-treated cells

H460/Cav-1, H460/control and H460/shCav-1 cells were seeded at 8×10^3 cells per well in a 96-well plate overnight. Next day, each cell was pre-treated with hydroxyl radical generator (ferrous sulfate) or blocker (deferoxamine). After 1 h, cells were treated with hydrogen peroxide (LC₅₀ of H460 cells) for optimum time. Cell viability of each cell was observed by MTT assay. Hoechst 33342 and propidium iodide (PI) co-staining assay was also used to detect apoptotic and necrotic cell death.

9.3.5. Effect of hydroxyl radical modulators on cellular ROS and hydroxyl radical level

H460/Cav-1, H460/control and H460/shCav-1 cells were seeded at 8×10^3 cells per well in a 96-well plate overnight. Next day, each cell was pre-treated with hydroxyl radical generator (ferrous sulfate) or blocker (deferoxamine) for 1 h and followed by medium containing 10 μ M of DCFH₂-DA or HPF at 4°C for 30 min. After that, the excess probe were removed and replaced by medium containing hydrogen peroxide (LC₅₀ of H460 cells). Intracellular ROS and hydroxyl radical were determined immediately by fluorescence microplate reader from 0 to 3 h and cellular fluorescence signals were also determined by fluorescence microscope.

CHAPTER IV

RESULTS

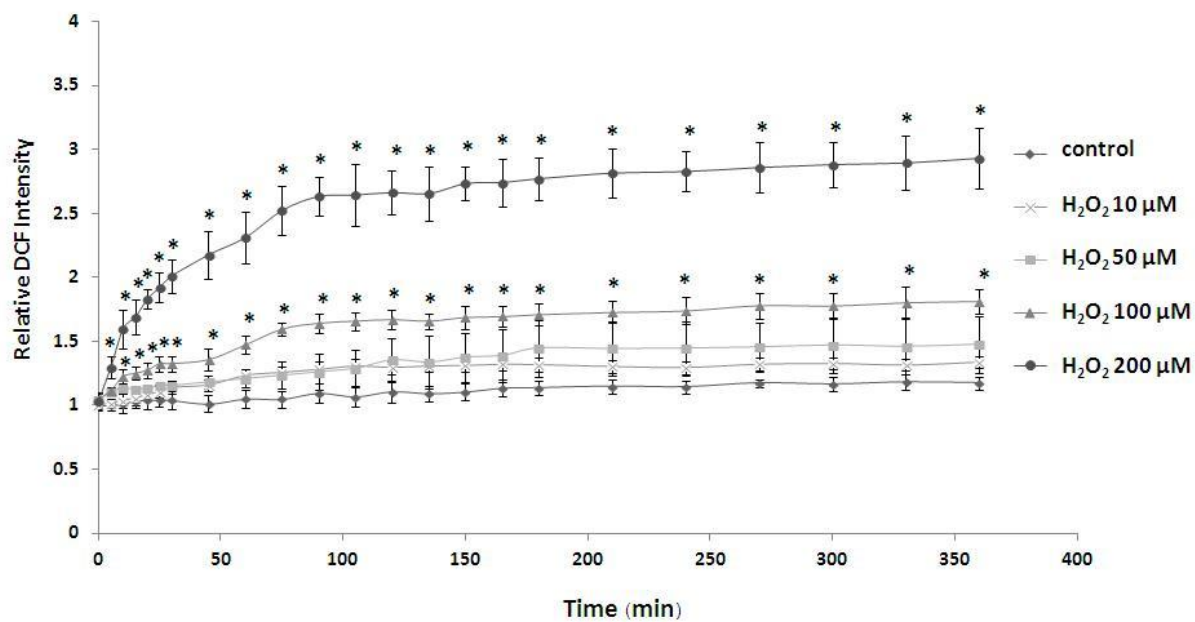
1. Hydrogen peroxide induced oxidative stress and cell death in human lung carcinoma H460 cells and hydroxyl radical was the main ROS which was responsible for oxidative damage induced by hydrogen peroxide.

1.1. Effect of hydrogen peroxide on oxidative stress in lung carcinoma cells.

First, to investigate the effect of hydrogen peroxide on oxidative stress in lung carcinoma cells, H460 cells were treated with various concentrations of hydrogen peroxide (0, 10, 50, 100 and 200 μM). Then, intracellular ROS were determined by DCFH₂-DA, ROS probe using fluorescence microplate reader from 0 to 6 h after hydrogen peroxide treatment. In addition, DCF signals also visualized by using fluorescence microscope to confirm the rising intracellular ROS.

The results showed that 10-200 μM hydrogen peroxide increased intracellular ROS in a dose-dependent manner from 0 to 6 h. Hydrogen peroxide at the concentration of 100 μM caused significantly increase in ROS level since 15 minutes after treatment compared to non-treated control cells while 200 μM hydrogen peroxide resulted in significantly higher ROS than control cells since 5 minute. Moreover, the intracellular ROS were found to be saturated after hydrogen peroxide treatment for 3 h. As a result of these characteristics, intracellular ROS would be observed from 0 to 3 h in further experiments.

A



B

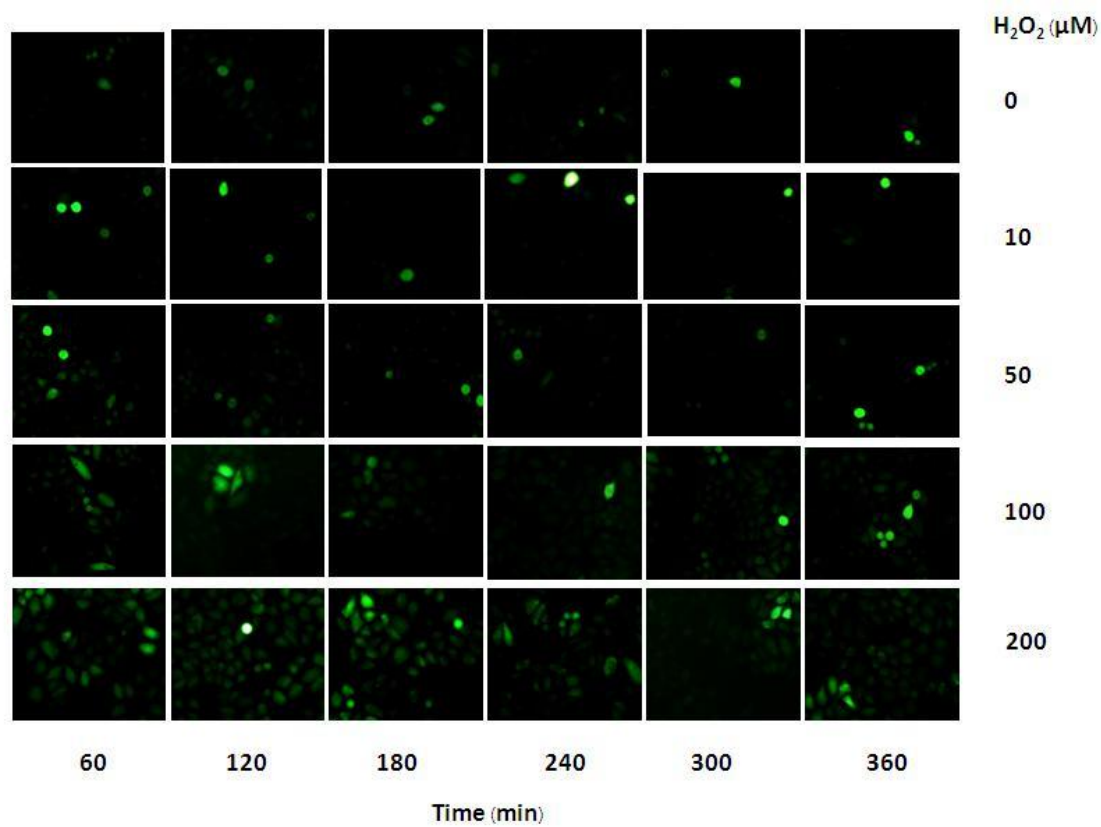


Figure 4.1 Effect of hydrogen peroxide on oxidative stress in H460 cells. A) Cells were treated with various concentrations of hydrogen peroxide (0, 10, 50, 100, and 200 μM). Intracellular ROS were determined by using DCFH₂-DA probe and measured from 0 to 6 h using fluorescence microplate reader. B) Intracellular ROS were also evaluated under a fluorescence microscope. Data points represent the mean \pm S.D. (n=3). * p <0.05 versus non-treated control.

1.2. Effect of hydrogen peroxide on cell death in lung carcinoma cells.

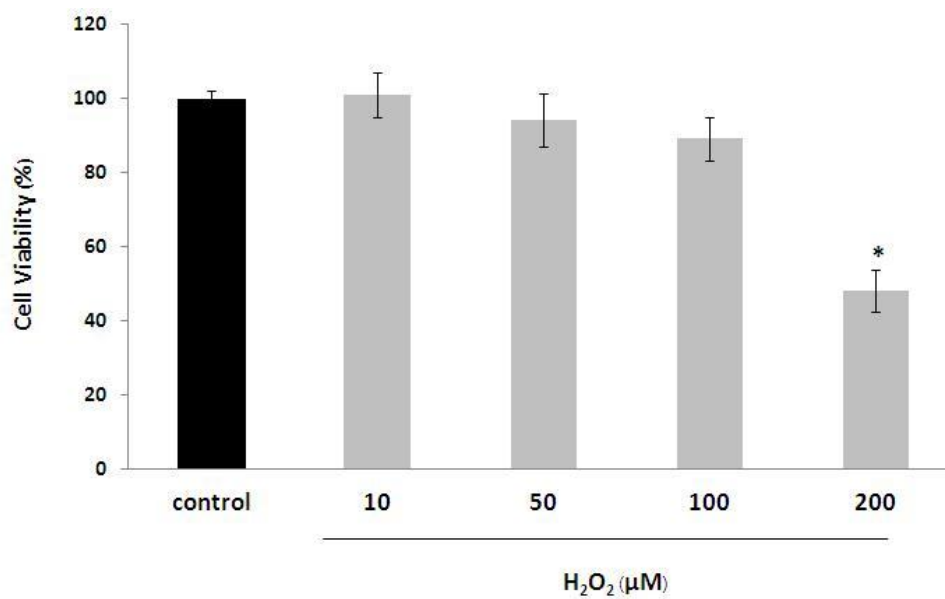
To characterize hydrogen peroxide-induced cell death, MTT assay was examined to study the effect of hydrogen peroxide on cell viability in H460 cells. Apoptosis and necrosis detection was also investigated by Hoechst 33342 and propidium iodide co-staining assay.

In a dose-dependent study, H460 cells were treated with various concentrations of hydrogen peroxide (0, 10, 50, 100, and 200 μM) and incubated for 24 h. Then, MTT assay and Hoechst 33342 and propidium iodide co-staining assay were performed.

The results clearly suggested that hydrogen peroxide dose-dependently reduced viability. At 24 h after treatment, 100 μM hydrogen peroxide reduced cell viability ($89.19 \pm 5.78\%$) and cell viability was significantly decreased when treated with 200 μM hydrogen peroxide with approximately 50% of the cells remaining viable ($48.05 \pm 5.77\%$). Hoechst 33342 and propidium iodide co-staining assay showed that the main mode of cell death was apoptosis. Apoptotic cells, indicated by chromatin condensation and/or nuclear fragmentation, stained with Hoechst. However, necrotic cell death was not detected since there was no cell stained with propidium iodide.

Since 200 μM of hydrogen peroxide significantly reduced cell viability and highly enhanced ROS level in H460 cells, this dose would be used in further experiments to detect cell death induced by hydrogen peroxide.

A



B

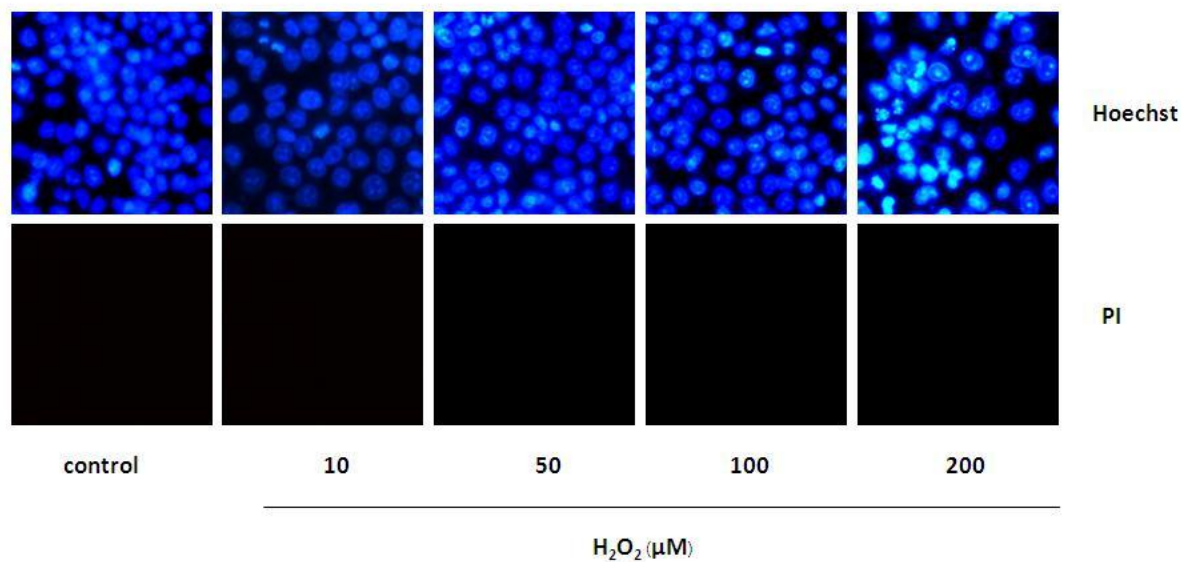


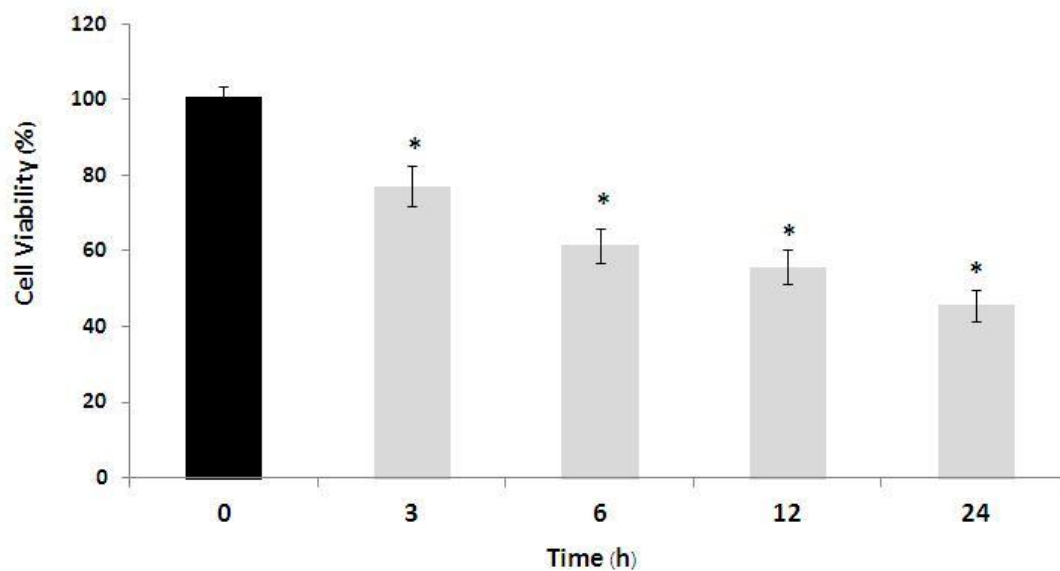
Figure 4.2 Effect of various concentrations of hydrogen peroxide on cell death in H460 cells. A) Cells were treated with various concentrations of hydrogen peroxide (0, 10, 50, 100, and 200 μM). After 24 h, MTT assay was performed to determine cell viability. B) Hoechst 33342 and propidium iodide co-staining assay was observed

under a fluorescence microscope to detect apoptotic and necrotic cell death. Data points represent the mean \pm S.D. (n=3). * p <0.05 versus non-treated control.

In a time-dependent study, H460 cells were treated with 200 μ M of hydrogen peroxide and incubated for 0, 3, 6, 12 and 24 h. After that, cell viability was investigated by MTT assay. Hoechst 33342 and propidium iodide co-staining assay was also performed.

The results showed that 200 μ M of hydrogen peroxide treatment contributed to significant reduction in viability after 3 h ($77.10 \pm 5.28\%$) and the viability continuously reduced until 24 h ($46.58 \pm 4.15\%$). Furthermore, Hoechst and propidium iodide co-staining assay revealed that apoptotic cells could be early seen at 12 h after hydrogen peroxide treatment. According to the gradually increasing number of the apoptotic cells until saturated at 24 h, this time point were used in further experiment to examined cell death induced by hydrogen peroxide.

A



B

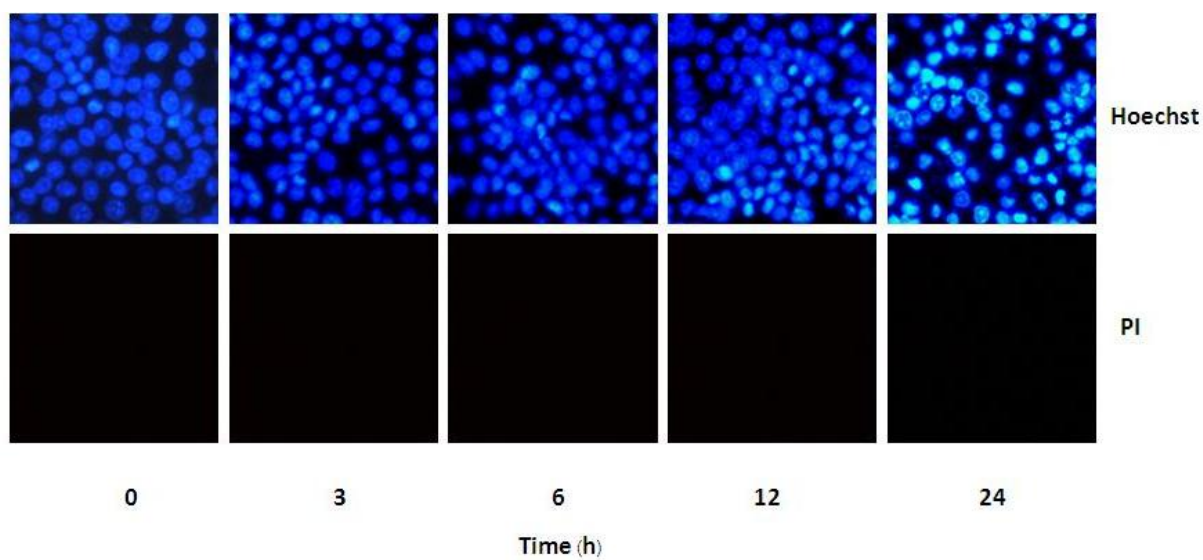


Figure 4.3 A time-dependent study of hydrogen peroxide-induced cell death in H460 cells. A) Cells were treated with 200 μ M of hydrogen peroxide and incubated for 0, 3, 6, 12 and 24 h. After that, MTT assay was performed. B) Hoechst 33342 and propidium iodide co-staining assay was also examined under a fluorescence

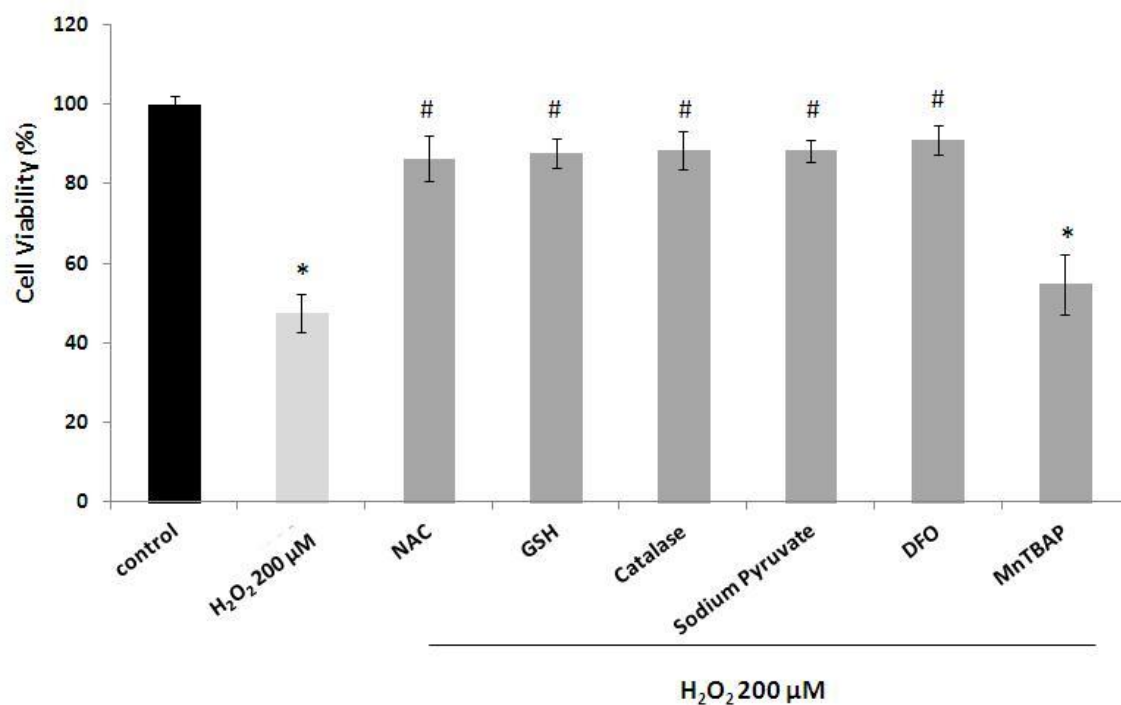
microscope. Data points represent the mean \pm S.D. (n=3). * p <0.05 versus non-treated control.

1.3. Effect of antioxidants on H460 cell death induced by hydrogen peroxide.

To investigate which antioxidants could protect cell death induced by hydrogen peroxide and to find out which specific ROS participated in cell death, cells were pretreated with pan-antioxidants (NAC and GSH) or specific antioxidants such as H₂O₂-scavenger (catalase and sodium pyruvate), hydroxyl radical inhibitor (deferoxamine) and superoxide anion scavenger (MnTBAP) for 1 h and followed by 200 μ M of hydrogen peroxide. After 24 h, cell viability was investigated by MTT assay and Hoechst 33342 and propidium iodide co-staining assay was performed to detect apoptotic and necrotic cell death.

The results showed that all antioxidants prevented hydrogen peroxide-induced cell death except MnTBAP. Indeed, viability of NAC, GSH, catalase, sodium pyruvate and deferoxamine-treated cells (86.44 ± 5.67 , 87.61 ± 3.67 , 88.38 ± 4.76 , 88.35 ± 2.86 , $91.91 \pm 3.75\%$, respectively) were significantly higher than hydrogen peroxide-treated cells ($47.44 \pm 4.77\%$). On the other hand, viability of MnTBAP-treated cells ($54.87 \pm 7.60\%$) was not significantly different from hydrogen peroxide-treated cells. Confirming study using Hoechst 33342 and propidium iodide co-staining assay also exhibited the similar results that MnTBAP did not prevent apoptosis caused by hydrogen peroxide. These findings suggested that superoxide anion was not associated with hydrogen peroxide-induced apoptosis.

A



B

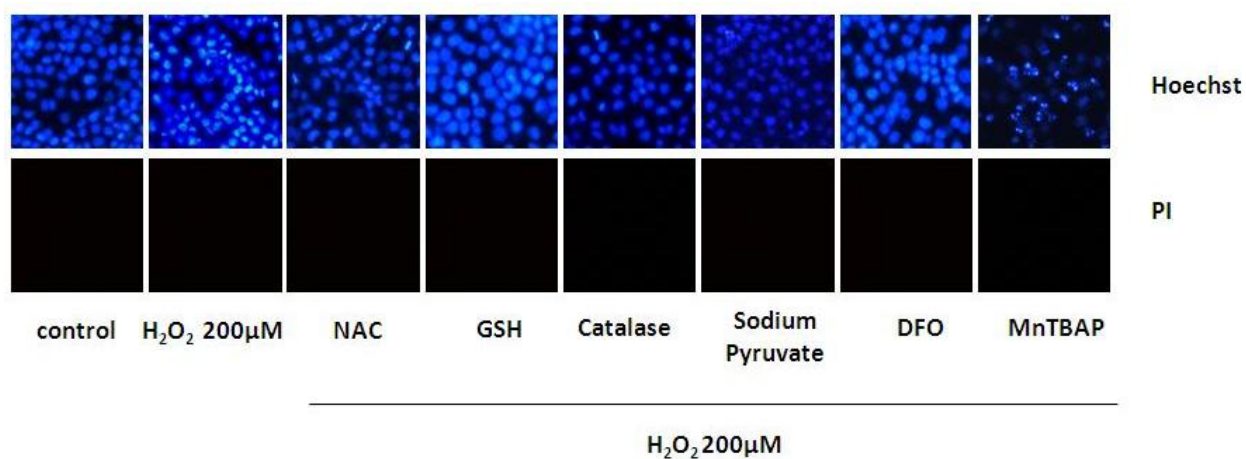


Figure 4.4 Effect of antioxidants on H460 cell death induced by hydrogen peroxide. A) Cells were pretreated with 1 mM N-acetylcysteine (NAC), 1 mM glutathione (GSH), 5,000 units/ml of catalase, 1 mM sodium pyruvate, 1 mM deferoxamine (DFO) or 50 μM Mn(III)tetrakis(4-benzoic acid)porphyrin chloride (MnTBAP) prior

to 200 μM of hydrogen peroxide (H_2O_2). After 24 h of incubation, MTT assay was performed. B) Hoechst 33342 and propidium iodide co-staining assay was also examined under a fluorescence microscope. Value represents the mean \pm S.D. ($n=3$). * $p<0.05$ versus non-treated control. # $p<0.05$ versus 200 μM H_2O_2 -treated cells.

To confirm that all concentration of antioxidants used in the experiments did not affect the cell viability, MTT assay was performed. H460 cells were treated with 1 mM N-acetylcysteine, 1 mM glutathione, 5,000 units/ml of catalase, 1 mM sodium pyruvate, 1 mM deferoxamine or 50 μM Mn(III)tetrakis(4-benzoic acid)porphyrin chloride (MnTBAP) and incubated for 24 h. The results showed that concentration of antioxidants used in the experiments did not significantly reduce viability of H460 cells.

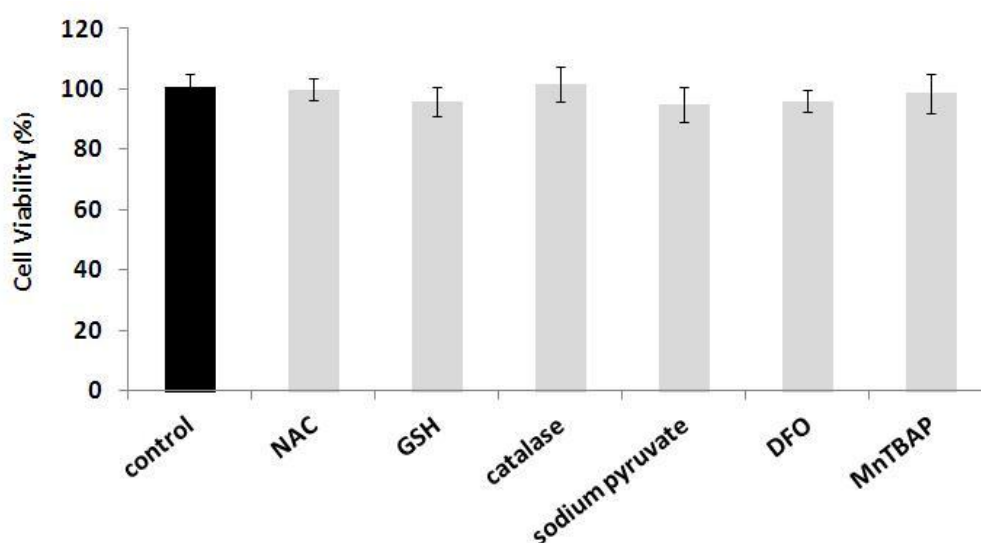


Figure 4.5 Effect of antioxidants on cell viability of H460 cells. Cells were treated with 1 mM N-acetylcysteine (NAC), 1 mM glutathione (GSH), 5,000 units/ml of catalase, 1 mM sodium pyruvate, 1 mM deferoxamine (DFO) or 50 μM Mn(III)tetrakis(4-benzoic acid)porphyrin chloride (MnTBAP). After 24 h of incubation, MTT assay was performed. Value represents the mean \pm S.D. ($n=3$).

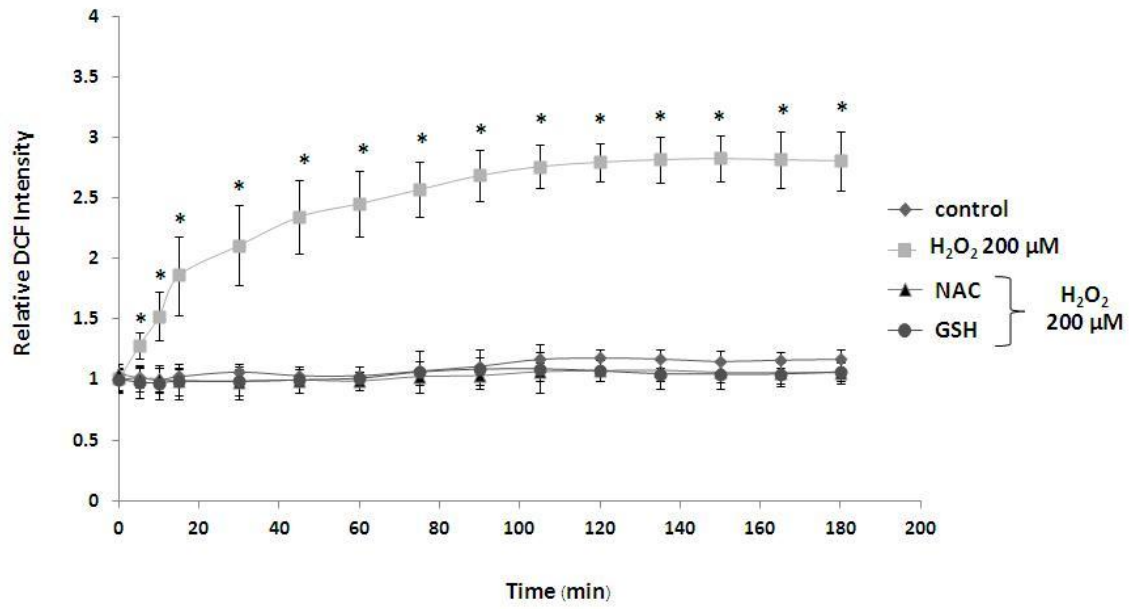
1.4. Effect of antioxidants on cellular oxidative stress induced by hydrogen peroxide in lung carcinoma cells.

To study the effect of antioxidants and to identify the principal ROS caused by hydrogen peroxide-induced oxidative stress in H460 cells. Cells were pretreated with pan- or specific antioxidants prior to 200 μ M hydrogen peroxide. Intracellular ROS were measured by DCFH₂-DA as ROS probe, analyzed using fluorescence microplate reader from 0 to 3 h and confirmed by visualizing under a fluorescence microscope.

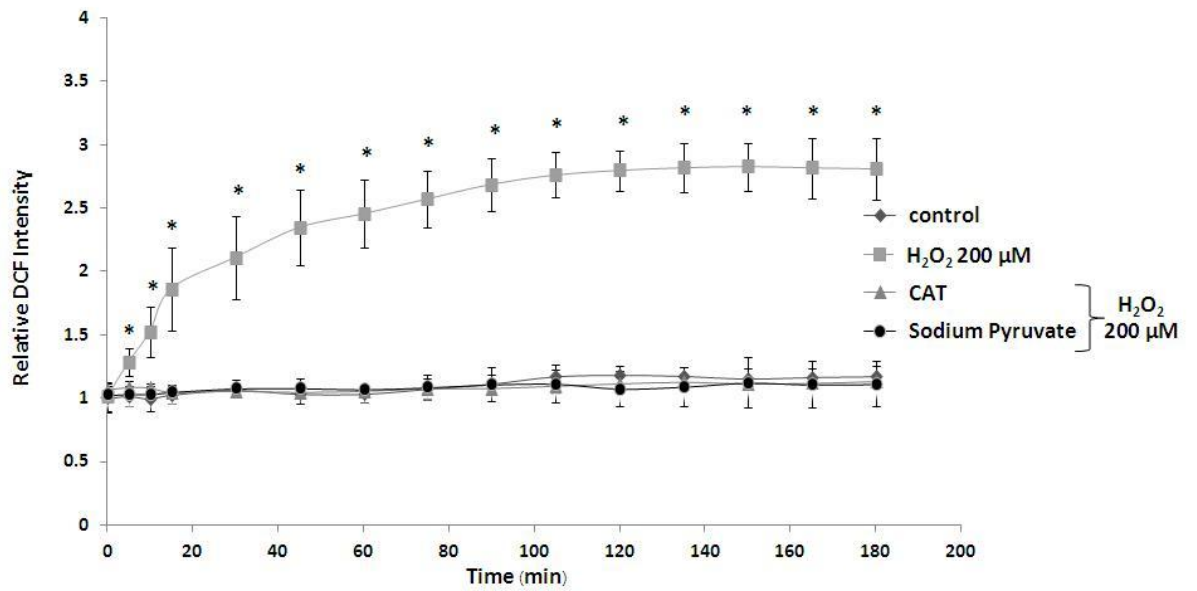
The results showed that all antioxidants prevented the increase of intracellular ROS induced by hydrogen peroxide (Figure 4.6) except MnTBAP, the superoxide anion scavenger. N-acetylcysteine and glutathione, pan-antioxidants, showed the protective effect in response to hydrogen peroxide. Pretreated cells with catalase and sodium pyruvate, the hydrogen peroxide scavengers, and deferoxamine, hydroxyl radical blocker, also had no increase in DCF signals as well as non-treated control cells. These results suggested that hydrogen peroxide and hydroxyl radical participated in these conditions. Since MnTBAP had no protective effect, superoxide anion was not the cause of cell death and oxidative stress induced by hydrogen peroxide.

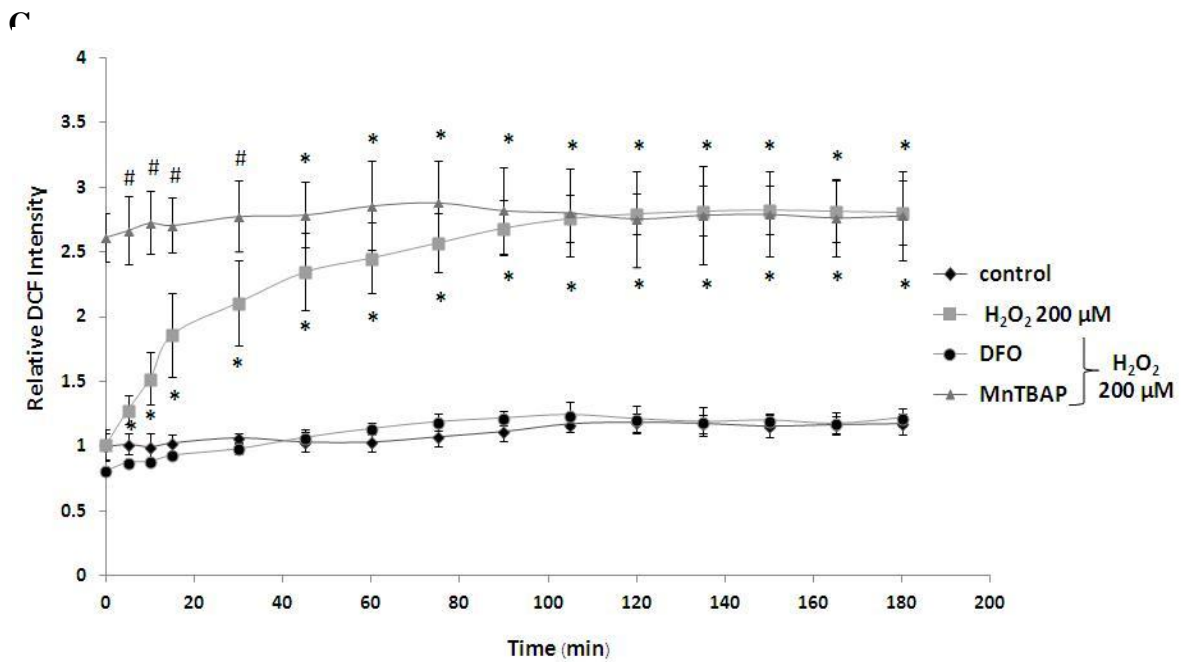
In addition, Figure 4.6D showed the DCF signals in response to hydrogen peroxide of antioxidant-treated cells from 0 to 3 h by using fluorescence microscope. Consistently, the results showed that the DCF signals increased by hydrogen peroxide treatment. Importantly, pretreatment with antioxidants reduced DCF signals except MnTBAP which confirmed the results from the previous experiment.

A



B





D

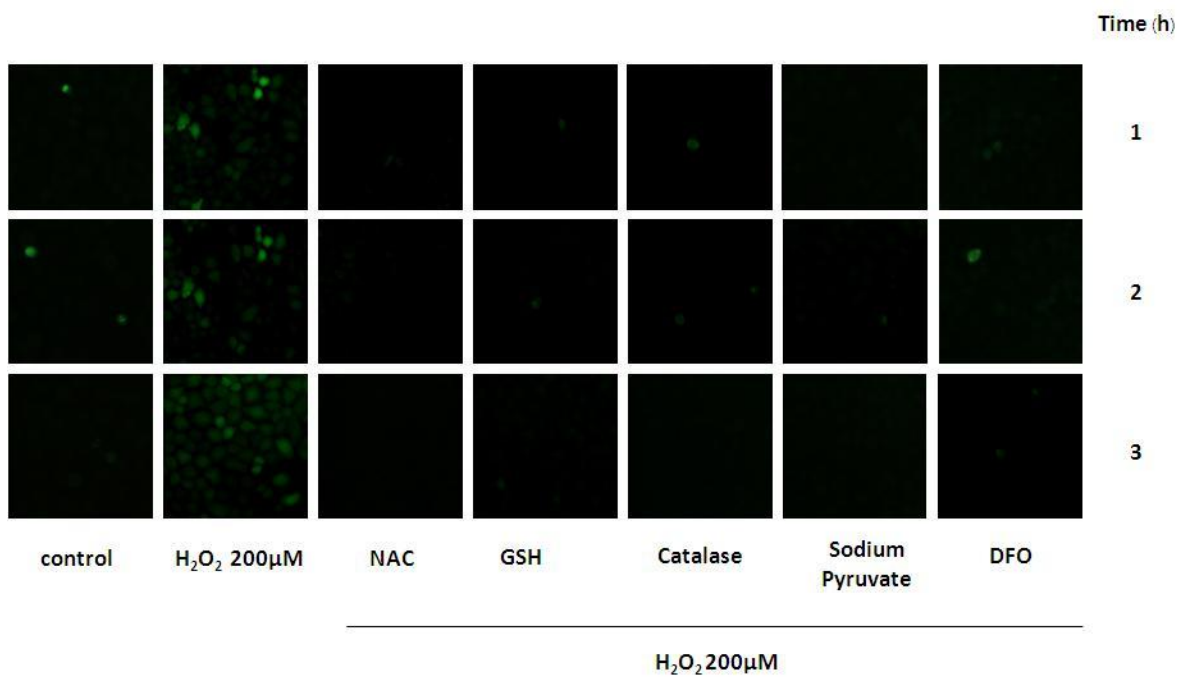


Figure 4.6 Effect of antioxidants on oxidative stress induced by hydrogen peroxide. A), B) and C) Cells were treated with 1 mM N-acetylcysteine (NAC), 1 mM glutathione (GSH), 5,000 units/ml of catalase (CAT), 1 mM sodium pyruvate, 1 mM

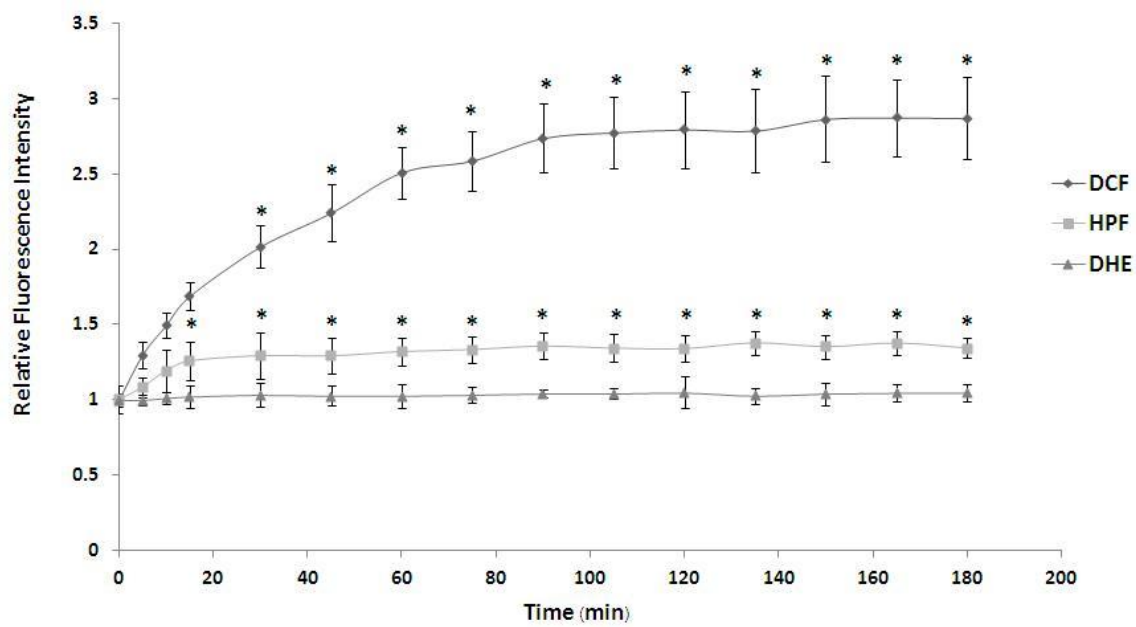
deferoxamine (DFO) or 50 μM Mn(III)tetrakis(4-benzoic acid)porphyrin chloride (MnTBAP) prior to 200 μM hydrogen peroxide. Using DCFH₂-DA as ROS probe, intracellular ROS were measured by fluorescence microplate reader from 0 to 3 h. D) Confirming study using fluorescence microscope. Data points represent the mean \pm S.D. (n=3). * p <0.05 versus non-treated control. # p <0.05 versus 200 μM H₂O₂-treated cells.

1.5. Hydroxyl radical was predominantly responsible for oxidative stress induced by hydrogen peroxide.

This study was investigated to confirm which specific ROS played an important role in hydrogen peroxide-induced oxidative stress by using various specific ROS probes. DCFH₂-DA (ROS probe), HPF (hydroxyl radical probe), or DHE (superoxide anion probe) were used to detect the increase of each species and 200 μM of hydrogen peroxide was added to induce oxidative stress. Intracellular ROS, hydroxyl radical or superoxide anion levels were determined by fluorescence microplate reader from 0 to 3 h using specific wavelength. Moreover, cellular fluorescence signals were determined by fluorescence microscope as well.

Interestingly, the results showed that intracellular ROS and hydroxyl radical level were increased due to rising DCF and HPF signals, respectively (Figure 4.7A). On the other hand, level of superoxide anion, indicated by DHE signals, remained the same as basal level. Furthermore, using fluorescence microscope to examine DHE signals was also performed. Although using the various concentration of hydrogen peroxide (0, 50, 100, and 200 μM) induced oxidative stress, there was no significant change in DHE signals (Figure 4.7B). These could be concluded that superoxide anion was not the specific ROS which was responsible for hydrogen peroxide-induced oxidative stress and hydrogen peroxide or hydroxyl radical may be the leading cause.

A



B

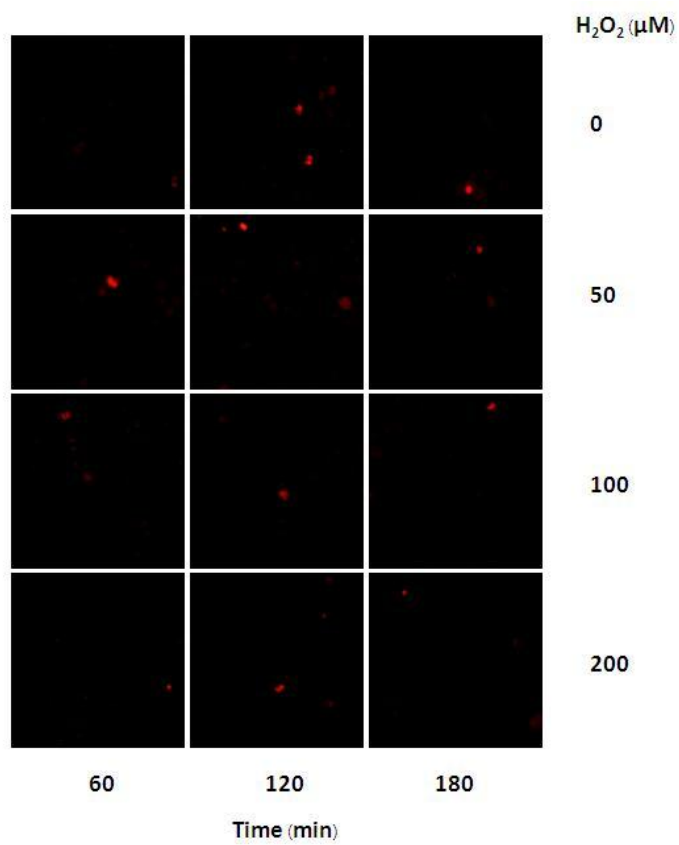


Figure 4.7 Superoxide anion was not the cause of oxidative stress induced by hydrogen peroxide. A) Cells were treated with 200 μM hydrogen peroxide. Intracellular ROS, hydroxyl radical and superoxide anion were detected by specific probes, DCFH₂-DA, HPF and DHE, respectively. Fluorescence intensity was measured by fluorescence microplate reader using each specific wavelength from 0 to 3 h. B) Confirming study using fluorescence microscope to observe DHE signals in H460 cells after treatment with various concentrations of hydrogen peroxide (0, 10, 50, 100, and 200 μM). Data points represent the mean \pm S.D. (n=3). * p <0.05 versus non-treated control at 0 min.

To find out whether hydrogen peroxide or hydroxyl radical was the main ROS which played a role in oxidative stress induced by hydrogen peroxide, H460 cells were pretreated with deferoxamine, hydroxyl radical blocker, prior to 200 μM hydrogen peroxide. Then, HPF was used to detect hydroxyl radical level.

The results obviously suggested that hydroxyl radical was the main ROS increasing inside the cells treated with hydrogen peroxide. Hydroxyl radical significantly increased higher than non-treated control cells as early as 15 minutes after hydrogen peroxide treatment. On the other hand, deferoxamine pretreatment could suppress hydroxyl radical level as shown in Figure 4.8. The hydroxyl radical level in deferoxamine-pretreated cells was not significantly different from non-treated control cells.

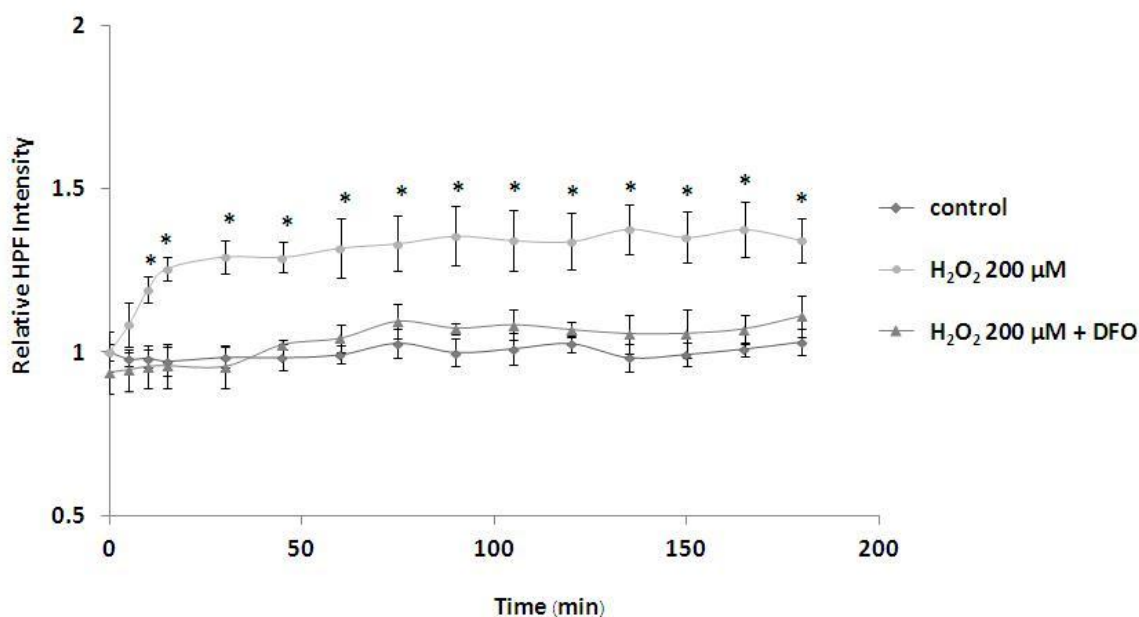


Figure 4.8 Hydroxyl radical played a predominant role in oxidative stress induced by hydrogen peroxide. H460 cells were pretreated or non-pretreated with 1 mM deferoxamine before adding 200 μ M hydrogen peroxide. Hydroxyl radical level was detected using 10 μ M of HPF probe and measured by fluorescence microplate reader from 0 to 3 h. Data points represent the mean \pm S.D. (n=3). * p <0.05 versus non-treated control.

2. Caveolin-1 attenuated oxidative stress and cell death induced by hydrogen peroxide in human lung carcinoma H460 cells.

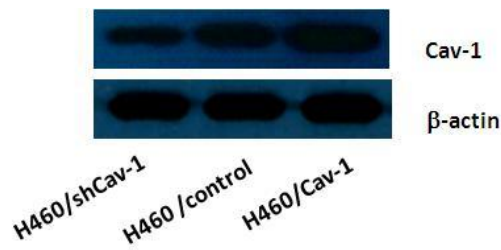
2.1. Caveolin-1 expression in lung carcinoma cells.

To study the effect of caveolin-1 on hydrogen peroxide-induced oxidative stress and cell death, H460 cells were transfected with Cav-1 overexpressing plasmid, mock control plasmid or Cav-1 shRNA plasmid in order to generate Cav-1 overexpressed H460 (H460/Cav-1), mock control transfected H460 (H460/control) and Cav-1 down-regulated H460 (H460/shCav-1) cells, respectively. After the process of selection, H460/Cav-1, H460/control and H460/shCav-1 cells were subjected to Western blotting to evaluate caveolin-1 expression. β -actin level was also

determined in each cell to confirm equal protein loading. The band intensity was quantified using analyst/PC densitometry software.

Figure 4.9A showed that H460/Cav-1 cells expressed the highest level of caveolin-1 while the level of H460/shCav-1 cells was the lowest among three cells. Using densitometry to determined caveolin-1 level in each cells, the relative band intensity of H460/Cav-1 and H460/shCav-1 were 3.25 ± 0.24 and 0.42 ± 0.08 , respectively, normalized to those of H460/control cells (1.00 ± 0.15) (Figure 4.9B). These cells were used in further experiments.

A



B

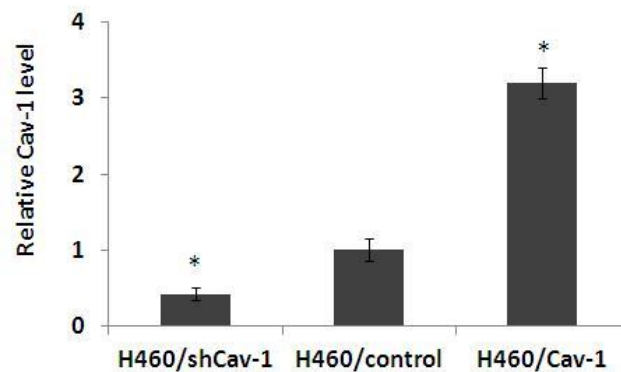


Figure 4.9 Caveolin-1 expression by Western blotting. A) After transfection and selection, H460/shCav-1, H460/Cav-1 and H460/control cells were subjected to western blot method. Blots were probed with caveolin-1 antibody to evaluate caveolin-1 expression of each cell. Then, blots were reprobated with β -actin antibody to evaluate β -actin level and confirm equal loading of the proteins. B) Relative Cav-1

level of each cell was analyzed by using densitometry. Data points represent the mean \pm S.D. (n=3). * p <0.05 versus H460/control.

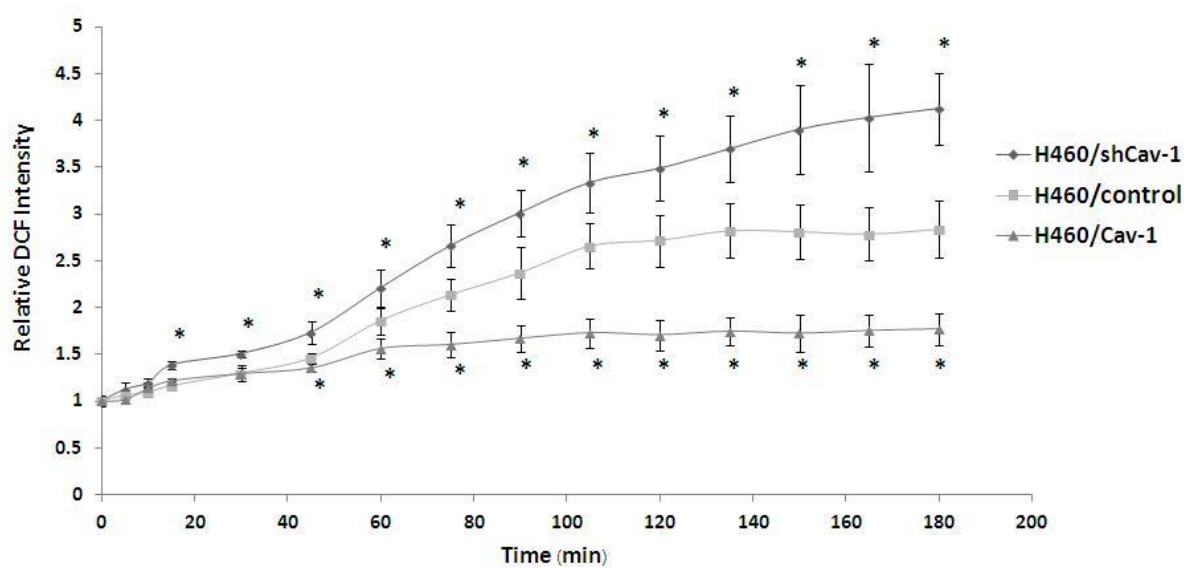
2.2. Effect of hydrogen peroxide on oxidative stress in H460/Cav-1 and H460/shCav-1 cells.

This study was investigated in order to compare the effect of hydrogen peroxide-induced oxidative stress between H460/Cav-1, H460/control and H460/shCav-1 cells. The increased ROS of each cell was evaluated by DCFH₂-DA probes. Each cell was treated with 200 μ M of hydrogen peroxide and DCF signals were immediately measured using fluorescence microplate reader from 0 to 3 h after treatment. Moreover, fluorescence microscope was used to detect DCF signals as well.

The results showed that DCF signal found in H460/shCav-1 cells was significantly higher than H460/control cells while H460/Cav-1 cells were shown the dramatic reduction of ROS level compared to H460/control cells (Figure 4.10A). H460/shCav-1 cells had increased in ROS level significantly higher than H460/control cells since 15 minutes after hydrogen peroxide treatment and reached 4.12 ± 0.38 -fold ROS level compared to non-treated control cells at 180 minute. In contrast, H460/Cav-1 cells exhibited the significant lower level of ROS than H460/control cells at 45 minutes after hydrogen peroxide exposure and still maintained approximately 1.76 ± 0.17 -fold ROS level compared to non-treated control cells at 180 minute. Indeed, at this time point, H460/control cells were shown with 2.83 ± 0.30 -fold ROS level compared to non-treated control cells.

Confirming study by using fluorescence microscope to detect DCF signals after hydrogen peroxide treatment was also investigated. H460/shCav-1 cells showed the highest increase of ROS level while H460/Cav-1 cells showed the lowest ROS signals among three cells. The results also suggested that overexpression of caveolin-1 reduced hydrogen peroxide-induced oxidative stress in H460 cells.

A



B

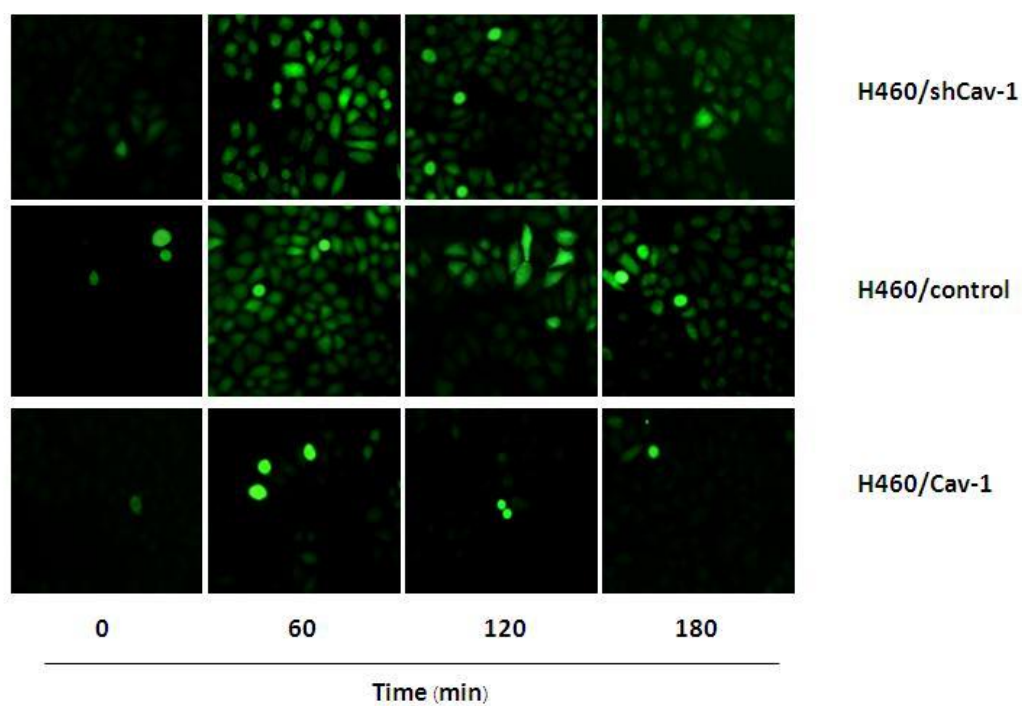


Figure 4.10 Caveolin-1 attenuated hydrogen peroxide-induced ROS in H460 cells. A) H460/Cav-1, H460/control and H460/shCav-1 cells were treated with 200 μM hydrogen peroxide and intracellular ROS were detected by DCFH₂-DA. DCF signal was measured by fluorescence microplate reader from 0 to 3 h. B) Confirming study

using fluorescence microscope to observe DCF signals. Data points represent the mean \pm S.D. (n=3). * p <0.05 versus H460/control at each time point.

Previous experiments found that hydroxyl radical was generated by hydrogen peroxide inside H460 cells and caused oxidative status and cell death. This study was examined whether caveolin-1 reduced hydroxyl radical level. Using HPF, hydroxyl radical probe, H460/Cav-1, H460/control and H460/shCav-1 cells were treated with 200 μ M hydrogen peroxide. Fluorescence intensity was immediately measured by fluorescence microplate reader from 0 to 3 h.

As expected, the results revealed that caveolin-1 reduced hydroxyl radical level in H460 cells. At 1 h after hydrogen peroxide treatment, H460/shCav-1 cells had the significant higher level of hydroxyl radical than H460/control and H460/Cav-1 cells. The relative HPF intensities are 1.56 ± 0.06 , 1.32 ± 0.09 and 1.03 ± 0.12 -fold compared to each non-treated cell, respectively. In addition, these characteristic continued until 180 minutes after hydrogen peroxide treatment. This study also confirmed the role of caveolin-1 in suppression of hydrogen peroxide-induced oxidative stress.

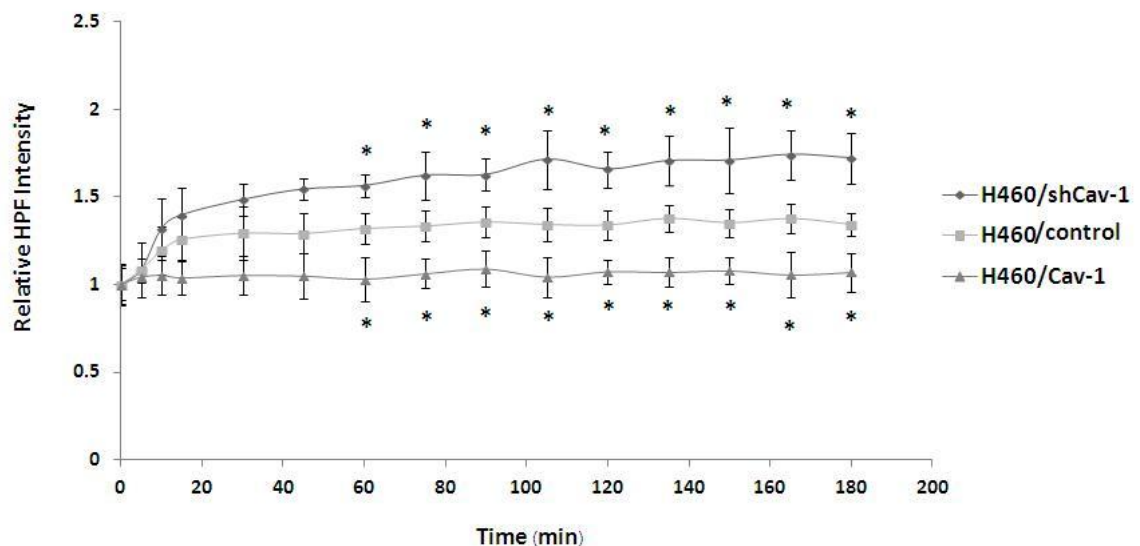


Figure 4.11 Caveolin-1 reduced hydroxyl radical level induced by hydrogen peroxide in H460 cells. A) H460/Cav-1, H460/control and H460/shCav-1 cells were treated

with 200 μM hydrogen peroxide. Intracellular hydroxyl radical were detected by HPF probe and measured by fluorescence microplate reader from 0 to 3 h. Data points represent the mean \pm S.D. (n=3). * p <0.05 versus H460/control at each time point.

2.3. Effect of hydrogen peroxide on cell death in H460/Cav-1 and H460/shCav-1 cells.

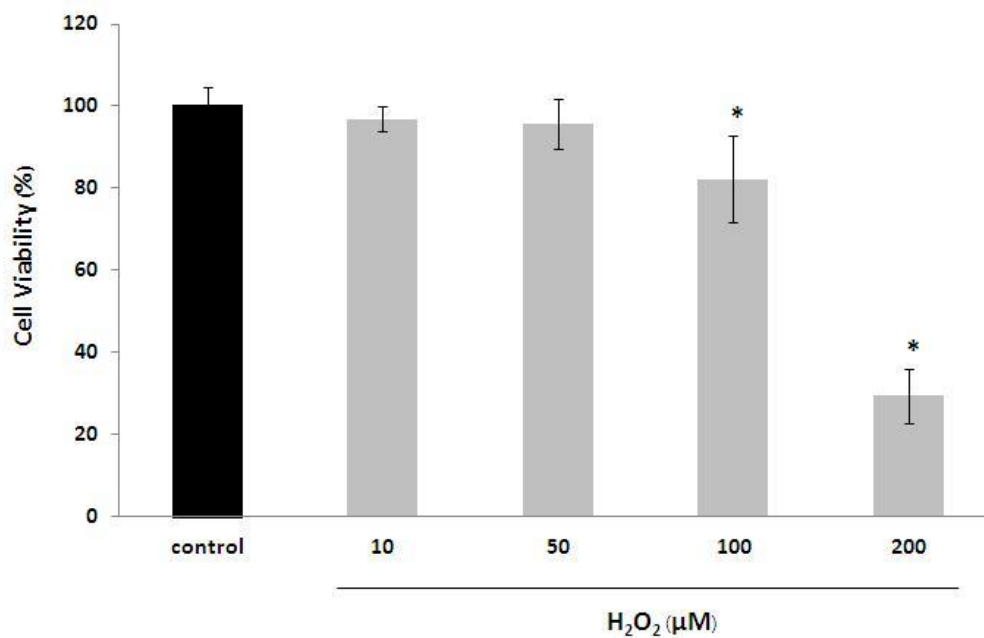
Hydrogen peroxide-induced cell death in H460/Cav-1 and H460/shCav-1 cells was determined in order to compare the effect of caveolin-1 to normal H460/control cells.

Caveolin-1 down-regulated H460 cells or H460/shCav-1 cells were treated with 0, 10, 50, 100 and 200 μM of hydrogen peroxide and incubated for 24 h. After that, MTT assay was performed to estimate cell viability. Hoechst 33342 and propidium iodide co-staining assay was also examined using a fluorescence microscope to characterize the mode of cell death.

The results in H460/shCav-1 cells which expressed low level of caveolin-1 showed that hydrogen peroxide caused cell viability reduction in a dose-dependent manner (Figure 4.12A). After 24 h of treatment, 100 μM hydrogen peroxide caused significantly decreased in cell viability ($82.92 \pm 6.04\%$) compared to non-treated control cell. Moreover, viability of H460/shCav-1 cells dramatically decreased by 200 μM hydrogen peroxide treatment ($29.37 \pm 6.64\%$).

Consistently, the results of Hoechst 33342 and PI co-staining assay also revealed that hydrogen peroxide caused cell apoptosis. Hydrogen peroxide caused dose-dependently increased in the number of apoptotic cells while there was no necrosis in this condition as shown in Figure 4.12B.

A



B

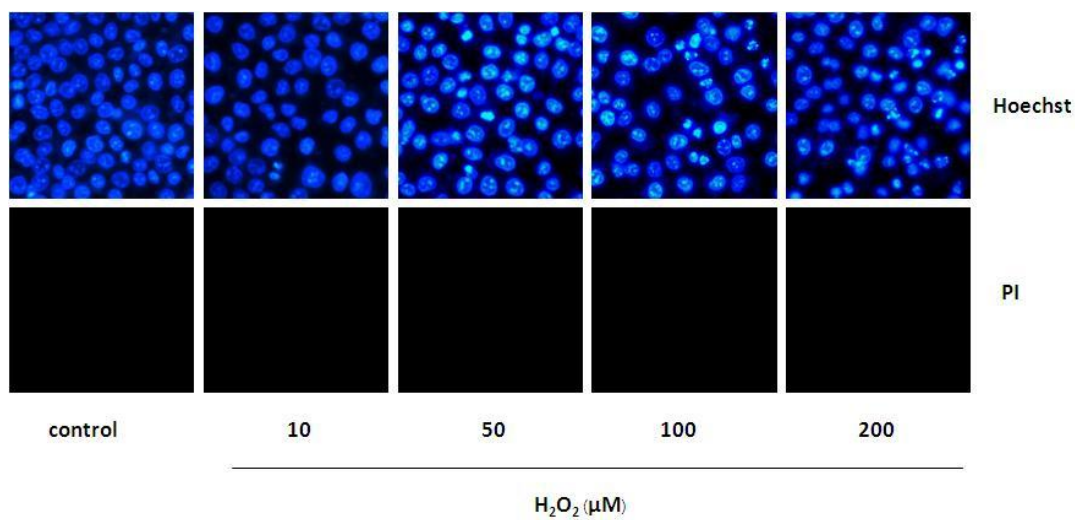


Figure 4.12 Hydrogen peroxide reduced viability of H460/shCav-1 cells and caused cell apoptosis in a dose-dependent manner. A) H460/shCav-1 cells were treated with 0, 10, 50, 100 and 200 μM hydrogen peroxide. After 24 h of incubation, MTT assay was performed. B) Nuclear morphology of apoptotic cells detected by Hoechst 33342 and

PI co-staining assay using fluorescence microscope. Data points represent the mean \pm S.D. (n=3). * p <0.05 versus non-treated control.

To investigate the effect of caveolin-1 on cell death induced by hydrogen peroxide, time-dependent experiment of H460/shCav-1 cells was examined as well. According to previous study that 200 μ M of hydrogen peroxide caused decreased in viability of H460 cells approximately 50%, this dose of hydrogen peroxide was used in this experiment in order to compare the percentage of cell viability between two cell types. H460/shCav-1 cells were treated with 200 μ M hydrogen peroxide and incubated for 0, 3, 6, 12 and 24 h. At each time point, MTT assay was performed. In addition, apoptosis and necrosis detection was also investigated by Hoechst 33342 and PI co-staining assay.

The results showed that viability of H460/shCav-1 cells significantly decreased since 3 h after hydrogen peroxide treatment ($68.33 \pm 4.98\%$) as shown in Figure 4.13A and continuously decreased until 24 h ($29.26 \pm 3.64\%$). Furthermore, Hoechst 33342 and PI co-staining assay showed that apoptotic cells were increased due to the effect of hydrogen peroxide and the results were consistent with the former MTT assay (Figure 4.13B).

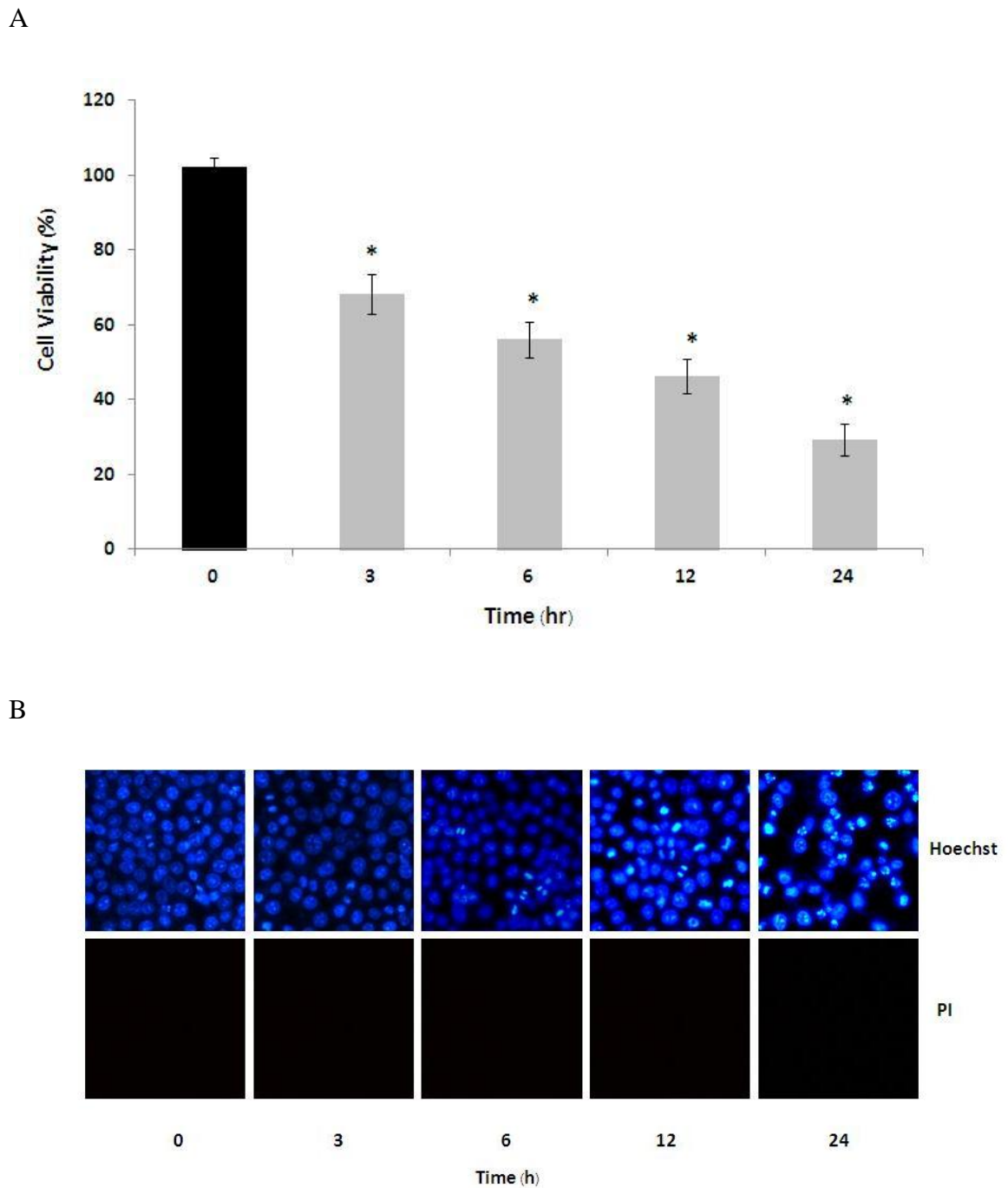
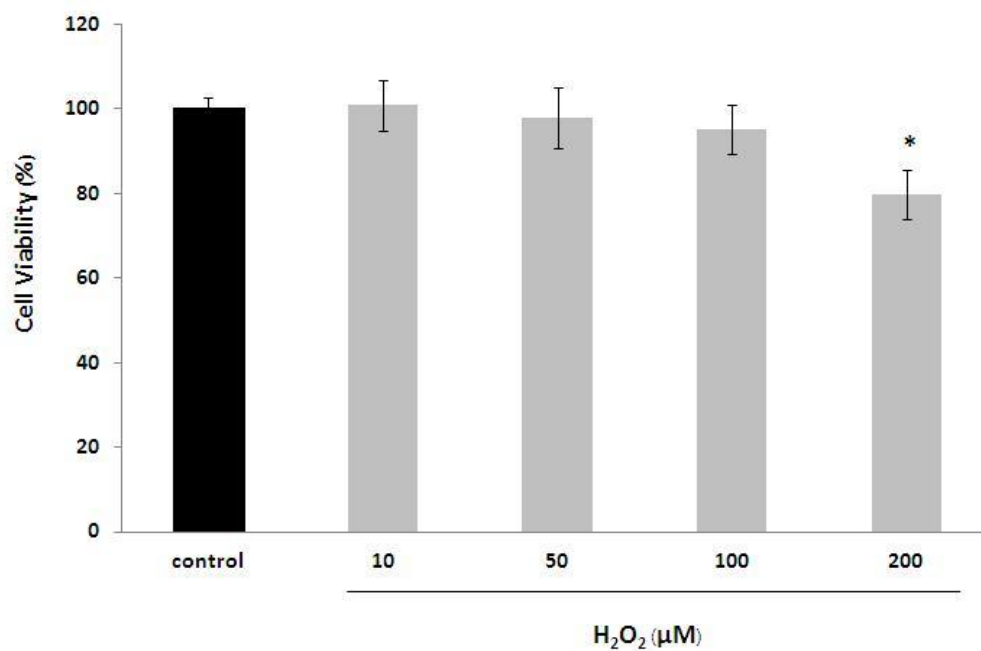


Figure 4.13 Hydrogen peroxide reduced viability of H460/shCav-1 cells and caused cell apoptosis in a time-dependent manner. A) H460/shCav-1 cells were treated with 200 μ M hydrogen peroxide. After 0, 3, 6, 12 and 24 h of incubation, MTT assay was performed at each time point. B) Nuclear morphology of apoptotic cells detected by Hoechst 33342 and PI co-staining assay using fluorescence microscope. Data points represent the mean \pm S.D. (n=3). * p <0.05 versus non-treated control.

To study the effect of caveolin-1 that overexpressed in H460 cells in response to hydrogen peroxide, H460/Cav-1 cells were treated with 0, 10, 50, 100 and 200 μM hydrogen peroxide. After 24 h of incubation, MTT assay was performed to obtain cell viability. Moreover, Hoechst 33342 and PI co-staining assay was also investigated.

The results strongly suggested that overexpression of caveolin-1 caused cells resistance to hydrogen peroxide-induced cell death. As shown in Figure 4.14A, treatment with 100 μM hydrogen peroxide did not significantly affect the viability of H460/Cav-1 cells ($95.25 \pm 2.97\%$) while this concentration caused significant reduction in viability of H460/shCav-1 cells ($82.92 \pm 6.04\%$) at 24 h. Viability of H460/Cav-1 cells was significantly decreased when treated with 200 μM hydrogen peroxide ($79.86 \pm 2.30\%$) but still higher than H460/shCav-1 cells ($29.37 \pm 6.64\%$). Besides, Hoechst 33342 and PI co-staining assay also confirmed that the number of apoptotic cells dose-dependently increased due to hydrogen peroxide and no necrotic cells were detected in this condition (Figure 4.14B).

A



B

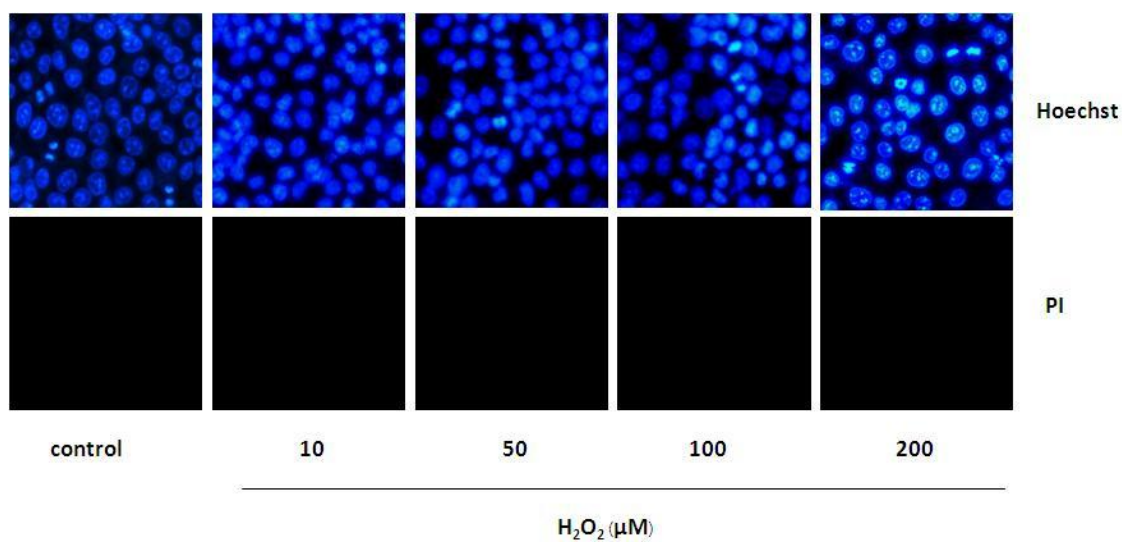


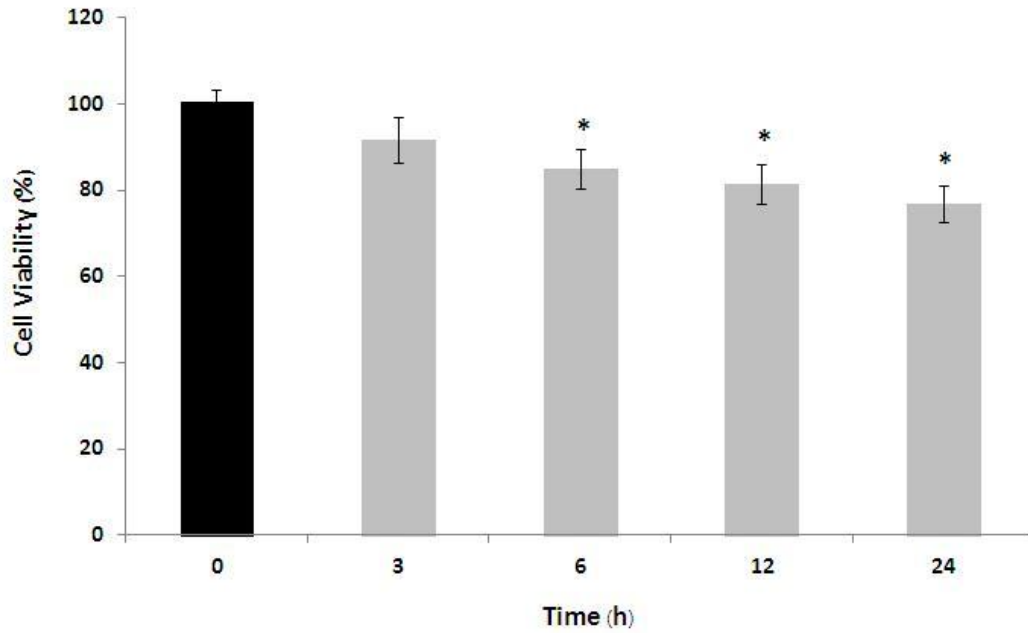
Figure 4.14 Hydrogen peroxide reduced viability of H460/Cav-1 cells and caused cell apoptosis in a dose-dependent manner. A) H460/Cav-1 cells were treated with 0, 10, 50, 100 and 200 μM hydrogen peroxide. After 24 h of incubation, MTT assay was performed. B) Nuclear morphology of apoptotic cells detected by Hoechst 33342 and

PI co-staining assay using fluorescence microscope. Data points represent the mean \pm S.D. (n=3). * p <0.05 versus non-treated control.

To compare the effect of caveolin-1 in response to hydrogen peroxide in H460 cells, time-dependent study of H460/Cav-1 cells was also examined. Since 200 μ M hydrogen peroxide reduced viability of H460 cells approximately 50%, this concentration was used in this experiment in order to compare the percent of cell viability between two cell types. H460/Cav-1 cells were treated with 200 μ M hydrogen peroxide and incubated for 0, 3, 6, 12 and 24 h. After each time point, MTT assay was performed. Furthermore, apoptosis and necrosis detection was also investigated by Hoechst 33342 and PI co-staining assay using fluorescence microscope.

As expected, the results suggested the role of caveolin-1 in protecting cell death overtime in response to hydrogen peroxide. Figure 4.15A showed that the viability of H460/Cav-1 cells did not significantly decrease until 6 h after treatment ($84.89 \pm 6.5\%$) while viabilities of H460 and H460/shCav-1 cells were significantly decreased since 3 h after hydrogen peroxide treatment ($77.09 \pm 5.28\%$ and $68.34 \pm 4.98\%$, respectively). In addition, the results from Hoechst 33342 and PI co-staining assay were also consistent with the results from MTT assay. Apoptotic cells were detected overtime until 24 h and no PI-positive cells were detected (Figure 4.15B). The results suggested that caveolin-1 overexpression lead to cell resistance to hydrogen peroxide-induced cell death and preserved higher viability compared to normal H460 and H460/shCav-1 cells, respectively.

A



B

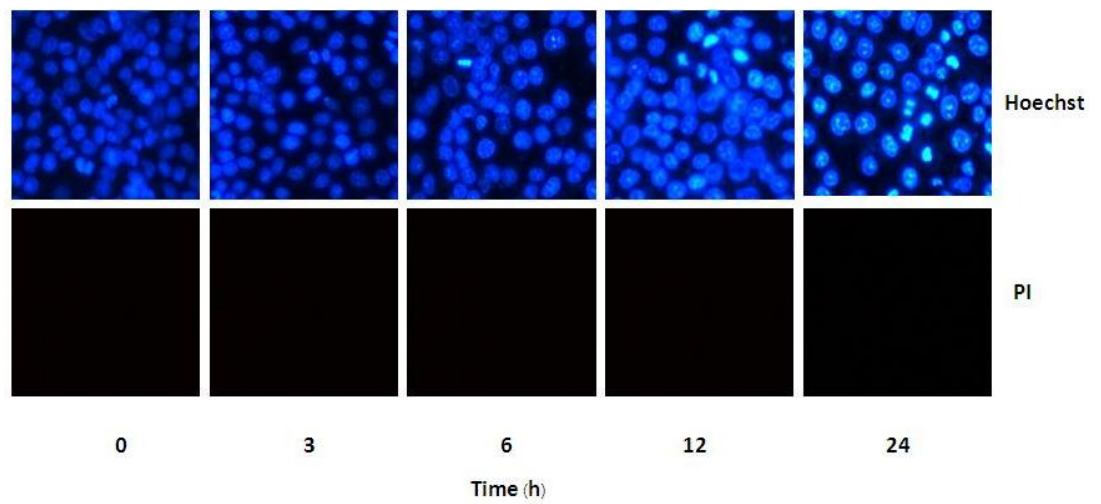


Figure 4.15 Hydrogen peroxide reduced viability of H460/Cav-1 cells and caused cell apoptosis in a time-dependent manner. A) H460/Cav-1 cells were treated with 200 μ M hydrogen peroxide. After 0, 3, 6, 12 and 24 h of incubation, MTT assay was performed at each time point. B) Nuclear morphology of apoptotic cells detected by

Hoechst 33342 and PI co-staining assay using fluorescence microscope. Data points represent the mean \pm S.D. (n=3). * p <0.05 versus non-treated control.

To investigate the effect of caveolin-1 on oxidative damage in response to hydrogen peroxide in H460 cells and to confirm that the process of transfection did not affect cell responses, caveolin-1 overexpressed (H460/Cav-1), caveolin-1 mock control transfected (H460/control) and cav-1 knockdown (H460/shCav-1) cells were treated with 200 μ M hydrogen peroxide. Then, MTT assay was performed after incubation for 24 h and viabilities of H460/Cav-1 and H460/shCav-1 cells were compared to H460/control cells.

The results showed that caveolin-1 attenuated oxidative damage to H460 cells. After 3 h of hydrogen peroxide (200 μ M) treatment, H460/Cav-1 significantly remained higher viability than H460/control and H460/shCav-1 cells ($91.61 \pm 3.53\%$, $77.10 \pm 5.28\%$ and $68.34 \pm 4.98\%$, respectively) as shown in Figure 4.16. At 6 h, viability of H460/Cav-1 cells ($84.89 \pm 6.51\%$) was continuously significantly higher than H460/control cells ($64.76 \pm 4.66\%$) and H460/shCav-1 cells ($56.09 \pm 3.73\%$). Moreover, at 24 after hydrogen peroxide treatment, viability of H460/Cav-1 cells was the highest among three cells ($76.85 \pm 4.48\%$) while survival cells of H460/control and H460/shCav-1 cells were lower ($45.58 \pm 4.15\%$ and $29.26 \pm 3.64\%$, respectively). This study obviously confirmed that caveolin-1 suppressed lung cancer cell death induced by hydrogen peroxide.

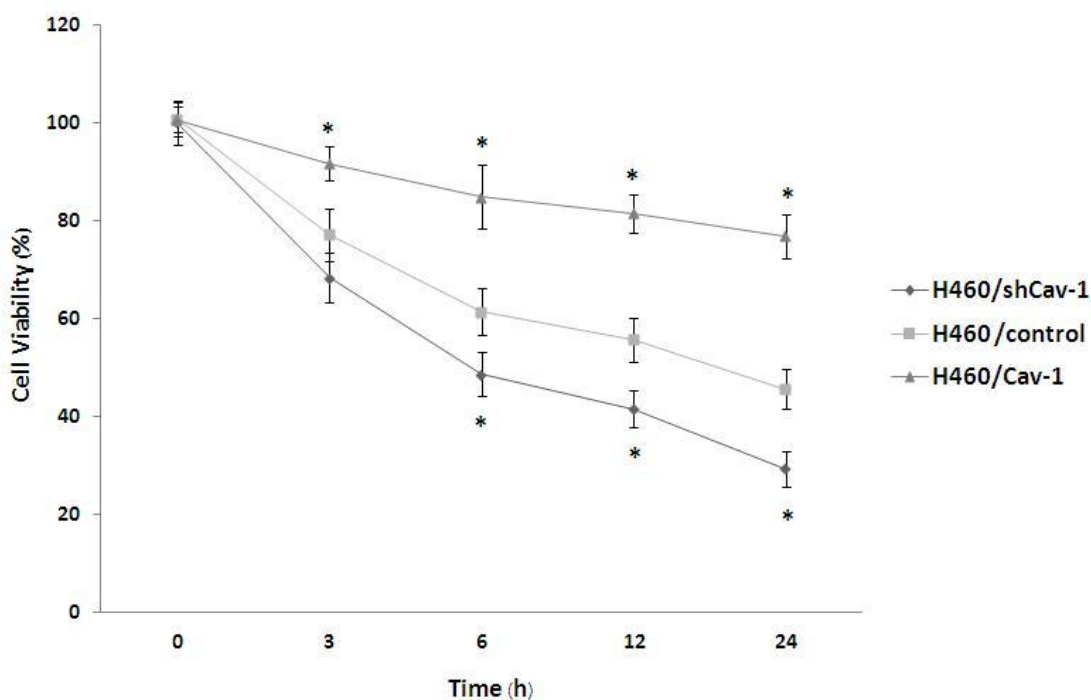


Figure 4.16 Caveolin-1 attenuated oxidative damage to H460 cells. H460/Cav-1, H460/control and H460/shCav-1 cells were treated with 200 μ M hydrogen peroxide and incubated for 0, 3, 6, 12 and 24 h. Each time point, cell viability of each cell was measured by MTT assay. Data points represent the mean \pm S.D. (n=3). * p <0.05 versus H460/control at each time point.

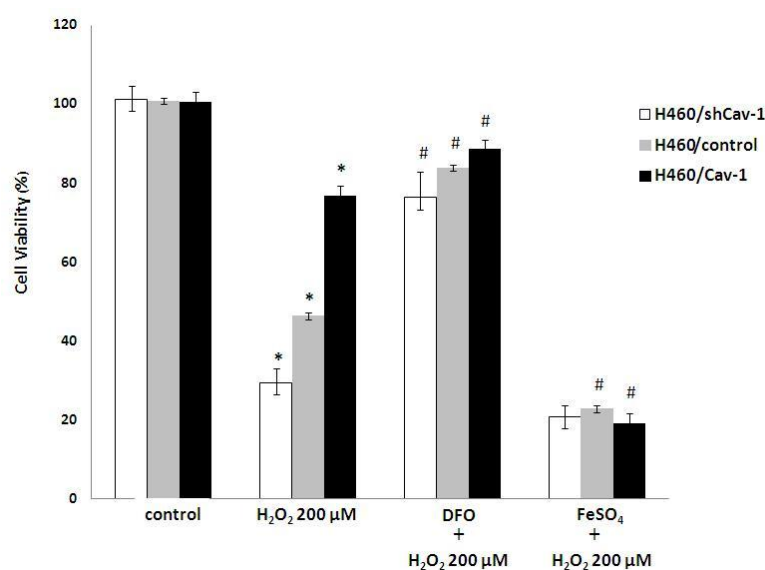
2.4. Effect of hydroxyl radical modulators on viability of H₂O₂-treated cells.

The previous experiments showed that hydroxyl radical was the main ROS causing oxidative stress and cell death in H460 cells. To confirm that hydroxyl radical affected cell death in caveolin-1 overexpressed or knockdown H460 cells, H460/Cav-1, H460/control and H460/shCav-1 cells were pretreated with hydroxyl radical modulators which were deferoxamine (hydroxyl radical blocker) and ferrous sulfate (hydroxyl radical generator) for 1 h before hydrogen peroxide (200 μ M) treatment. Then, cells were incubated for 24 h and MTT assay was performed to obtain cell viability. In addition, Hoechst 33342 and PI co-staining assay was also investigated to detect apoptotic and necrotic cell death.

Figure 4.17A showed the results from MTT assay. After 24 h of hydrogen peroxide treatment (200 μ M), viability of H460/Cav-1, H460/control and H460/shCav-1 cells was significantly decreased ($76.85 \pm 4.48\%$, $46.33 \pm 5.17\%$ and $29.26 \pm 3.64\%$, respectively) compared to each non-treated control cell. As expected, deferoxamine, ferrous iron chelator, could protect cell death from hydrogen peroxide. Pretreatment with 1 mM deferoxamine prior to hydrogen peroxide significantly preserved viability of H460/Cav-1, H460/control and H460/shCav-1 cells ($88.63 \pm 6.17\%$, $83.83 \pm 4.52\%$ and $76.26 \pm 6.48\%$, respectively). In contrast, pretreatment with 50 μ M ferrous sulfate, catalyst in Fenton reaction, enhanced cell death in all three cells. The viability of H460/Cav-1, H460/control and H460/shCav-1 cells was dramatically reduced ($19.11 \pm 2.42\%$, $22.79 \pm 0.82\%$ and $20.71 \pm 2.94\%$, respectively) compared to each hydrogen peroxide-treated cell.

Furthermore, the result from Hoechst 33342 and PI co-staining assay was also consistent with the result from MTT assay (Figure 4.17B). The number of apoptotic cells increased due to hydrogen peroxide treatment. Pretreatment with deferoxamine significantly prevented cell death while ferrous sulfate enhanced apoptotic cell death in all H460/Cav-1, H460/control and H460/shCav-1 cells. The result highly suggested that hydroxyl radical caused cell death induced by hydrogen peroxide.

A



B

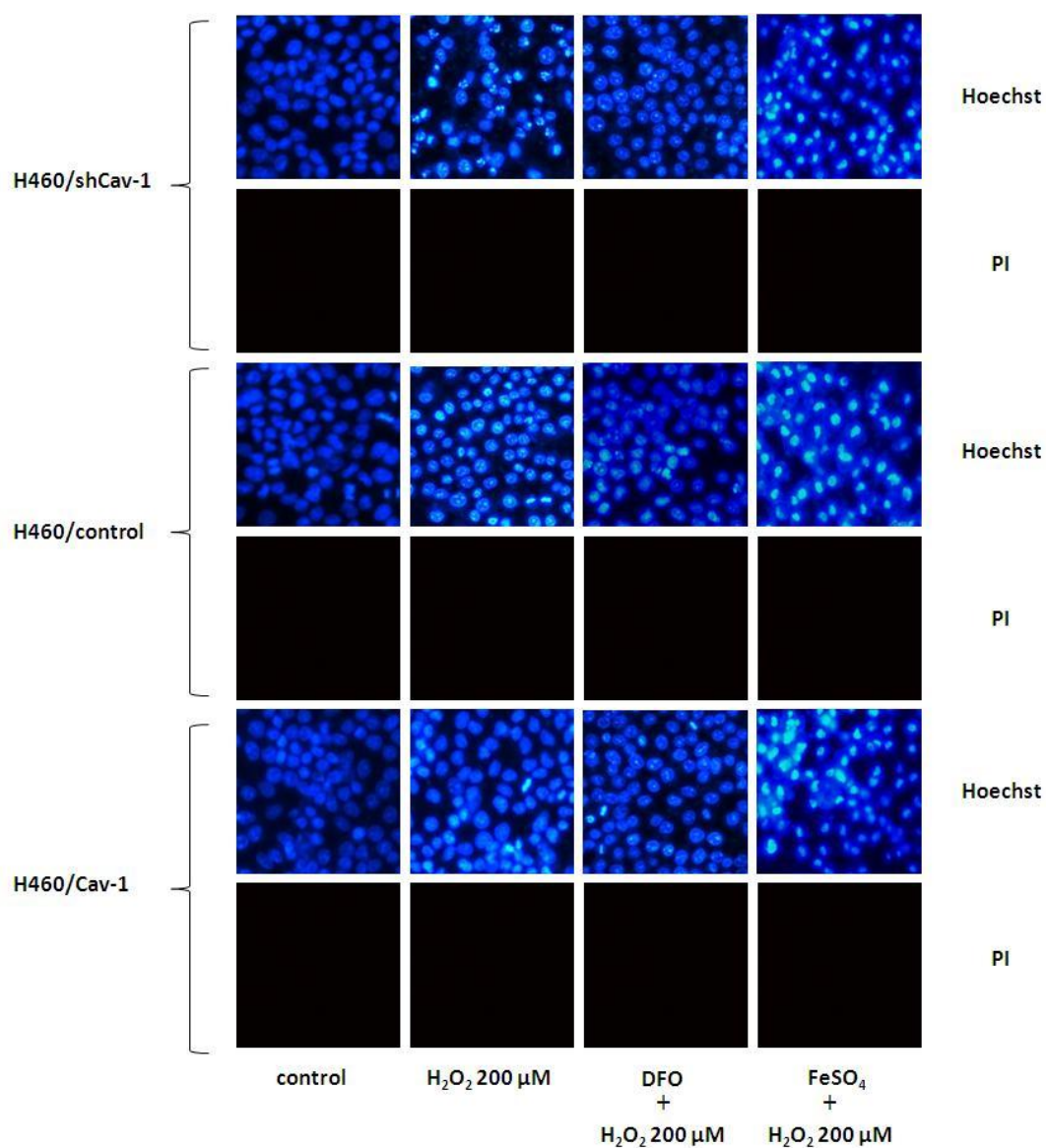


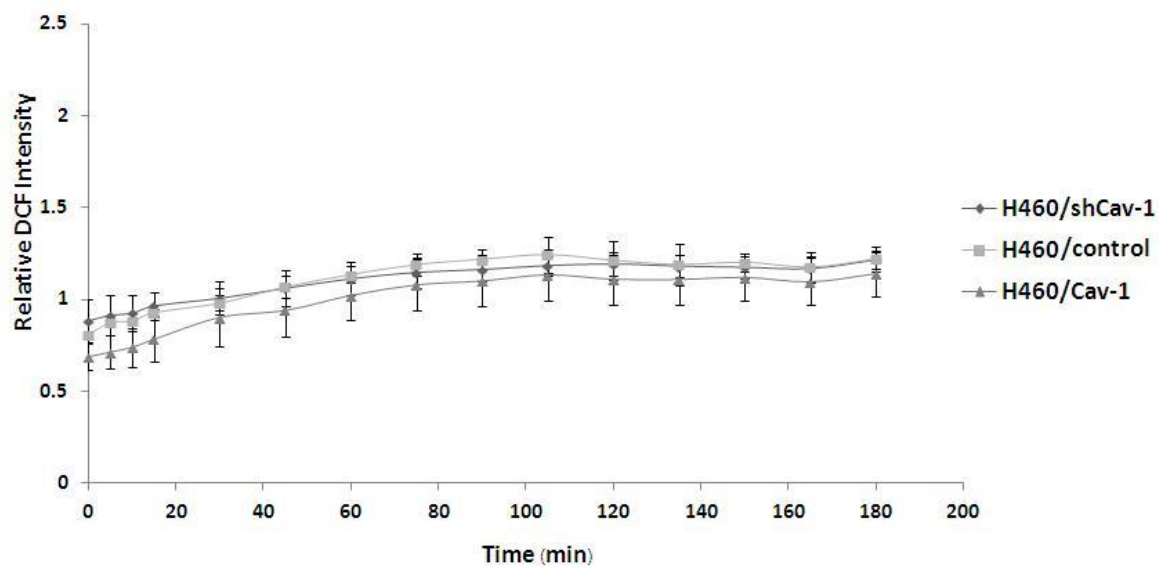
Figure 4.17 Effect of hydroxyl radical on cell death induced by hydrogen peroxide in H460/Cav-1, H460/control and H460/shCav-1 cells. A) H460/Cav-1, H460/control and H460/shCav-1 cells were pretreated with 1 mM deferoxamine (hydroxyl radical blocker) or 50 μM ferrous sulfate (hydroxyl radical generator) for 1 h followed by 200 μM hydrogen peroxide. After 24 h of incubation, MTT assay was performed. B) Nuclear morphology of apoptotic cells detected by Hoechst 33342 and PI co-staining assay using fluorescence microscope. Data points represent the mean \pm S.D. (n=3). * p <0.05 versus non-treated control cells. # p <0.05 versus each H₂O₂-treated cells.

2.5. Effect of hydroxyl radical modulators on cellular ROS and hydroxyl radical level.

The former experiments showed that hydroxyl radical was the cause of oxidative stress and cell death in H460 cells. To investigate how hydroxyl radical affected cellular ROS and the effect of hydroxyl radical modulators on cells which expressed different level of caveolin-1, H460/Cav-1, H460/control and H460/shCav-1 cells were pretreated with deferoxamine (hydroxyl radical blocker) or ferrous sulfate (hydroxyl radical generator) for 1 h. Then, each cell was probed with DCFH₂-DA, ROS probe, for 30 minute at 4 °C. After that, cells were treated with hydrogen peroxide, and ROS level were immediately measured by fluorescence microplate reader from 0 to 3 h. Moreover, intracellular ROS was also measured by fluorescence microscope.

The result clearly showed that pretreatment with 1 mM deferoxamine, hydroxyl radical blocker, reduced cellular ROS in three cells. The DCF signals of each cell indicated that ROS levels of H460/shCav-1 and H460/Cav-1 cells were not significantly different from H460/control cells after treatment overtime until 3 h (Figure 4.18A). Interestingly, as a result of deferoxamine, ROS level of all cells diminished and were lower than the basal level (non-treated control cells) in all hydrogen peroxide-treated group at the beginning of ROS measurement. The result by using fluorescence microscope also revealed in the same way that DCF signals detected were not different between three cell types (Figure 4.18B).

A



B

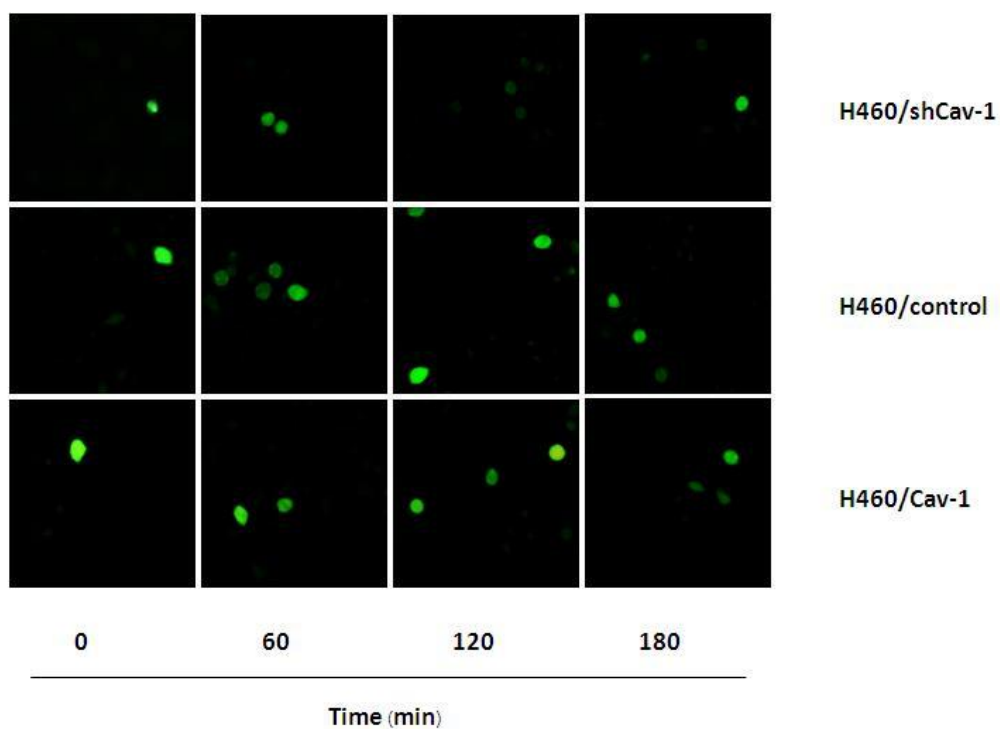
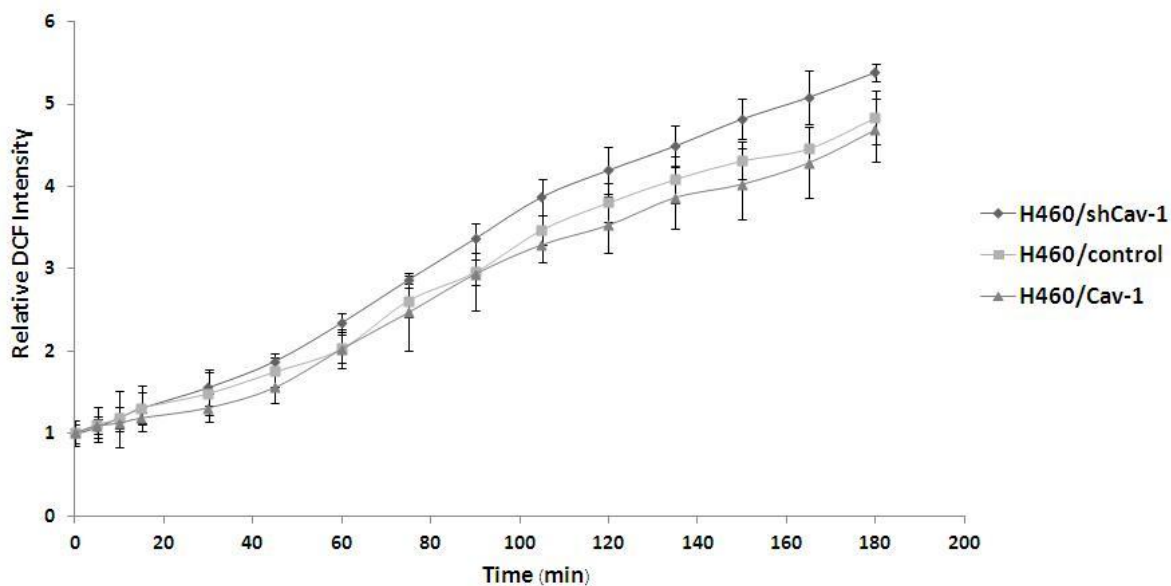


Figure 4.18 Effect of hydroxyl radical inhibitor on cellular oxidative stress. A) H460/Cav-1, H460/control and H460/shCav-1 cells were pretreated with 1 mM

deferoxamine for 1 h followed by 200 μ M hydrogen peroxide. After 24 h of incubation, MTT assay was performed. B) Nuclear morphology of apoptotic cells detected by Hoechst 33342 and PI co-staining assay using fluorescence microscope. Data points represent the mean \pm S.D. (n=3).

In contrast, pretreatment with 50 μ M ferrous sulfate, hydroxyl radical generator, highly enhanced cellular ROS in all cells. However, as shown in Figure 4.19A, the DCF signals of H460/shCav-1 and H460/Cav-1 cells were not significantly different from H460/control cells. In addition, the result from fluorescence microscope also showed the similar result (Figure 4.19B). The results suggested that hydroxyl radical was the principal ROS that mediated cellular oxidative stress in response to hydrogen peroxide.

A



B

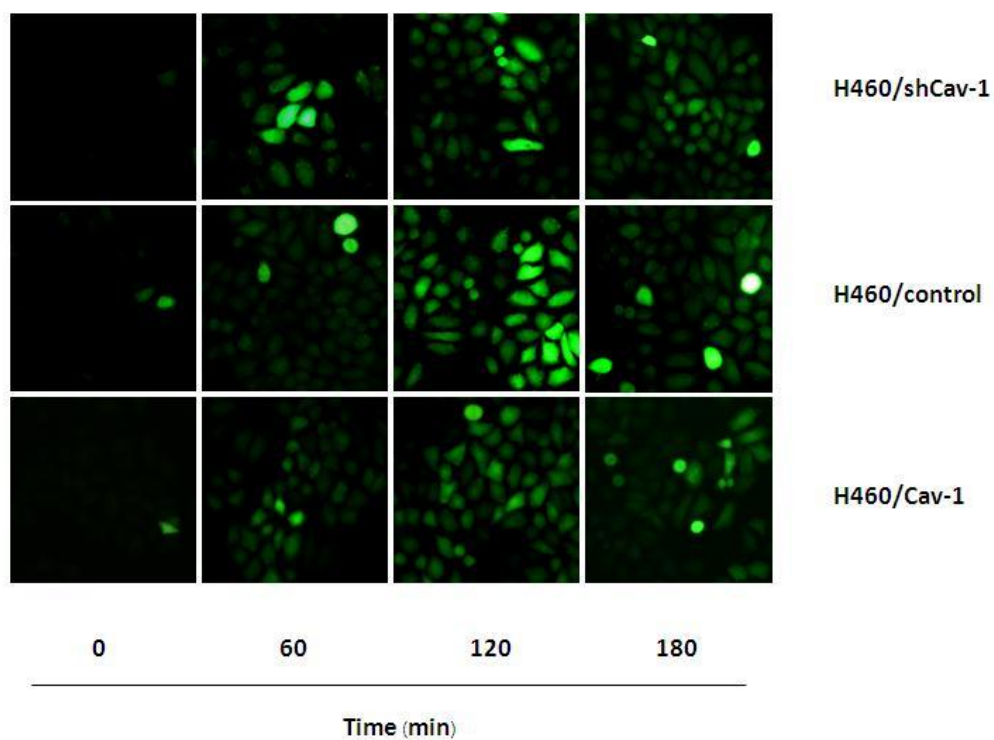


Figure 4.19 Effect of hydroxyl radical generator on cellular oxidative stress. A) H460/Cav-1, H460/control and H460/shCav-1 cells were pretreated with 50 μ M

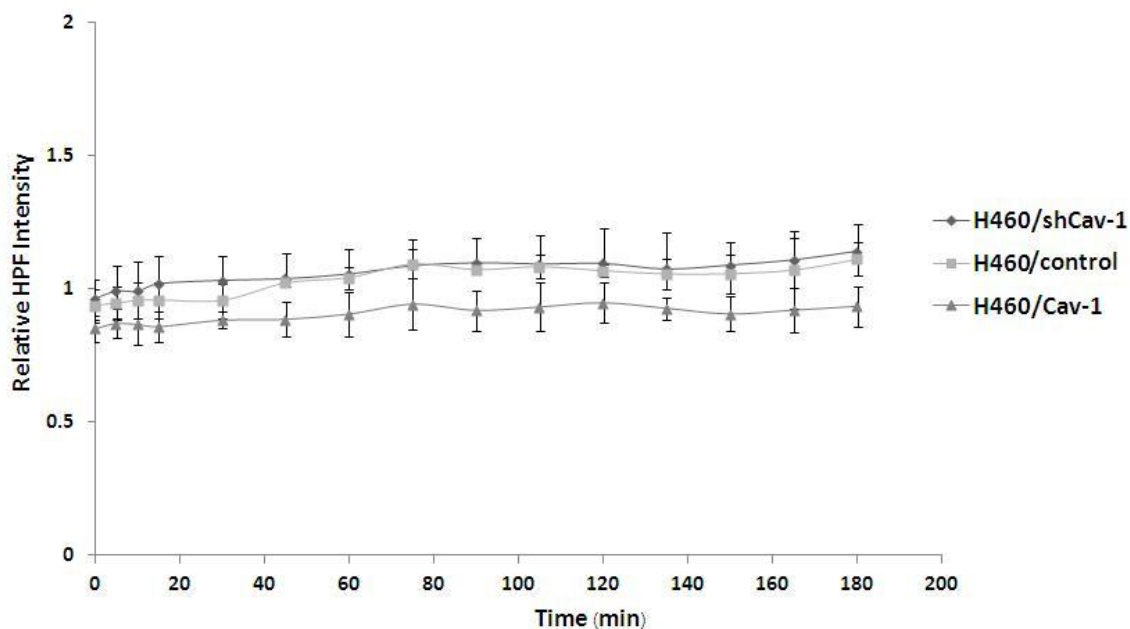
ferrous sulfate for 1 h and then followed by 200 μ M hydrogen peroxide. After 24 h of incubation, MTT assay was performed. B) Nuclear morphology of apoptotic cells detected by Hoechst 33342 and PI co-staining assay using fluorescence microscope. Data points represent the mean \pm S.D. (n=3).

The last experiment was examined in order to confirm that hydroxyl radical was the key ROS resulting in oxidative stress in H460 cells. This study also used hydroxyl radical modulators to examine hydroxyl radical level in H460 cells which expressed different level of caveolin-1, H460/Cav-1, H460/control and H460/shCav-1 cells. Each cell was pretreated with 1 mM deferoxamine (hydroxyl radical blocker) or 50 μ M ferrous sulfate (hydroxyl radical generator) for 1 h. After that, each cell was probed with HPF, specific hydroxyl radical probe, for 30 minute at 4 $^{\circ}$ C. Then, after removing the excess probe, cells were treated with hydrogen peroxide, and ROS level were immediately measured by fluorescence microplate reader from 0 to 3 h.

The results clearly showed that deferoxamine, the ferrous ion chelator, decreased level of hydroxyl radical in all cells since 0 to 3 h after hydrogen peroxide treatment (Figure 4.20A). Interestingly, at the beginning of measurement, hydroxyl radical level in all deferoxamine-pretreated cells was lower than each non-treated control cells.

On the other hand, pretreatment with ferrous sulfate, the catalyst of Fenton reaction to generate hydroxyl radical, highly increased hydroxyl radical level in response to hydrogen peroxide. Although the hydroxyl radical level in H460/shCav-1 cells seems to be the highest among three cells, however, relative HPF intensities of H460/shCav-1 and H460/Cav-1 cells were not significantly different compared to H460/control cells (Figure 4.20B).

A



B

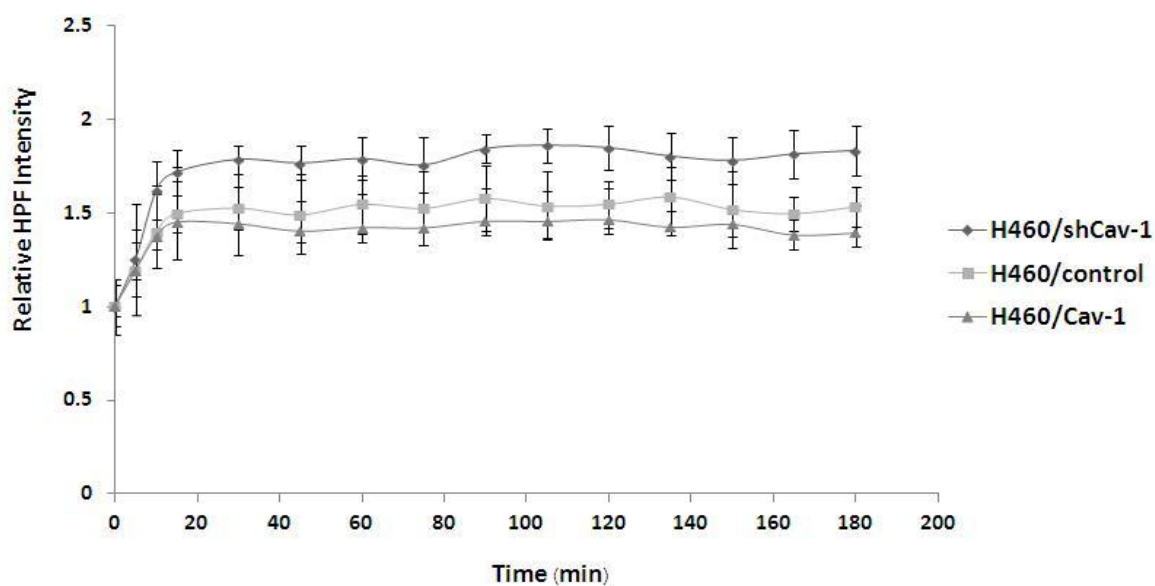


Figure 4.20 Effect of hydroxyl radical modulators on cellular hydroxyl radical level. H460/Cav-1, H460/control and H460/shCav-1 cells were pretreated with A) 1 mM deferoxamine or B) 50 μ M ferrous sulfate for 1 h. Then, cells were probed with HPF at 4 $^{\circ}$ C for 30 minute. After removed excess probe, 200 μ M hydrogen peroxide was

added and the hydroxyl radical level was immediately measured by fluorescence microplate reader. Data points represent the mean \pm S.D. (n=3).

CHAPTER V

DISCUSSION AND CONCLUSION

Although ROS are widely accepted as important mediators for normal cell processes, when in excess, ROS cause oxidative stress implicating in the damage of cellular components and subsequently cell death. For cancer, ROS are considered as carcinogens since several evidences have indicated their roles in facilitating carcinogenesis, and tumor progression (Dreher and Junod, 1996; Ha *et al.*, 2000; Nakamura *et al.*, 1988).

Chronic inflammation that found in the environments of several human cancers including lung cancer, is likely to be a significant cause of an increase ROS in such microenvironments. Indeed, ROS, including superoxide anion, hydrogen peroxide, and singlet oxygen, are released from inflammatory cells of the innate immune system (Ames, Gold, and Willett, 1995; Coussens and Werb, 2002), and cause oxidative damage to surrounding cancer cells. Among key ROS presenting in physiological and pathological conditions, H₂O₂ is the one to gain most attentions since it is relatively stable in comparison to other principle ROS and can pass through biological membrane and spread in tissues (Bienert *et al.*, 2006; Li and Jackson, 2002; Waldron and Rozengurt, 2000).

As expected, treatment with H₂O₂ induced oxidative stress in human lung carcinoma H460 cells. The detection of ROS using specific ROS probe revealed that intracellular ROS were increased in a time- and concentration-dependent manners. Cell viability assay further revealed that the toxicity of such H₂O₂ treatment in these cells was mainly through apoptosis. These observations were consistent with the previous finding that H₂O₂ exposure mediated cytotoxicity through apoptosis induction in human gastric carcinoma cells (Mao *et al.*, 2006) and neuroblastoma cells (Jagtap *et al.*, 2003). However, apoptosis and necrosis was found in H₂O₂ -treated macrophage as well (Lin *et al.*, 2010). Indeed, the range of concentration used in Lin *et al.* experiment (0 - 500 μM) was higher than that of the present study (0 – 200 μM)

and may be the explanation of different mechanism of action of such ROS besides the difference of cell model.

Next, to identify which specific ROS were responsible for oxidative stress and cell death induced by H₂O₂, pan- and specific ROS probes and antioxidants were used. Pretreatment with all antioxidants but MnTBAP, the superoxide anion scavenger, reduced intracellular ROS levels induced by H₂O₂ and preserved cell viability of H460 cells. This study suggested that superoxide anion was not involved in the oxidative damage mediated by H₂O₂. Furthermore, the results consistent with the experiments that H₂O₂ caused significant increase of hydroxyl radical level while the level of superoxide anion did not change. Importantly, pretreatment with deferoxamine, the ferrous ion chelator, reduced ROS and hydroxyl radical level and thus in turn suppressed cell death induced by H₂O₂. These experiments strongly suggested that hydroxyl radical was the main ROS participating in H₂O₂-induced oxidative damage.

It has been shown in the present study that cellular oxidative stresses as well as cytotoxicity caused by H₂O₂ exposure were attenuated in the Cav-1 overexpressed lung cancer cells while shRNA-mediated Cav-1 down-regulated cells were highly susceptible for H₂O₂-induced cell damage. It is well documented that H₂O₂ could be detoxified by cellular antioxidant enzymes including glutathione peroxidase and catalase to water (Valko *et al.*, 2004; Li *et al.*, 2000); however, in the presence of reduced transition metal ion such as iron or copper, H₂O₂ could be rapidly converted to highly reactive hydroxyl radical through Fenton-like reactions (Valko *et al.*, 2004; Lloyd, Hanna, and Mason, 1997).

H₂O₂ treatment resulted in an induction of cellular ROS, namely H₂O₂ and hydroxyl radical. The evidence has indicated different roles of specific ROS in regulation of cell behaviors. Previous experiments indicated that superoxide anion and H₂O₂ inhibited lung cancer cell migration and invasion whereas hydroxyl radical had opposite effects (Luanpitpong *et al.*, 2010). Also, endogenous H₂O₂ but not hydroxyl radical could render cancer cell resist to detachment-induced apoptosis (Rungtabnapa *et al.*, 2011). Previous experiments indicated that H₂O₂ generated in response to

cisplatin treatment mediated renal cell necrosis, whereas hydroxyl radical play a principle role in apoptosis induction (Baek *et al.*, 2003). This finding is consistent with this study that the blockage of hydroxyl radical forming by deferoxamine pre-treatment dramatically inhibited H₂O₂-induced cell death in H460 cells.

Up-regulation of Cav-1 has been observed in lung cancer cells (Sunaga *et al.*, 2004; Ho *et al.*, 2002). The increase level of Cav-1 was shown to associate with several cancer behaviors, such as anoikis resistance (Chanvorachote *et al.*, 2009; Rungtabnapa *et al.*, 2011), migration, and invasion (Luanpitpong *et al.*, 2010) . However, its role in controlling redox status of the cells is still largely unknown. The cell stably transfected with Cav-1 overexpressing plasmids showed a sufficient increase of Cav-1 level over that of parental H460 cells and the shRNA-transfected cells showed dramatically reduced Cav-1 level. Indeed, Cav-1 rendered this lung carcinoma cells to H₂O₂-mediated death. In certain experiments, Cav-1 has been shown to sensitize cancer cell apoptosis in response to death stimuli. The reduction of Cav-1 level was shown to contribute chemotherapeutic cisplatin and carboplatin resistance (David, 2007). Further, the mechanism of Cav-1 in sensitizing cisplatin-induced cell death was through the superoxide anion induction (Pongjit and Chanvorachote, 2011). In contrast to the above findings, this study herein revealed that there was only minimal change in cellular superoxide anion in response to H₂O₂ treatment and Cav-1 overexpression was able to protect cell death. Although the further investigations are necessary to clarify the mechanism(s) by which Cav-1 possess such opposite effects on specific ROS machinery of cells, the present study has revealed for the first time that Cav-1 could attenuate oxidative stress induced by H₂O₂.

In conclusion, the present study has suggested that Cav-1 functioned to the modification of cellular oxidative stress induced by H₂O₂ treatment and render lung cancer cell resist to apoptosis. Since sustained or elevated Cav-1 expression and H₂O₂ level could be concomitantly found in certain cancers, especially lung cancer, the findings of this study may purport the better understanding in cancer biology.

REFERENCES

- Ames, B. N., Gold, L. S., and Willett, W. C. 1995. The causes and prevention of cancer. Proceedings of the National Academy of Sciences of the United States of America 92: 5258-5265.
- Agelaki, S., et al. 2009. Caveolin-1 regulates EGFR signaling in MCF-7 breast cancer cells and enhances gefitinib-induced tumor cell inhibition. Cancer Biology & Therapy 8: 1470-1477.
- Alan, E. 1987. The formation, isolation and characterization of DNA adducts produced by anticancer platinum complexes. Pharmacology & Therapeutics 34: 155-166.
- Arbiser, J. L., et al. 2002. Reactive oxygen generated by Nox1 triggers the angiogenic switch. Proceedings of the National Academy of Sciences of the United States of America 99: 715-720.
- Baek, S. M., Kwon, C. H., Kim, J. H., Woo, J. S., Jung, J. S., and Kim, Y. K. 2003. Differential roles of hydrogen peroxide and hydroxyl radical in cisplatin-induced cell death in renal proximal tubular epithelial cells. Journal of Laboratory and Clinical Medicine 142: 178-186.
- Bates, D. A., and Winterbourn, C. C. 1982. Deoxyribose breakdown by the adriamycin semiquinone and H₂O₂: evidence for hydroxyl radical participation. FEBS Letters 145: 137-142.
- Berlett, B. S., and Stadtman, E. R. 1997. Protein oxidation in aging, disease, and oxidative stress. The Journal of Biological Chemistry 272: 20313-20316.
- Bienert, G. P., Schjoerring, J. K., and Jahn, T. P. 2006. Membrane transport of hydrogen peroxide. Biochimica et Biophysica Acta (BBA) - Biomembranes 1758: 994-1003.
- Brown, M. R., et al. 1999. Overexpression of human catalase inhibits proliferation and promotes apoptosis in vascular smooth muscle cells. Circulation Research 85: 524-533.

- Brozovic, A., Ambriovic-Ristov, A., and Osmak, M. 2010. The relationship between cisplatin-induced reactive oxygen species, glutathione, and BCL-2 and resistance to cisplatin. Critical Reviews in Toxicology 40: 347-359.
- Burdon, R. H. 1995. Superoxide and hydrogen peroxide in relation to mammalian cell proliferation. Free Radical Biology & Medicine 18: 775-794.
- Carver, L. A., and Schnitzer, J. E. 2003. Caveolae: mining little caves for new cancer targets. Nature Review. Cancer 3: 571-581.
- Chandra, J., Samali, A., and Orrenius, S. 2000. Triggering and modulation of apoptosis by oxidative stress. Free Radical Biology & Medicine 29: 323-333.
- Chanvorachote, P., Nimmannit, U., Lu, Y., Talbott, S., Jiang, B. H., and Rojanasakul, Y. 2009. Nitric oxide regulates lung carcinoma cell anoikis through inhibition of ubiquitin-proteasomal degradation of caveolin-1. The Journal of Biological Chemistry 284: 28476-28484.
- Chen, Q., et al. 2005. Pharmacologic ascorbic acid concentrations selectively kill cancer cells: action as a pro-drug to deliver hydrogen peroxide to tissues. Proceedings of the National Academy of Sciences of the United States of America 102: 13604-13609.
- Chung-man Ho, J., Zheng, S., Comhair, S. A., Farver, C., and Erzurum, S. C. 2001. Differential expression of manganese superoxide dismutase and catalase in lung cancer. Cancer Research 61: 8578-8585.
- Circu, M. L., and Aw, T. Y. 2010. Reactive oxygen species, cellular redox systems, and apoptosis. Free Radical Biology & Medicine 48: 749-762.
- Coussens, L. M., and Werb, Z. 2002. Inflammation and cancer. Nature 420: 860-867.
- David J, S. 2007. Mechanisms of resistance to cisplatin and carboplatin. Critical Reviews in Oncology/Hematology 63: 12-31.
- del Bello, B., Paolicchi, A., Comporti, M., Pompella, A., and Maellaro, E. 1999. Hydrogen peroxide produced during gamma-glutamyl transpeptidase activity is involved in prevention of apoptosis and maintenance of proliferation in U937 cells. The FASEB journal : official publication of the Federation of American Societies for Experimental Biology 13: 69-79.
- DeLong, M. J. 1998. Apoptosis: a modulator of cellular homeostasis and disease states. Annals of the New York Academy of Sciences 842: 82-90.

- Dreher, D., and Junod, A. F. 1996. Role of oxygen free radicals in cancer development. European Journal of Cancer 32A: 30-38.
- Droge, W. 2002. Free radicals in the physiological control of cell function. Physiological Reviews 82: 47-95.
- Fang, J., Seki, T., and Maeda, H. 2009. Therapeutic strategies by modulating oxygen stress in cancer and inflammation. Advanced Drug Delivery Reviews 61: 290-302.
- Fiucci, G., Ravid, D., Reich, R., and Liscovitch, M. 2002. Caveolin-1 inhibits anchorage-independent growth, anoikis and invasiveness in MCF-7 human breast cancer cells. Oncogene 21: 2365-2375.
- Fujino, S., et al. 1996. A comparison of epidermal growth factor receptor levels and other prognostic parameters in non-small cell lung cancer. European Journal of Cancer 32A: 2070-2074.
- Garcia-Cardena, G., Oh, P., Liu, J., Schnitzer, J. E., and Sessa, W. C. 1996. Targeting of nitric oxide synthase to endothelial cell caveolae via palmitoylation: implications for nitric oxide signaling. Proceedings of the National Academy of Sciences of the United States of America 93: 6448-6453.
- Gewirtz, D. A. 1999. A critical evaluation of the mechanisms of action proposed for the antitumor effects of the anthracycline antibiotics adriamycin and daunorubicin. Biochemical Pharmacology 57: 727-741.
- Giannoni, E., Fiaschi, T., Ramponi, G., and Chiarugi, P. 2009. Redox regulation of anoikis resistance of metastatic prostate cancer cells: key role for Src and EGFR-mediated pro-survival signals. Oncogene 28: 2074-2086.
- Gueraud, F., et al. 2010. Chemistry and biochemistry of lipid peroxidation products. Free Radical Research 44: 1098-1124.
- Ha, H. C., Thiagalingam, A., Nelkin, B. D., and Casero, R. A., Jr. 2000. Reactive oxygen species are critical for the growth and differentiation of medullary thyroid carcinoma cells. Clinical Cancer Research 6: 3783-3787.
- Herbst, R. S., Heymach, J. V., and Lippman, S. M. 2008. Lung cancer. The New England Journal of Medicine 359: 1367-1380.
- Ho, C. C., Huang, P. H., Huang, H. Y., Chen, Y. H., Yang, P. C., and Hsu, S. M. 2002. Up-regulated caveolin-1 accentuates the metastasis capability of lung

- adenocarcinoma by inducing filopodia formation. The American Journal of Pathology 161: 1647-1656.
- Hunt, C. R., et al. (1998). Genomic instability and catalase gene amplification induced by chronic exposure to oxidative stress. Cancer Research 58: 3986-3992.
- Hynes, N. E., and Lane, H. A. 2005. ERBB receptors and cancer: the complexity of targeted inhibitors. Nature Review. Cancer 5: 341-354.
- Jackson, J. H. 1994. Potential molecular mechanisms of oxidant-induced carcinogenesis. Environment Health Perspective 102: 155-157.
- Jagtap, J. C., Chandele, A., Chopde, B.A., and Shastry, P. 2003. Sodium pyruvate protects against H₂O₂ mediated apoptosis in human neuroblastoma cell line-SK-N-MC. Journal of Chemical Neuroanatomy 26: 109-118.
- Janku, F., Stewart, D. J., and Kurzrock, R. 2010. Targeted therapy in non-small-cell lung cancer--is it becoming a reality? Nature Review. Clinical Oncology 7: 401-414.
- Jemal, A., Siegel, R., Xu, J., and Ward, E. 2010. Cancer statistics, 2010. CA: A Cancer Journal for Clinicians 60: 277-300.
- Karam, J. A., Lotan, Y., Roehrborn, C. G., Ashfaq, R., Karakiewicz, P. I., and Shariat, S. F. 2007. Caveolin-1 overexpression is associated with aggressive prostate cancer recurrence. Prostate 67: 614-622.
- Khan, E. M., Heidinger, J. M., Levy, M., Lisanti, M. P., Ravid, T., and Goldkorn, T. 2006. Epidermal growth factor receptor exposed to oxidative stress undergoes Src- and caveolin-1-dependent perinuclear trafficking. The Journal of Biological Chemistry 281: 14486-14493.
- Klaunig, J. E., Kamendulis, L. M., and Hocevar, B. A. 2010. Oxidative stress and oxidative damage in carcinogenesis. Toxicologic Pathology 38: 96-109.
- Koleske, A. J., Baltimore, D., and Lisanti, M. P. 1995. Reduction of caveolin and caveolae in oncogenically transformed cells. Proceedings of the National Academy of Sciences of the United States of America 92: 1381-1385.
- Kruidering, M., Van de Water, B., de Heer, E., Mulder, G. J., and Nagelkerke, J. F. 1997. Cisplatin-induced nephrotoxicity in porcine proximal tubular cells: mitochondrial dysfunction by inhibition of complexes I to IV of the

- respiratory chain. The Journal of Pharmacology and Experimental Therapeutics 280: 638-649.
- Leist, M., et al. 1999. Inhibition of Mitochondrial ATP Generation by Nitric Oxide Switches Apoptosis to Necrosis. Experimental Cell Research 249: 396-403.
- Li, C., and Jackson, R. M. 2002. Reactive species mechanisms of cellular hypoxia-reoxygenation injury. American Journal of Physiology - Cell Physiology 282: C227-241.
- Li, L., Ren, C. H., Tahir, S. A., Ren, C., and Thompson, T. C. 2003. Caveolin-1 maintains activated Akt in prostate cancer cells through scaffolding domain binding site interactions with and inhibition of serine/threonine protein phosphatases PP1 and PP2A. Molecular and Cellular Biology 23: 9389-9404.
- Li, S., Couet, J., and Lisanti, M. P. 1996. Src tyrosine kinases, Galpha subunits, and H-Ras share a common membrane-anchored scaffolding protein, caveolin. Caveolin binding negatively regulates the auto-activation of Src tyrosine kinases. The Journal of Biological Chemistry 271: 29182-29190.
- Li, S., Yan, T., Yang, J. Q., Oberley, T. D., and Oberley, L. W. 2000. The role of cellular glutathione peroxidase redox regulation in the suppression of tumor cell growth by manganese superoxide dismutase. Cancer Research 60: 3927-3939.
- Li, S., et al. 1995. Evidence for a regulated interaction between heterotrimeric G proteins and caveolin. The Journal of Biological Chemistry 270: 15693-15701.
- Lin, X., Sun, T., Cai, M., and Shen, P. 2010. Cell-death-mode switch from necrosis to apoptosis in hydrogen peroxide treated macrophages. Science China. Life Sciences 53: 1196-1203.
- Lloyd, P. G., and Hardin, C. D. 2011. Caveolae in cancer: two sides of the same coin? Focus on "Hydrogen peroxide inhibits non-small cell lung cancer cell anoikis through the inhibition of caveolin-1 degradation". American Journal of Physiology. Cell Physiology 300: C232-234.
- Lloyd, R. V., Hanna, P. M., and Mason, R. P. 1997. The Origin of the hydroxyl radical oxygen in the Fenton reaction. Free Radical Biology and Medicine 22: 885-888.

- Luanpitpong, S., et al. 2010. Regulation of lung cancer cell migration and invasion by reactive oxygen species and caveolin-1. The Journal of Biological Chemistry 285: 38832-38840.
- Madamanchi, N. R., Vendrov, A., and Runge, M. S. 2005. Oxidative stress and vascular disease. Arteriosclerosis, Thrombosis, and Vascular Biology 25: 29-38.
- Mao, Y., et al. 2006. Hydrogen peroxide-induced apoptosis in human gastric carcinoma MGC803 cells. Cell Biology International 30: 332-337.
- Miguel, L.-L. 2007. Dual role of hydrogen peroxide in cancer: Possible relevance to cancer chemoprevention and therapy. Cancer Letters 252: 1-8.
- Misthos, P., et al. 2005. Postresectional pulmonary oxidative stress in lung cancer patients. The role of one-lung ventilation. European journal of cardio-thoracic surgery 27: 379-382
- Moon, K. C., et al. 2005. Expression of caveolin-1 in pleomorphic carcinoma of the lung is correlated with a poor prognosis. Anticancer Research 25: 4631-4637.
- Nakamura, Y., Gindhart, T. D., Winterstein, D., Tomita, I., Seed, J. L., and Colburn, N. H. 1988. Early superoxide dismutase-sensitive event promotes neoplastic transformation in mouse epidermal JB6 cells. Carcinogenesis 9: 203-207.
- Negre-Salvayre, A., et al. 2010. Pathological aspects of lipid peroxidation. Free Radical Research 44: 1125-1171.
- Nicholson, D. W., and Thornberry, N. A. 1997. Caspases: killer proteases. Trends in Biochemical Sciences 22: 299-306.
- Nobel, C. S., Burgess, D. H., Zhivotovsky, B., Burkitt, M. J., Orrenius, S., and Slater, A. F. 1997. Mechanism of dithiocarbamate inhibition of apoptosis: thiol oxidation by dithiocarbamate disulfides directly inhibits processing of the caspase-3 proenzyme. Chemical Research in Toxicology 10: 636-643.
- Ohno, Y., and Gallin, J. I. 1985. Diffusion of extracellular hydrogen peroxide into intracellular compartments of human neutrophils. Studies utilizing the inactivation of myeloperoxidase by hydrogen peroxide and azide. The Journal of Biological Chemistry 260: 8438-8446.
- Okamoto, T., Schlegel, A., Scherer, P. E., and Lisanti, M. P. 1998. Caveolins, a family of scaffolding proteins for organizing "preassembled signaling

- complexes" at the plasma membrane. The Journal of Biological Chemistry 273: 5419-5422.
- Ono, K., Iwanaga, Y., Hirayama, M., Kawamura, T., Sowa, N., and Hasegawa, K. 2004. Contribution of caveolin-1 alpha and Akt to TNF-alpha-induced cell death. American Journal of Physiology. Lung Cellular and Molecular Physiology 287: L201-209.
- Parton, R. G., and Simons, K. 2007. The multiple faces of caveolae. Nature Reviews. Molecular Cell Biology 8: 185-194.
- Patel, H. H., Murray, F., and Insel, P. A. 2008. Caveolae as organizers of pharmacologically relevant signal transduction molecules. Annual Review of Pharmacology and Toxicology 48: 359-391.
- Pelle, E., Mammone, T., Maes, D., and Frenkel, K. 2005. Keratinocytes act as a source of reactive oxygen species by transferring hydrogen peroxide to melanocytes. The Journal of Investigative Dermatology 124: 793-797.
- Polytarchou, C., Hatziapostolou, M., and Papadimitriou, E. 2005. Hydrogen peroxide stimulates proliferation and migration of human prostate cancer cells through activation of activator protein-1 and up-regulation of the heparin affinity regulatory peptide gene. The Journal of Biological Chemistry 280: 40428-40435.
- Pongjit, K., and Chanvorachote, P. 2011. Caveolin-1 sensitizes cisplatin-induced lung cancer cell apoptosis via superoxide anion-dependent mechanism. Molecular and Cellular Biochemistry 358: 365-373.
- Ravid, T., Heidinger, J. M., Gee, P., Khan, E. M., and Goldkorn, T. 2004. c-Cbl-mediated ubiquitinylation is required for epidermal growth factor receptor exit from the early endosomes. The Journal of Biological Chemistry 279: 37153-37162.
- Reth, M. 2002. Hydrogen peroxide as second messenger in lymphocyte activation. Nature Immunology 3: 1129-1134.
- Rhee, S. G., Kang, S. W., Jeong, W., Chang, T.-S., Yang, K.-S., and Woo, H. A. 2005. Intracellular messenger function of hydrogen peroxide and its regulation by peroxiredoxins. Current Opinion in Cell Biology 17: 183-189.

- Rosell, R., et al. 2001. The role of chemotherapy in early non-small-cell lung cancer management. Lung Cancer 34 Suppl 3: S63-74.
- Rungtabnapa, P., Nimmannit, U., Halim, H., Rojanasakul, Y., and Chanvorachote, P. 2011. Hydrogen peroxide inhibits non-small cell lung cancer cell anoikis through the inhibition of caveolin-1 degradation. American Journal of Physiology. Cell Physiology 300: C235-245.
- Sargiacomo, M., et al. 1995. Oligomeric structure of caveolin: implications for caveolae membrane organization. Proceedings of the National Academy of Sciences of the United States of America 92: 9407-9411.
- Shaul, P. W., et al. 1996. Acylation targets endothelial nitric-oxide synthase to plasmalemmal caveolae. The Journal of Biological Chemistry 271: 6518-6522.
- Song, K. S., Li, S., Okamoto, T., Quilliam, L. A., Sargiacomo, M., and Lisanti, M. P. 1996. Co-purification and direct interaction of Ras with caveolin, an integral membrane protein of caveolae microdomains. Detergent-free purification of caveolae microdomains. The Journal of Biological Chemistry 271: 9690-9697.
- Sunaga, N., et al. 2004. Different roles for caveolin-1 in the development of non-small cell lung cancer versus small cell lung cancer. Cancer Research 64: 4277-4285.
- Tahir, S. A., et al. 2001. Secreted caveolin-1 stimulates cell survival/clonal growth and contributes to metastasis in androgen-insensitive prostate cancer. Cancer Research 61: 3882-3885.
- Thomas, G. M., and Huganir, R. L. 2004. MAPK cascade signalling and synaptic plasticity. Nature Reviews. Neuroscience 5: 173-183.
- Valko, M., Izakovic, M., Mazur, M., Rhodes, C. J., and Telser, J. 2004. Role of oxygen radicals in DNA damage and cancer incidence. Molecular and Cellular Biochemistry 266: 37-56.
- Vivanco, I., and Sawyers, C. L. 2002. The phosphatidylinositol 3-Kinase AKT pathway in human cancer. Nature Reviews. Cancer 2:489-501.
- Waghray, M., et al. 2005. Hydrogen peroxide is a diffusible paracrine signal for the induction of epithelial cell death by activated myofibroblasts. The FASEB Journal : Official Publication of the Federation of American Societies for Experimental Biology 19: 854-856.

- Waldron, R. T., and Rozengurt, E. 2000. Oxidative stress induces protein kinase D activation in intact cells. Involvement of Src and dependence on protein kinase C. The Journal of Biological Chemistry 275: 17114-17121.
- Wang, D., and Lippard, S. J. 2005. Cellular processing of platinum anticancer drugs. Nature Reviews. Drug Discovery 4: 307-320.
- Wang, L., et al. 2008. Peroxide is a key mediator of Bcl-2 down-regulation and apoptosis induction by cisplatin in human lung cancer cells. Molecular Pharmacology 73: 119-127.
- Yang, C. P., Galbiati, F., Volonte, D., Horwitz, S. B., and Lisanti, M. P. 1998. Upregulation of caveolin-1 and caveolae organelles in Taxol-resistant A549 cells. FEBS Letters 439: 368-372.
- Zanetti, M., Katusic, Z. S., and O'Brien, T. 2002. Adenoviral-mediated overexpression of catalase inhibits endothelial cell proliferation. American Journal of Physiology. Heart and Circulatory Physiology 283: H2620-2626.

APPENDIX

APPENDIX

TABLES OF EXPERIMENTAL RESULTS

Table 1. ROS intensity of H460 cells after treatment with various concentration of hydrogen peroxide and determined by using DCFH₂-DA probe. The DCF signal of each concentration at each time point was normalized to non-treated control and reported as relative DCF intensity. Data points represent the mean \pm S.D. (n=3).

Time (min)	Relative DCF intensity				
	control	H ₂ O ₂ 10 μ M	H ₂ O ₂ 50 μ M	H ₂ O ₂ 100 μ M	H ₂ O ₂ 200 μ M
0	1.00 \pm 0.04	1.00 \pm 0.00	1.04 \pm 0.05	1.04 \pm 0.06	1.02 \pm 0.07
5	1.00 \pm 0.04	1.01 \pm 0.00	1.11 \pm 0.01	1.11 \pm 0.03	1.30 \pm 0.09
10	1.01 \pm 0.07	1.03 \pm 0.06	1.13 \pm 0.01	1.22 \pm 0.05	1.59 \pm 0.15
15	1.03 \pm 0.06	1.05 \pm 0.06	1.13 \pm 0.02	1.25 \pm 0.05	1.69 \pm 0.14
20	1.04 \pm 0.06	1.08 \pm 0.04	1.13 \pm 0.02	1.27 \pm 0.06	1.83 \pm 0.07
25	1.04 \pm 0.06	1.11 \pm 0.05	1.15 \pm 0.01	1.32 \pm 0.06	1.92 \pm 0.11
30	1.04 \pm 0.07	1.14 \pm 0.05	1.15 \pm 0.03	1.32 \pm 0.06	2.01 \pm 0.13
45	1.01 \pm 0.06	1.16 \pm 0.05	1.18 \pm 0.05	1.35 \pm 0.08	2.17 \pm 0.19
60	1.05 \pm 0.07	1.23 \pm 0.04	1.21 \pm 0.07	1.47 \pm 0.07	2.31 \pm 0.21
75	1.05 \pm 0.06	1.26 \pm 0.05	1.23 \pm 0.11	1.59 \pm 0.05	2.52 \pm 0.19
90	1.09 \pm 0.07	1.28 \pm 0.06	1.26 \pm 0.14	1.64 \pm 0.07	2.63 \pm 0.15

Time (min)	Relative DCF intensity				
	control	H ₂ O ₂ 10 μM	H ₂ O ₂ 50 μM	H ₂ O ₂ 100 μM	H ₂ O ₂ 200 μM
105	1.07 ± 0.08	1.31 ± 0.05	1.29 ± 0.17	1.66 ± 0.07	2.64 ± 0.23
120	1.10 ± 0.08	1.29 ± 0.05	1.35 ± 0.17	1.67 ± 0.08	2.66 ± 0.17
135	1.09 ± 0.06	1.31 ± 0.05	1.33 ± 0.20	1.66 ± 0.06	2.65 ± 0.21
150	1.10 ± 0.06	1.31 ± 0.05	1.37 ± 0.19	1.68 ± 0.09	2.73 ± 0.13
165	1.13 ± 0.06	1.32 ± 0.05	1.39 ± 0.20	1.69 ± 0.08	2.74 ± 0.19
180	1.14 ± 0.06	1.32 ± 0.05	1.44 ± 0.22	1.71 ± 0.09	2.77 ± 0.17
210	1.15 ± 0.06	1.30 ± 0.05	1.44 ± 0.21	1.73 ± 0.09	2.81 ± 0.19
240	1.14 ± 0.05	1.29 ± 0.05	1.44 ± 0.19	1.74 ± 0.11	2.83 ± 0.15
270	1.17 ± 0.03	1.32 ± 0.05	1.45 ± 0.19	1.78 ± 0.10	2.86 ± 0.20
300	1.16 ± 0.06	1.33 ± 0.05	1.47 ± 0.22	1.78 ± 0.10	2.88 ± 0.17
330	1.17 ± 0.06	1.31 ± 0.05	1.46 ± 0.22	1.80 ± 0.12	2.89 ± 0.21
360	1.18 ± 0.05	1.34 ± 0.05	1.47 ± 0.22	1.81 ± 0.10	2.93 ± 0.23

Table 2. The percentage of H460 cell viability was determined by MTT assay after treatment with various concentration of hydrogen peroxide for 24 h. Value represents the mean \pm S.D. (n=3).

Hydrogen peroxide (μ M)	Cell viability (%)
control	99.83 \pm 2.37
10	100.89 \pm 6.00
50	94.10 \pm 7.19
100	89.19 \pm 5.78
200	48.05 \pm 5.78

Table 3. The percentage of H460 cell viability was determined by MTT assay after treatment with 200 μ M hydrogen peroxide at various time point. Value represents the mean \pm S.D. (n=3).

Time (h)	Cell viability (%)
0	100.78 \pm 2.59
3	77.10 \pm 5.28
6	61.40 \pm 4.66
12	55.69 \pm 4.51
24	46.58 \pm 4.15

Table 4. The percentage of H460 cell viability was determined by MTT assay after pretreatment with various kinds of antioxidant prior to 200 μ M hydrogen peroxide at 24 h. Value represents the mean \pm S.D. (n=3).

Treatment	Cell viability (%)
control	100.00 \pm 2.05
H ₂ O ₂ 200 μ M	47.44 \pm 4.77
NAC 1 mM + H ₂ O ₂ 200 μ M	86.44 \pm 5.67
GSH 1 mM + H ₂ O ₂ 200 μ M	87.61 \pm 3.67
CAT 5,000 units/ml + H ₂ O ₂ 200 μ M	88.38 \pm 4.76
Sodium pyruvate 1 mM + H ₂ O ₂ 200 μ M	88.35 \pm 2.86
DFO 1 mM + H ₂ O ₂ 200 μ M	91.10 \pm 3.75
MnTBAP 50 μ M + H ₂ O ₂ 200 μ M	54.84 \pm 7.60

Table 5. The percentage of H460 cell viability was determined by MTT assay after treatment with various kinds of antioxidant at 24 h. Value represents the mean \pm S.D. (n=3).

Treatment	Cell viability (%)
control	100.50 \pm 4.36
NAC 1 mM	99.91 \pm 3.75
GSH 1 mM	95.84 \pm 4.67
CAT 5,000 units/ml	101.59 \pm 5.86
Sodium pyruvate 1 mM	94.95 \pm 5.89
DFO 1 mM	96.00 \pm 3.75
MnTBAP 50 μ M	98.54 \pm 6.53

Table 6. ROS intensity of H460 cells after pretreatment with various kinds of antioxidant prior to 200 μ M of hydrogen peroxide and determined by using DCFH₂-DA probe. The DCF signal of each concentration at each time point was normalized to non-treated control and reported as relative DCF intensity. Data points represent the mean \pm S.D. (n=3).

Time (min)	Relative DCF intensity							
	control	H ₂ O ₂ 200 μ M	NAC + H ₂ O ₂ 200 μ M	GSH + H ₂ O ₂ 200 μ M	CAT + H ₂ O ₂ 200 μ M	Sodium pyruvate + H ₂ O ₂ 200 μ M	DFO + H ₂ O ₂ 200 μ M	MnTBAP + H ₂ O ₂ 200 μ M
0	1.00 \pm 0.10	1.01 \pm 0.12	1.05 \pm 0.36	1.00 \pm 0.08	1.06 \pm 0.05	1.03 \pm 0.07	0.81 \pm 0.01	2.61 \pm 0.19
5	1.02 \pm 0.08	1.28 \pm 0.11	1.01 \pm 0.11	0.98 \pm 0.13	1.08 \pm 0.05	1.03 \pm 0.02	0.87 \pm 0.01	2.67 \pm 0.26
10	1.00 \pm 0.10	1.52 \pm 0.20	1.01 \pm 0.11	0.97 \pm 0.13	1.08 \pm 0.04	1.03 \pm 0.04	0.88 \pm 0.02	2.73 \pm 0.24
15	1.03 \pm 0.06	1.86 \pm 0.32	0.98 \pm 0.11	0.99 \pm 0.14	1.04 \pm 0.03	1.05 \pm 0.05	0.93 \pm 0.01	2.71 \pm 0.21
30	1.07 \pm 0.04	2.11 \pm 0.32	0.98 \pm 0.11	0.99 \pm 0.15	1.05 \pm 0.04	1.08 \pm 0.07	0.98 \pm 0.43	2.78 \pm 0.27
45	1.03 \pm 0.07	2.34 \pm 0.30	0.99 \pm 0.10	1.00 \pm 0.02	1.04 \pm 0.04	1.08 \pm 0.07	1.07 \pm 0.06	2.79 \pm 0.25
60	1.03 \pm 0.07	2.45 \pm 0.27	0.99 \pm 0.07	1.01 \pm 0.06	1.05 \pm 0.04	1.07 \pm 0.04	1.13 \pm 0.04	2.86 \pm 0.34
75	1.07 \pm 0.08	2.57 \pm 0.23	1.02 \pm 0.07	1.06 \pm 0.17	1.07 \pm 0.04	1.09 \pm 0.10	1.19 \pm 0.06	2.88 \pm 0.32

Time (min)	Relative DCF intensity							
	control	H ₂ O ₂ 200 μM	NAC + H ₂ O ₂ 200 μM	GSH + H ₂ O ₂ 200 μM	CAT + H ₂ O ₂ 200 μM	Sodium pyruvate + H ₂ O ₂ 200 μM	DFO + H ₂ O ₂ 200 μM	MnTBAP + H ₂ O ₂ 200 μM
90	1.11 ± 0.07	2.69 ± 0.21	1.03 ± 0.07	1.09 ± 0.16	1.07 ± 0.04	1.11 ± 0.14	1.22 ± 0.06	2.82 ± 0.33
105	1.17 ± 0.06	2.76 ± 0.18	1.06 ± 0.08	1.09 ± 0.20	1.10 ± 0.05	1.12 ± 0.15	1.24 ± 0.10	2.80 ± 0.34
120	1.18 ± 0.07	2.80 ± 0.16	1.05 ± 0.13	1.07 ± 0.09	1.11 ± 0.05	1.08 ± 0.14	1.21 ± 0.11	2.75 ± 0.37
135	1.17 ± 0.07	2.81 ± 0.19	1.08 ± 0.09	1.05 ± 0.12	1.13 ± 0.05	1.09 ± 0.15	1.19 ± 0.11	2.79 ± 0.38
150	1.15 ± 0.08	2.83 ± 0.19	1.06 ± 0.08	1.04 ± 0.12	1.11 ± 0.05	1.12 ± 0.20	1.20 ± 0.05	2.79 ± 0.33
165	1.16 ± 0.07	2.82 ± 0.24	1.06 ± 0.08	1.05 ± 0.10	1.12 ± 0.05	1.11 ± 0.18	1.17 ± 0.08	2.77 ± 0.30
180	1.17 ± 0.08	2.81 ± 0.25	1.06 ± 0.09	1.06 ± 0.08	1.13 ± 0.05	1.11 ± 0.17	1.23 ± 0.07	2.78 ± 0.34

Table 7. Specific ROS intensity of H460 cells after 200 μ M of hydrogen peroxide treatment and determined by using DCFH₂-DA, HPF and DHE. Each fluorescence signal at each time point was normalized to non-treated control and reported as relative fluorescence intensity. Data points represent the mean \pm S.D. (n=3).

Time (min)	Relative fluorescence intensity		
	DCF	HPF	DHE
0	1.00 \pm 0.01	1.00 \pm 0.09	1.00 \pm 0.03
5	1.30 \pm 0.09	1.08 \pm 0.07	1.00 \pm 0.03
10	1.49 \pm 0.08	1.19 \pm 0.14	1.01 \pm 0.03
15	1.69 \pm 0.09	1.26 \pm 0.13	1.02 \pm 0.08
30	2.02 \pm 0.14	1.29 \pm 0.15	1.03 \pm 0.08
45	2.24 \pm 0.19	1.29 \pm 0.12	1.02 \pm 0.06
60	2.51 \pm 0.17	1.32 \pm 0.09	1.02 \pm 0.05
75	2.59 \pm 0.19	1.33 \pm 0.08	1.03 \pm 0.05
90	2.74 \pm 0.23	1.36 \pm 0.09	1.04 \pm 0.02
105	2.78 \pm 0.24	1.34 \pm 0.09	1.04 \pm 0.03
120	2.80 \pm 0.25	1.34 \pm 0.09	1.05 \pm 0.10
135	2.79 \pm 0.28	1.38 \pm 0.08	1.03 \pm 0.05
150	2.87 \pm 0.29	1.35 \pm 0.07	1.04 \pm 0.07
165	2.87 \pm 0.25	1.38 \pm 0.08	1.05 \pm 0.06
180	2.87 \pm 0.27	1.34 \pm 0.08	1.05 \pm 0.06

Table 8. HPF intensity of H460 cells after 200 μM of hydrogen peroxide treatment with or without pretreatment with deferoxamine and determined by using HPF probe. The HPF signal at each time point was normalized to non-treated control and reported as relative HPF intensity. Data points represent the mean \pm S.D. (n=3).

Time (min)	Relative HPF intensity		
	control	H ₂ O ₂ 200 μM	DFO + H ₂ O ₂ 200 μM
0	1.00 \pm 0.02	1.00 \pm 0.06	0.94 \pm 0.06
5	0.98 \pm 0.02	1.08 \pm 0.06	0.95 \pm 0.06
10	0.98 \pm 0.02	1.19 \pm 0.04	0.95 \pm 0.07
15	0.97 \pm 0.04	1.26 \pm 0.04	0.96 \pm 0.07
30	0.98 \pm 0.03	1.29 \pm 0.05	0.96 \pm 0.06
45	0.98 \pm 0.04	1.29 \pm 0.04	1.02 \pm 0.01
60	0.99 \pm 0.02	1.32 \pm 0.09	1.04 \pm 0.04
75	1.03 \pm 0.04	1.33 \pm 0.08	1.09 \pm 0.05
90	1.00 \pm 0.04	1.36 \pm 0.09	1.07 \pm 0.02
105	1.01 \pm 0.05	1.34 \pm 0.09	1.08 \pm 0.05
120	1.03 \pm 0.03	1.34 \pm 0.09	1.07 \pm 0.02
135	0.98 \pm 0.04	1.38 \pm 0.08	1.06 \pm 0.06
150	0.99 \pm 0.04	1.35 \pm 0.08	1.06 \pm 0.07
165	1.00 \pm 0.02	1.38 \pm 0.08	1.07 \pm 0.04
180	1.03 \pm 0.04	1.34 \pm 0.07	1.11 \pm 0.06

Table 9. DCF intensity of H460/control, H460/shCav-1 and H460/Cav-1 cells after 200 μ M of hydrogen peroxide treatment and determined by using DCFH₂-DA. The DCF signal at each time point was normalized to non-treated control and reported as relative DCF intensity. Data points represent the mean \pm S.D. (n=3).

Time (min)	Relative DCF intensity		
	H460/shCav-1	H460/control	H460/Cav-1
0	1.00 \pm 0.02	1.00 \pm 0.02	1.00 \pm 0.05
5	1.12 \pm 0.08	1.06 \pm 0.04	1.02 \pm 0.05
10	1.19 \pm 0.05	1.09 \pm 0.06	1.14 \pm 0.06
15	1.38 \pm 0.04	1.16 \pm 0.05	1.22 \pm 0.02
30	1.51 \pm 0.04	1.30 \pm 0.08	1.29 \pm 0.06
45	1.73 \pm 0.12	1.46 \pm 0.05	1.35 \pm 0.04
60	2.21 \pm 0.20	1.86 \pm 0.14	1.56 \pm 0.10
75	2.66 \pm 0.23	2.13 \pm 0.18	1.60 \pm 0.13
90	3.01 \pm 0.25	2.36 \pm 0.28	1.69 \pm 0.14
105	3.33 \pm 0.31	2.66 \pm 0.24	1.73 \pm 0.15
120	3.48 \pm 0.35	2.72 \pm 0.27	1.71 \pm 0.16
135	3.69 \pm 0.35	2.82 \pm 0.29	1.74 \pm 0.14
150	3.90 \pm 0.47	2.81 \pm 0.29	1.72 \pm 0.19
165	4.03 \pm 0.57	2.78 \pm 0.28	1.75 \pm 0.17
180	4.12 \pm 0.38	2.83 \pm 0.30	1.77 \pm 0.17

Table 10. HPF intensity of H460/control, H460/shCav-1 and H460/Cav-1 cells after 200 μ M of hydrogen peroxide treatment and determined by using HPF probe. The HPF signal at each time point was normalized to non-treated control and reported as relative HPF intensity. Data points represent the mean \pm S.D. (n=3).

Time (min)	Relative HPF intensity		
	H460/shCav-1	H460/control	H460/Cav-1
0	1.00 \pm 0.12	1.00 \pm 0.09	1.00 \pm 0.11
5	1.08 \pm 0.16	1.08 \pm 0.07	1.04 \pm 0.04
10	1.32 \pm 0.18	1.19 \pm 0.14	1.05 \pm 0.11
15	1.40 \pm 0.15	1.26 \pm 0.13	1.04 \pm 0.10
30	1.48 \pm 0.09	1.29 \pm 0.17	1.05 \pm 0.11
45	1.54 \pm 0.06	1.29 \pm 0.12	1.05 \pm 0.13
60	1.56 \pm 0.06	1.32 \pm 0.09	1.03 \pm 0.12
75	1.62 \pm 0.13	1.33 \pm 0.08	1.06 \pm 0.08
90	1.63 \pm 0.09	1.36 \pm 0.09	1.09 \pm 0.10
105	1.71 \pm 0.17	1.34 \pm 0.09	1.04 \pm 0.11
120	1.66 \pm 0.10	1.34 \pm 0.09	1.07 \pm 0.07
135	1.71 \pm 0.14	1.38 \pm 0.08	1.07 \pm 0.08
150	1.71 \pm 0.19	1.35 \pm 0.08	1.08 \pm 0.08
165	1.74 \pm 0.14	1.38 \pm 0.08	1.06 \pm 0.13
180	1.72 \pm 0.14	1.34 \pm 0.07	1.07 \pm 0.11

Table 11. The percentage of H460/shCav-1 cell viability was determined by MTT assay after treatment with various concentration of hydrogen peroxide for 24 h. Value represents the mean \pm S.D. (n=3).

Hydrogen peroxide (μ M)	Cell viability (%)
control	100.47 \pm 4.23
10	96.90 \pm 3.10
50	95.72 \pm 5.94
100	82.92 \pm 6.04
200	29.37 \pm 6.64

Table 12. The percentage of H460/Cav-1 cell viability was determined by MTT assay after treatment with various concentration of hydrogen peroxide for 24 h. Value represents the mean \pm S.D. (n=3).

Hydrogen peroxide (μ M)	Cell viability (%)
control	100.23 \pm 3.97
10	100.87 \pm 6.46
50	97.78 \pm 5.65
100	95.26 \pm 2.97
200	79.86 \pm 2.30

Table 13. The percentage of H460/control, H460/shCav-1 and H460/Cav-1 cell viability was determined by MTT assay after treatment with 200 μ M of hydrogen peroxide for various time point. Value represents the mean \pm S.D. (n=3).

Time (h)	Cell viability (%)		
	H460/shCav-1	H460/control	H460/Cav-1
0	101.13 \pm 5.95	100.78 \pm 2.59	100.65 \pm 3.56
3	68.34 \pm 4.98	77.10 \pm 5.28	91.61 \pm 3.53
6	56.08 \pm 3.73	61.40 \pm 4.66	84.89 \pm 6.51
12	46.23 \pm 3.02	55.69 \pm 4.51	81.50 \pm 3.86
24	29.26 \pm 3.64	45.58 \pm 4.16	76.85 \pm 4.48

Table 14. The percentage of H460/control, H460/shCav-1 and H460/Cav-1 cell viability was determined by MTT assay after treatment with 200 μ M of hydrogen peroxide with the presence or absence of hydroxyl radical modulators for 24 h. Value represents the mean \pm S.D. (n=3).

Treatment	Cell viability (%)		
	H460/shCav-1	H460/control	H460/Cav-1
control	101.13 \pm 3.50	100.78 \pm 2.59	100.65 \pm 3.56
H ₂ O ₂ 200 μ M	29.26 \pm 3.64	45.58 \pm 4.16	76.85 \pm 4.48
DFO + H ₂ O ₂ 200 μ M	76.26 \pm 6.48	83.83 \pm 4.52	88.63 \pm 6.13
FeSO ₄ + H ₂ O ₂ 200 μ M	20.71 \pm 2.94	22.79 \pm 0.82	19.11 \pm 2.42

Table 15. DCF intensity of H460/control, H460/shCav-1 and H460/Cav-1 cells after pretreatment with deferoxamine prior to 200 μ M hydrogen peroxide and determined by using DCFH₂-DA. The DCF signal was normalized to non-treated control and reported as relative DCF intensity. Data points represent the mean \pm S.D. (n=3).

Time (min)	Relative DCF intensity		
	H460/shCav-1	H460/control	H460/Cav-1
0	0.88 \pm 0.12	0.81 \pm 0.01	0.68 \pm 0.07
5	0.91 \pm 0.11	0.87 \pm 0.02	0.71 \pm 0.09
10	0.93 \pm 0.099	0.88 \pm 0.02	0.74 \pm 0.11
15	0.96 \pm 0.07	0.93 \pm 0.02	0.78 \pm 0.12
30	1.01 \pm 0.09	0.98 \pm 0.04	0.90 \pm 0.15
45	1.06 \pm 0.10	1.07 \pm 0.06	0.94 \pm 0.14
60	1.11 \pm 0.09	1.13 \pm 0.04	1.02 \pm 0.13
75	1.15 \pm 0.08	1.19 \pm 0.06	1.08 \pm 0.14
90	1.16 \pm 0.06	1.22 \pm 0.06	1.10 \pm 0.14
105	1.18 \pm 0.05	1.24 \pm 0.10	1.14 \pm 0.14
120	1.19 \pm 0.06	1.21 \pm 0.11	1.11 \pm 0.14
135	1.18 \pm 0.06	1.19 \pm 0.11	1.11 \pm 0.13
150	1.17 \pm 0.06	1.20 \pm 0.05	1.12 \pm 0.13
165	1.17 \pm 0.07	1.17 \pm 0.08	1.10 \pm 0.12
180	1.21 \pm 0.04	1.22 \pm 0.07	1.14 \pm 0.12

Table 16. DCF intensity of H460/control, H460/shCav-1 and H460/Cav-1 cells after pretreatment with ferrous sulfate prior to 200 μ M hydrogen peroxide and determined by using DCFH₂-DA. The DCF signal was normalized to non-treated control and reported as relative DCF intensity. Data points represent the mean \pm S.D. (n=3).

Time (min)	Relative DCF intensity		
	H460/shCav-1	H460/control	H460/Cav-1
0	0.99 \pm 0.12	1.00 \pm 0.16	1.00 \pm 0.02
5	1.08 \pm 0.13	1.11 \pm 0.22	1.09 \pm 0.09
10	1.19 \pm 0.12	1.18 \pm 0.34	1.12 \pm 0.10
15	1.31 \pm 0.19	1.31 \pm 0.27	1.19 \pm 0.06
30	1.56 \pm 0.22	1.49 \pm 0.26	1.31 \pm 0.17
45	1.88 \pm 0.10	1.75 \pm 1.18	1.56 \pm 0.18
60	2.35 \pm 0.12	2.03 \pm 0.17	2.02 \pm 0.23
75	2.87 \pm 0.09	2.61 \pm 0.21	2.47 \pm 0.46
90	3.37 \pm 0.18	2.95 \pm 0.16	2.93 \pm 0.44
105	3.87 \pm 0.22	3.47 \pm 0.17	3.29 \pm 0.20
120	4.20 \pm 0.28	3.80 \pm 0.24	3.53 \pm 0.34
135	4.49 \pm 0.24	4.09 \pm 0.28	3.87 \pm 0.37
150	4.82 \pm 0.24	4.31 \pm 0.23	4.03 \pm 0.43
165	5.08 \pm 0.32	4.46 \pm 0.05	4.29 \pm 0.43
180	5.38 \pm 0.10	4.84 \pm 0.32	4.69 \pm 0.38

Table 17. HPF intensity of H460/control, H460/shCav-1 and H460/Cav-1 cells after pretreatment with deferoxamine prior to 200 μ M hydrogen peroxide and determined by using HPF probe. The HPF signal was normalized to non-treated control and reported as relative HPF intensity. Data points represent the mean \pm S.D. (n=3).

Time (min)	Relative HPF intensity		
	H460/shCav-1	H460/control	H460/Cav-1
0	0.96 \pm 0.07	0.94 \pm 0.06	0.85 \pm 0.05
5	0.99 \pm 0.10	0.95 \pm 0.06	0.87 \pm 0.05
10	0.99 \pm 0.11	0.96 \pm 0.07	0.87 \pm 0.08
15	1.02 \pm 0.10	0.96 \pm 0.07	0.86 \pm 0.05
30	1.03 \pm 0.09	0.96 \pm 0.06	0.88 \pm 0.03
45	1.04 \pm 0.09	1.02 \pm 0.01	0.89 \pm 0.06
60	1.06 \pm 0.10	1.04 \pm 0.04	0.91 \pm 0.08
75	1.09 \pm 0.10	1.09 \pm 0.05	0.94 \pm 0.09
90	1.10 \pm 0.09	1.07 \pm 0.02	0.92 \pm 0.07
105	1.09 \pm 0.11	1.08 \pm 0.04	0.93 \pm 0.09
120	1.09 \pm 0.13	1.07 \pm 0.02	0.95 \pm 0.08
135	1.07 \pm 0.14	1.06 \pm 0.06	0.93 \pm 0.08
150	1.09 \pm 0.08	1.06 \pm 0.07	0.91 \pm 0.07
165	1.11 \pm 0.08	1.07 \pm 0.14	0.92 \pm 0.08
180	1.14 \pm 0.10	1.11 \pm 0.06	0.93 \pm 0.08

Table 18. HPF intensity of H460/control, H460/shCav-1 and H460/Cav-1 cells after pretreatment with ferrous sulfate prior to 200 μ M hydrogen peroxide and determined by using HPF probe. The HPF signal was normalized to non-treated control and reported as relative HPF intensity. Data points represent the mean \pm S.D. (n=3).

Time (min)	Relative HPF intensity		
	H460/shCav-1	H460/control	H460/Cav-1
0	1.00 \pm 0.14	1.01 \pm 0.11	1.00 \pm 0.15
5	1.25 \pm 0.30	1.20 \pm 0.14	1.20 \pm 0.21
10	1.62 \pm 0.16	1.40 \pm 0.20	1.38 \pm 0.27
15	1.72 \pm 0.12	1.50 \pm 0.25	1.45 \pm 0.22
30	1.79 \pm 0.07	1.53 \pm 0.26	1.44 \pm 0.19
45	1.77 \pm 0.09	1.49 \pm 0.21	1.40 \pm 0.16
60	1.79 \pm 0.11	1.55 \pm 0.16	1.42 \pm 0.18
75	1.76 \pm 0.14	1.53 \pm 0.19	1.42 \pm 0.11
90	1.84 \pm 0.08	1.58 \pm 0.17	1.46 \pm 0.17
105	1.86 \pm 0.09	1.54 \pm 0.18	1.46 \pm 0.16
120	1.85 \pm 0.12	1.55 \pm 0.13	1.47 \pm 0.16
135	1.80 \pm 0.13	1.59 \pm 0.16	1.43 \pm 0.08
150	1.78 \pm 0.12	1.52 \pm 0.21	1.44 \pm 0.10
165	1.81 \pm 0.13	1.51 \pm 0.11	1.38 \pm 0.08
180	1.83 \pm 0.13	1.53 \pm 0.11	1.39 \pm 0.15

VITA

Mr. Wongsakorn Suchaoin was born on July 23, 1984 in Phayao. He received his B.Pharm (1st class honor) from the faculty of Pharmacy, Chiang Mai University in 2007.